Advanced Endoscopic Imaging

Guest Editors: Helmut Neumann, Klaus Mönkemüller,
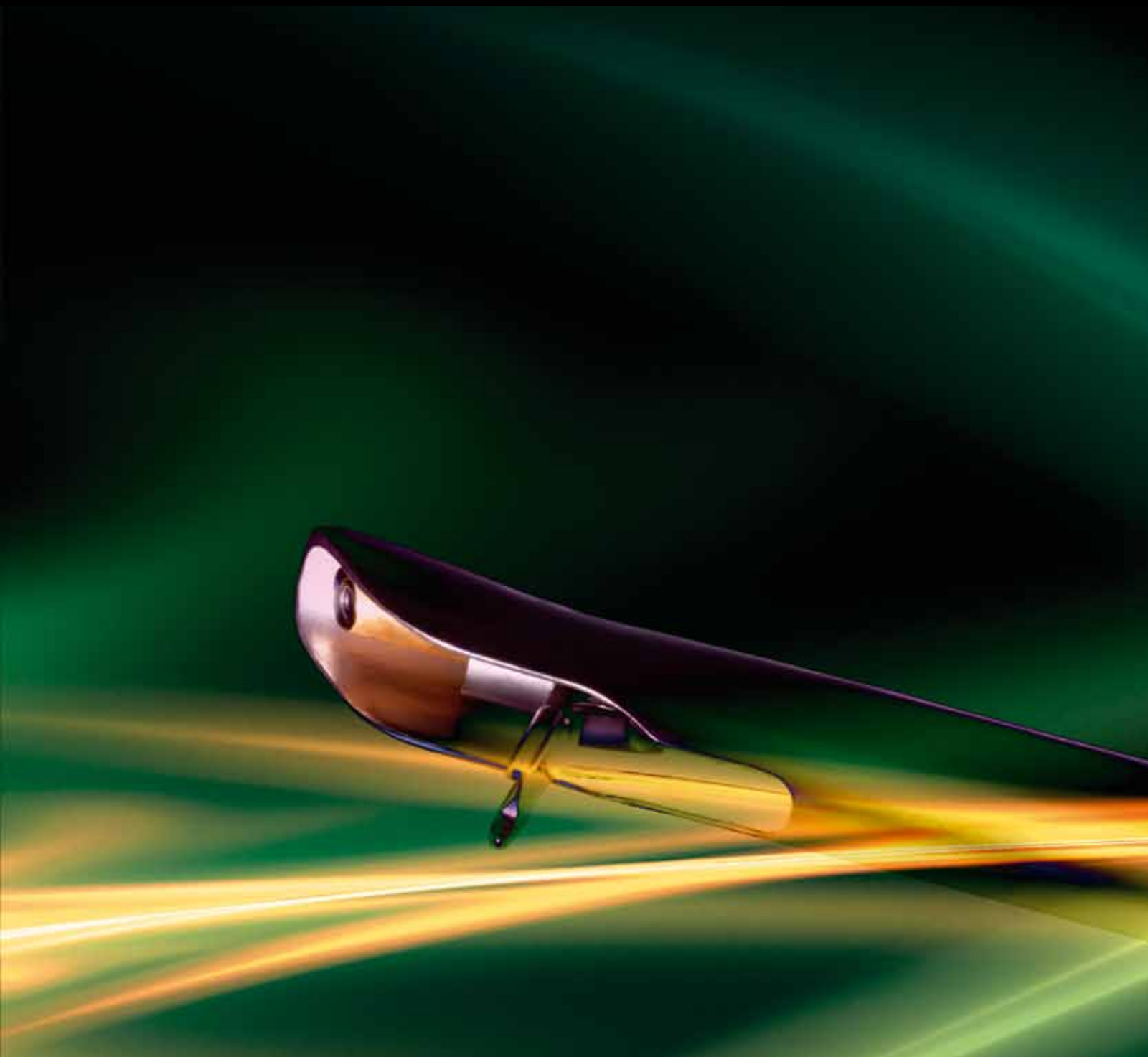Markus F. Neurath, Arthur Hoffman, and Charles Melbern Wilcox

Diagnostic and Therapeutic Endoscopy

Advanced Endoscopic Imaging

Guest Editors: Helmut Neumann, Klaus Mönkemüller,
Markus F. Neurath, Arthur Hoffman,
and Charles Melbern Wilcox

Editorial Board

Contents

Editorial
Advanced Endoscopic Imaging

Helmut Neumann,[1] Klaus Mönkemüller,[2] Markus F. Neurath,[1] Arthur Hoffman,[3] and Charles Melbern Wilcox[2]

[1] *Department of Medicine I, University of Erlangen-Nuremberg, Ulmenweg 18, 91054 Erlangen, Germany*
[2] *Basil Hirschowitz Endoscopic Center of Excellence, University of Alabama, Birmingham, AL, USA*
[3] *St. Marienkrankenhaus Katharina-Kasper, Richard-Wagner Straße 14, 60318 Frankfurt am Main, Germany*

Correspondence should be addressed to Helmut Neumann; helmut.neumann@uk-erlangen.de

It was in the late 18th century when the American essayist, poet, and philosopher Henry David Thoreau quoted "*It's not what you look at that matters, it's what you see.*" Indeed, more than 200 years later, this phrase is still valid and relevant, especially in the field of gastrointestinal (GI) endoscopy.

Endoscopists in the whole world are working hard to improve diagnosis and therapy of our patients. Despite these efforts, we are still confronted with some limitations of GI endoscopy including the lack of detection of colon polyps (i.e., significant adenoma miss rates), delayed diagnosis, and difficult areas to access, like the pancreatobiliary tract or the small bowel.

In the attempt to overcome these limitations, new endoscopic techniques are constantly being introduced. New endoscopic imaging techniques now allow for a more detailed analysis of mucosal and submucosal structures and include virtual chromoendoscopy, magnification endoscopy, and endocytoscopy. Various studies have shown the usefulness of these imaging techniques for conditions such as Barrett's esophagus, colon polyps, and early neoplasias of the luminal GI tract. Moreover, the recently introduced confocal laser endomicroscopy (CLE) system allows us to analyze structures at the cellular and subcellular layer thereby obtaining an optical biopsy during ongoing endoscopy. Besides, CLE has the potential to visualize fluorescence labeled structures against specific epitopes, that is, in gastrointestinal cancer or inflammatory bowel disease, thus adding molecular imaging to the field of endoscopic research. Furthermore, with the development of balloon-assisted endoscopy and capsule endoscopy, the endoscopist is now able to visualize the entire small bowel. Lastly, visualization beyond the mucosa is also important. This is accomplished with endoscopic ultrasonography (EUS). EUS plays now a pivotal role for the management and therapy of various diseases. Through EUS, the "eye" of the endoscopist is extended beyond the lumen allowing for a detailed examination of most adjacent structures to the luminal GI tract.

This special issue focuses on the exiting new developments of GI endoscopy. We are proud to present original articles and state-of-the-art reviews on the latest developments in the field of advanced endoscopic imaging. We are aware that it is impossible to cover the entire spectrum of advanced endoscopy in only one issue. The presented topics, however, highlight some of the most current aspects, controversies, and recommendations in selected areas of advanced GI imaging.

B. E. Bluen and coworkers analyzed the impact of EUS-FNA on patient management. Files from 268 patients were evaluated. In the conclusion, the authors suggest that the diagnostic accuracy of EUS-FNA might be improved further by taking more FNA passes from suspected lesions, optimizing needle selection, having an experienced echo-endoscopist available during the learning curve, and lastly having a cytologist present during the procedure. C. Xu et al. reviewed the technique and applications of contrast-enhanced harmonic EUS (CH-EUS) in pancreatic diseases and compared the technique to computed tomography, magnetic resonance imaging, and conventional EUS. The authors concluded that CH-EUS could be used for adequate sampling

of pancreatic tumors but could not replace EUS-FNA now. Mohammad-Alizadeh and coworkers evaluated the efficacy of limited sphincterotomy plus large balloon dilation for removal of biliary stones in a prospective nonrandomized study including 50 patients. The authors described that the combined approach is an effective and safe treatment in patients with challenging bile duct stones.

M. Iwatate et al. evaluated NBI (Olympus, Tokyo, Japan) and NBI combined with magnification for the evaluation of colorectal lesions and additionally gave an outlook on future prospects. Digital chromoendoscopy techniques were evaluated in two different trials of this special issue. C. E. O. dos Santos and coworkers presented the results of a prospective randomized study comparing the accuracy of Fujinon Intelligent Color Enhancement (FICE; Fujifilm, Tokyo, Japan) and real-time chromoendoscopy for the differential diagnosis of diminutive (<5 mm) neoplastic and nonneoplastic colorectal lesions and found that both approaches showed high accuracy for the histopathological diagnosis of diminutive colorectal lesions. S. Hancock et al. described the potential of i-scan (Pentax, Tokyo, Japan) in clinical endoscopic practice in upper and lower endoscopic procedures and described the potential usefulness of this technique for real-time diagnosis and characterization of GI lesions. The small bowel was discussed in two manuscripts of this special issue. H. Suzuki et al. described the successful treatment of early stage jejunal adenocarcinoma by endoscopic mucosal resection using double-balloon enteroscopy. Whereas there are several reports on polypectomy of the small bowel, this is the first report of EMR of this part of the GI tract. J. Chen and J. Lee reviewed the current development of machine-vision-based analysis of wireless capsule endoscopy, thereby focusing on the research that identifies specific gastrointestinal pathology and methods of shot boundary detection. CLE is an advanced endoscopic imaging technique. R. Pittayanon et al. described for the first time the learning curve of CLE for assessment of gastric intestinal metaplasia. The authors found that after a short session of training, even beginners could achieve a high level of accuracy with a substantial level of interobserver agreement. Foersch et al. described the potential of molecular imaging using CLE for imaging of COX-2 activity in murine sporadic and colitis-associated colorectal cancer. The authors pose a proof of concept and suggested the use of CLE for the detection of COX-2 expression during colorectal cancer surveillance. Finally, S. Peter et al. presented a state-of-the-art review on the potential of CLE for real-time histopathological evaluation of the pancreaticobiliary system. They concluded that the novel use of this technique is particularly of significance in differentiating indeterminate biliary strictures as treatment depends on an accurate and prompt diagnosis.

We highly appreciate the excellent contributions of all authors of this special issue and want to encourage all readers to be receptive on the rapidly growing field of advanced endoscopic imaging. Nonetheless, just utilizing a new method is not enough; a clear understanding of how the method is used and how the findings are interpreted is the key for a successful endoscopy: "*It's not what you look at that matters, it's what you see.*"

Helmut Neumann
Klaus Mönkemüller
Markus F. Neurath
Arthur Hoffman
Charles Melbern Wilcox

Review Article

Endomicroscopy of the Pancreaticobiliary System

Shajan Peter, Ji Young Bang, Klaus Mönkemuller, Shyam Varardarajulu, and C. Mel Wilcox

Division of Gastroenterology and Hepatology, University of Alabama at Birmingham, Birmingham, AL 35294-0012, USA

Correspondence should be addressed to C. Mel Wilcox; melw@uab.edu

It is often difficult to accurately differentiate between benign and malignant pancreaticobiliary strictures, and some are interpreted as indeterminate despite ERCP, EUS, or radiological imaging techniques, thereby making it difficult for the clinician to make appropriate management decisions. Probe-based confocal laser endomicroscopy (pCLE) is an innovative imaging tool integrating real-time in vivo imaging of these difficult-to-interpret strictures in the pancreaticobiliary system during endoscopy. Recent studies of endomicroscopy have shown a promising role with improved accuracy in distinguishing these lesions, thus paving the way for future research addressing improving precise interpretation, training, and long long-term impact.

1. Introduction

Over the past few years, advanced imaging techniques have improved the diagnosis of pancreaticobiliary disorders. While there have been improvements in technology involving procedures such as endoscopic retrograde cholangiopancreaticography (ERCP), endoscopic ultrasound (EUS), computed tomography (CT) scan, magnetic resonance imaging (MRCP), and direct cholangioscopy/SpyGlass, there have also been major advancements in not only diagnosis but also in tissue procurement combined with therapeutic potential. However, in spite of such progress, it remains difficult to accurately differentiate between benign and malignant lesions such as strictures, which are vital for decision-making and appropriate management [1] (Figure 1). Often, conventional methods such as intraductal biopsy, cytological brushings, or FNA remain inconclusive or indeterminate resulting in low diagnostic accuracy [2] (Figure 5). These scenarios lead to further testing or intervention; delay diagnosis is important for a potential candidate requiring surgical resection or palliative therapy. Probe-based confocal laser endomicroscopy (pCLE) is one innovative tool that allows for real-time in vivo imaging of these difficult-to-interpret strictures in the pancreaticobiliary system.

Current diagnostic modalities (biopsy, brush cytology, or fine needle aspiration (FNA) through ERCP or EUS guided routes) have their limitations in accurate diagnosis of biliary strictures, and the sensitivity of tissue sampling varies between 20% and 60% [3–5]. The sensitivity increases when two sampling methods are utilized such as combining brush cytology with forceps yielding a sensitivity ranging from 54% to 70.4% and specificity from 97% to 100% [6]. Adding EUS-guided FNA to these methods increased the sensitivity marginally to 71% with specificity of 100%, though the EUS technique is the best method for diagnosing intrapancreatic lesions. In a recent study, standard ERCP-guided tissue sampling in indeterminate biliary strictures had 76% sensitivity and 88% accuracy, while these values were 57% and 78%, respectively, for cholangioscopic-directed (Spy Bite) biopsies [7]. These data show that given the best available techniques, the yield is still suboptimal. The site of stricture such as proximal versus distal, nature of sampling, superficial versus deep, and difficulty in focal targeting add to the existing challenges facing the diagnostic dilemma while evaluating indeterminate biliary strictures thereby underlying the dire need for improving overall accuracy.

Confocal laser endomicroscopy (CLE) has emerged as a new endoscopic imaging modality helping the endoscopist

become an endopathologist by obtaining in vivo histological assessment. Thus it offers an additional or alternative method to tissue "sampling" in assessing strictures. There are two commercially available systems: (a) the endoscope-based CLE system where the confocal mechanism is incorporated in the tip of a conventional endoscope, integrated CLE (iCLE), and (b) the probe-based CLE (pCLE) system that can be passed through the biopsy channel of the endoscope. For real-time imaging of the biliary system owing to accessibility and delivery the latter system is currently being used [8].

The pCLE probe that is FDA approved specifically for pancreaticobiliary use is the CholangioFlex^{UHD} miniprobe (Mauna Kea Technologies, Paris, France) [9]. This probe consists of several fiber light bundles (>10000 optical fibers) with distal lens through which the laser beam is transmitted while being connected to a laser-scanning unit and light source. The diameter is smaller than a GastroFlex^{UHD} miniprobe, which is used for another upper gastrointestinal imaging. The specifications are listed in Table 1.

The CLE images are then sent to a laser scanning unit (LSU) that interprets the images and sends them to a processor. Data are collected at 12 frames per second. These images and acquired sequences are stored on computer systems, where they can be viewed and interpreted as real time or recorded and saved. They can be then reviewed, magnified, or exported. The specially designed software package (Cellvizio viewer) allows image correction and stabilization.

2. Contrast Agents

Exogenous fluorescent agents are needed for detection of cellular details while performing a CLE test. Intravenous fluorescein sodium is commonly used at 10% concentration, which then helps in highlighting vessels, intercellular spaces, vascular pattern, lamina propria, and overall cellular architecture. It does not stain nuclei. Thus, disruption of cellular architecture or vasculature or leaky blood vessels are indicative of disease. When used mostly by ophthalmologists fluorescent agents have shown a high safety profile, and adverse events are few [10]. One must caution the patient that they may experience transient yellowing of the skin, eyes, and urine that could persist for a few hours. Typically an injection of 2.5 to 5.0 mL of fluorescein is sufficient for visualization of epithelial cells, and the effect lasts for 30 minutes.

3. Technique

The pCLE probe is inserted through the working channel of an ERCP scope or through various catheter devices (Table 2). It is advanced until the radiopaque tip is visible under fluoroscopic vision or cholangioscopic visualization. It is then positioned in direct contact with the mucosa of the biliary tract or site of interest. It might be preferred to go from an area of normal mucosa to abnormality. After injecting fluorescein intravenously, using the foot pedals provided or from the computer screen activates the laser, and real-time endomicroscopy is performed. Given the narrowing of lumen

TABLE 1: Specifications of pCLE probe for pancreatico-biliary evaluation.

	Mini probe (CholangioFlex)
Laser wavelength	488 nm
Depth of imaging (μm)	40–60
Plane depth (μm)	0–50
Max field of view (mm)	325
Lateral resolution (μm)	3.5
Axial resolution (μm)	15
Imaging rate (frames/s)	12
External diameter (mm)	0.94

TABLE 2: Type of catheters for pCLE access.

Catheter device	Manufacturer
Cotton Graduated Dilatation Catheter	Cook Medical
OASIS One Action Stent Introduction System	Cook Medical
Memory Dormia Basket	Cook Medical
Howell Biliary Introducer	Cook Medical
Geenen Graduated Dilatation Catheter	Cook Medical
Swing Tip ERCP Cannula	Olympus Medical

specially while imaging biliary duct strictures, the main challenge is positioning the probe to maintain it perpendicular to the mucosa rather than parallel. The video sequences and images can be captured or recorded. Tissue sampling such as for cytology or biopsies are preferably done after image acquisition by pCLE as they could result in art factual errors. Access of the pCLE probe can also be achieved through the SpyGlass system (Boston Scientific, Natick, Massachusetts, USA), Olympus cholangioscopes (Olympus Corp, Tokyo, Japan), and Storz prototype cholangioscope (Karl Storz GmbH, Tuttlingen, Germany) [17].

4. Interpretation

Features that differentiate benign mucosa from malignant mucosa include loss of the reticular pattern of epithelial bands <20 μm, irregular epithelial lining, gland-like structures, tortuous dilated vessels with abnormal branching, and clumps of black areas showing focal decreased areas of fluorescein or fluorescein leakage (Figures 2, 3, and 4). Putting all these observations together, the Miami classification has been adopted for classification of biliary and pancreatic lesions especially for indeterminate strictures [18]. Using specific criteria such as thick white bands (>20 μm), or thick dark bands (>40 μm) or dark clumps and epithelial structures, resulted in sensitivity of 97%, specificity (33%), PPV (80%), and NPV, (80%) compared with 45%, 100%, 100%, and 69%, respectively, for standard cytopathology. The interobserver variability was moderate for most criteria. In retrospective analysis, combining two or more criteria increased the sensitivity as compared to single criteria interpretation.

(a) (b)
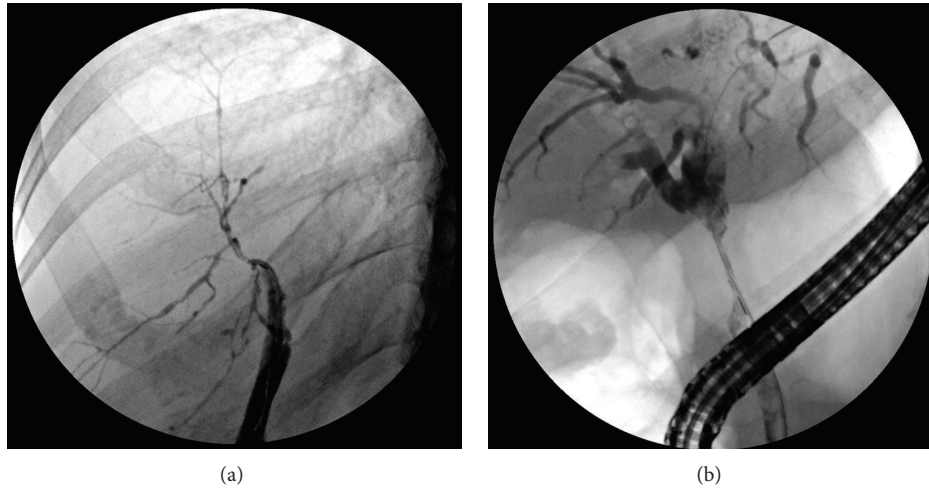
Figure 1: ERCP images of biliary strictures.

(a) (b)
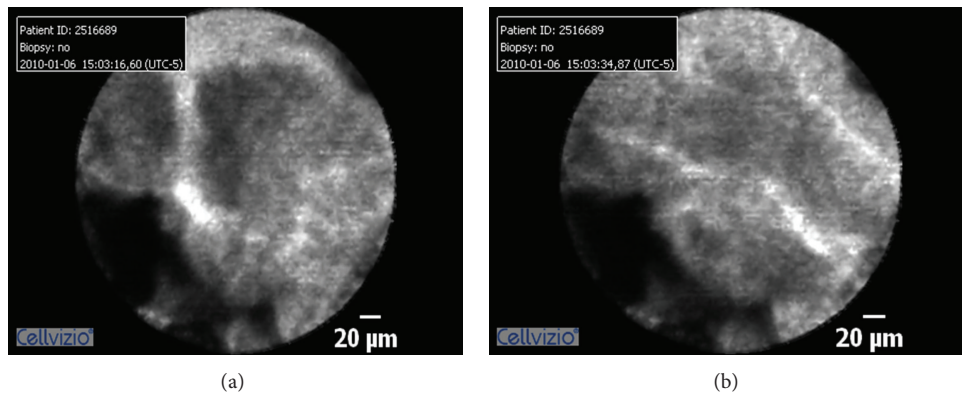
Figure 2: Normal appearing bile duct with fine, reticular pattern.

5. Studies

Few studies have evaluated the role of pCLE in evaluating pancreaticobiliary strictures (Table 3). Shieh et al. used the GastroFlex miniprobe for CBD evaluation and noted that cellular architecture was better visualized using this probe as compared to the CholangioFlex probe with no major side effects [13]. Giovannini et al. used the Cholangioflex probe in 37 patients who had ERCP for bile duct stones or stenosis and interpreted images in 33 [15]. Their study predicted an accuracy of 86%, sensitivity of 83%, and specificity of 75% compared to routine biopsies with respective values of 53%, 65%, and 53%. Meining et al. conducted a multicenter study in 89 patients with indeterminate biliary strictures using the CholangioFlex probe with a one-month followup after the procedure [19]. They were able to predict malignancy in 40 patients that was subsequently confirmed on followup. pCLE had a sensitivity of 98%, specificity of 67%, and accuracy of 81% as compared to 45%, 100%, and 75%, respectively, for index pathology. Accuracy for combination of ERCP and pCLE was also significantly higher compared with ERCP and tissue acquisition (90% versus 73%). Also of interest, there was no improvement in pCLE diagnostic accuracy during

the course of the study suggesting a short learning curve. Loeser et al. evaluated a smaller sample of 14 patients with indeterminate strictures of bile ducts using both the Cholangioflex and occasionally the GastroFlex probes [14]. They pointed to a normal reticular network pattern in benign lesions and comparison was made to multiphoton reconstructions of intact rat bile ducts [16]. The similarly observed reticular pattern corresponded to lymphatic structures, and presumably distortion of this pattern could be occurring in malignancy. Other criteria such as dilated blood vessels were not specific as they were observed in both benign and malignant strictures such that the negative predictive value suggests ruling out a malignancy.

6. Limitations and Promising Role

These studies shed light on the emerging role of pCLE for evaluation of indeterminate biliary strictures although limited by small sample size and specific population subsets. The diagnostic criteria are still evolving, and the exact anatomic correlates that result in the observed "abnormal" features remain undefined. One might speculate that white bands

TABLE 3: Relevant studies for pCLE of the biliary system [11].

Study (year)	Number of patients	Number malignant	Specificity	Sensitivity	Accuracy
Meining et al. [12] (2008)	14	6	88	83	86
Shieh et al. [13] (2012)	11	NA	NA	NA	NA
Loeser et al. [14] (2011)	14	6	NA	NA	NA
Giovannini et al. [15] (2011)	37	23	75	83	86
Meining et al. [19] (2011)	89	40	67	98	81

(a)

(b)
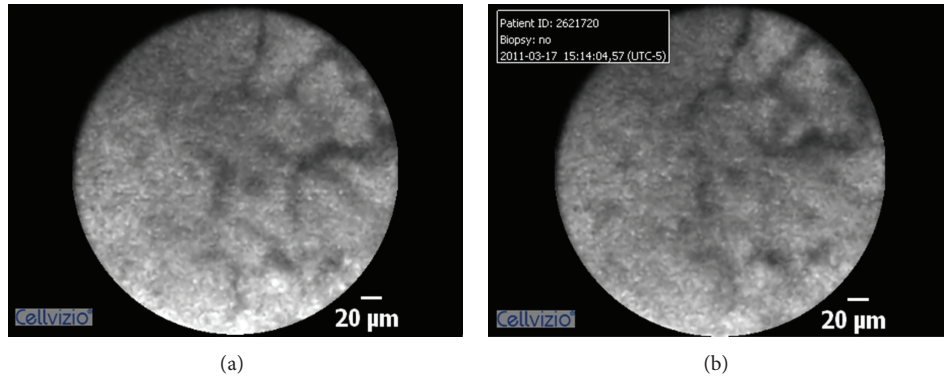
FIGURE 3: Normal appearing bile duct and reticular pattern.

(a)

(b)

(c)
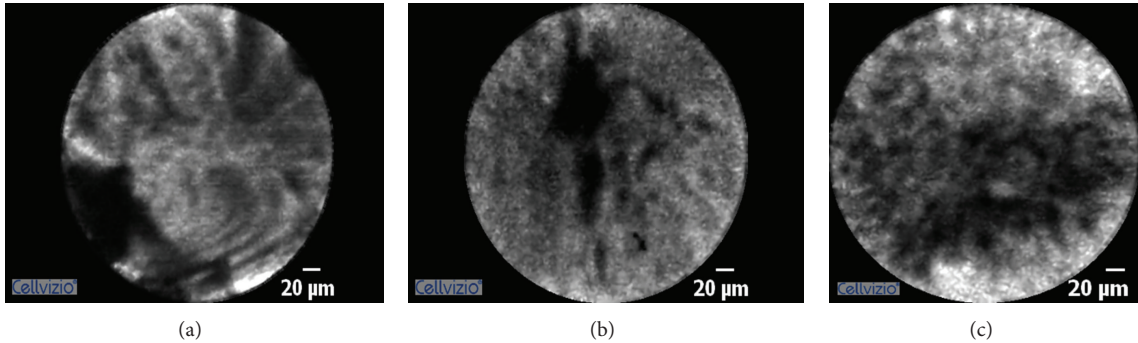
FIGURE 4: Biliary malignancy showing features of dark irregular structures, thick bands >20 μm, tortuous dilated blood vessels, and areas of dark clumps.

reflect blood vessels and increased neovascularization. Black bands could resemble lymphatic vessels, and the "clumps-" like structures correspond to tissue proliferation patterns, or these could mirror a paraneoplastic phenomenon. Observations such as the mucosal band and clump thickness are visual estimates and therefore subject to interpreter error. Also it is yet not clear which of these findings are specific to biliary versus pancreatic malignancies. In many of these studies, the endoscopists were aware of the clinical history and ERCP/CT or MRI findings while interpreting the imaging resulting in an interpreter bias. In a recent multicenter study, twenty-five deidentified pCLE video clips of indeterminate biliary strictures were sent to 6 observers at 5 institutions. Using the Miami Classification for standard image interpretation, they concluded that overall interobserver agreement with Kappa scores was poor to fair [20]. Further, the choice of

optimal access delivery catheter versus cholangioscopic is still not clear and needs to be investigated, as well as the difference between using a larger diameter probe (Gastroflex) from the miniprobe (Cholangioflex) keeping in mind the respective spatial resolution and image quality. These factors may be important while manipulating and targeting those challenging malignant lesions in the bile duct especially when growth occurs longitudinally along the wall rather than an intraluminal ingrowth manner. The cost effectiveness of pCLE is yet to be determined as it is not clear whether this tool is sufficient enough to replace histology. Nevertheless, it could prevent repeated endoscopic evaluations with attempt at biopsies in indeterminate cases. The possibilities of use during laparoscopy or laparotomy identifying disease-free margins are other potential areas where pCLE might play an expanding role.

(a)   (b)
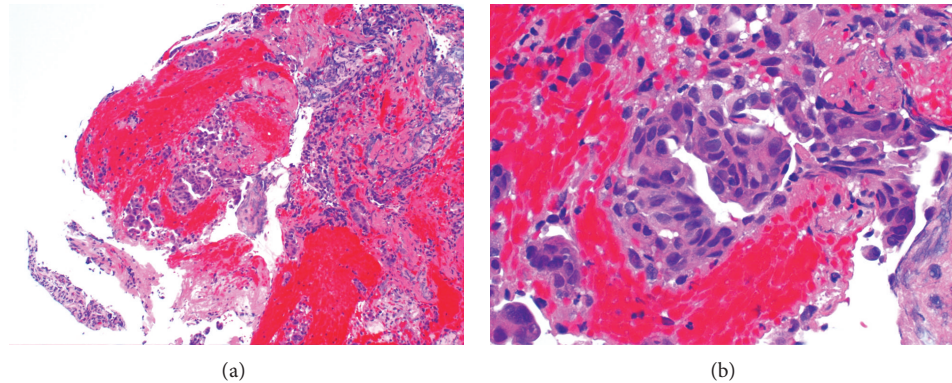
Figure 5: Cytopathology images of malignant biliary strictures (a) 10x resolution and (b) 40x resolution.

7. Future

Clearly, further studies are needed before pCLE is adopted as an integral technique for evaluation of pancreaticobiliary disease. Future studies should focus on prospective validating while defining one or more specific criteria for pancreaticobiliary disorders ranging from normal to inflammatory, early neoplastic, to disease specific such as cholangiocarcinomas, gallbladder malignancies, infiltrative pancreatic cancers, and primary-sclerosing-cholangitis-(PSC-) related tumors. Modification of probes for better image stability and resolution will be technical innovative challenge. Use of EUS-guided FNA needles is being studied and could potentially help to reach territories such as pancreatic cysts. Molecular imaging using fluorescent-tagged peptides developed from bacteriophage libraries selective to biliary tissues focuses on newer areas of research [21]. These peptides could then be detected by CLE and differentiate between benign and dysplastic/neoplastic tissues.

8. Conclusions

The newer endoscopic imaging modality of CLE has kindled an interest in the field of advanced imaging offering real-time histopathologic evaluation of the pancreaticobiliary system. It has strengthened and extended the arm of the gastroenterologist from a therapeutic endoscopist to an endopathologist. The novel use of this technique is particularly of significance in differentiating indeterminate biliary strictures as treatment depends on an accurate and prompt diagnosis. More studies will ultimately determine its precise role in the immediate or long-term impact as well in combination with available modalities in the treatment of pancreaticobiliary disorders.

References

[1] D. Uhlmann, M. Wiedmann, F. Schmidt et al., "Management and outcome in patients with Klatskin-mimicking lesions of the biliary tree," *Journal of Gastrointestinal Surgery*, vol. 10, no. 8, pp. 1144–1150, 2006.

[2] J. J. Bennett and R. H. Green, "Malignant masquerade: dilemmas in diagnosing biliary obstruction," *Surgical Oncology Clinics of North America*, vol. 18, no. 2, pp. 207–214, 2009.

[3] T. Ponchon, P. Gagnon, F. Berger et al., "Value of endobiliary brush cytology and biopsies for the diagnosis of malignant bile duct stenosis: results of a prospective study," *Gastrointestinal Endoscopy*, vol. 42, no. 6, pp. 565–572, 1995.

[4] R. Schoefl, M. Haefner, F. Wrba et al., "Forceps biopsy and brush cytology during endoscopic retrograde cholangiopancreatography for the diagnosis of biliary stenoses," *Scandinavian Journal of Gastroenterology*, vol. 32, no. 4, pp. 363–368, 1997.

[5] T. Rösch, K. Hofrichter, E. Frimberger et al., "ERCP or EUS for tissue diagnosis of biliary strictures? A prospective comparative study," *Gastrointestinal Endoscopy*, vol. 60, no. 3, pp. 390–396, 2004.

[6] A. Weber, R. M. Schmid, and C. Prinz, "Diagnostic approaches for cholangiocarcinoma," *World Journal of Gastroenterology*, vol. 14, no. 26, pp. 4131–4136, 2008.

[7] D. J. Hartman, A. Slivka, D. A. Giusto, and A. M. Krasinskas, "Tissue yield and diagnostic efficacy of fluoroscopic and cholangioscopic techniques to assess indeterminate biliary strictures," *Clinical Gastroenterology and Hepatology*, vol. 10, no. 9, pp. 1042–1046, 2012.

[8] A. Meining, D. Saur, M. Bajbouj et al., "In vivo histopathology for detection of gastrointestinal neoplasia with a portable, confocal miniprobe: an examiner blinded analysis," *Clinical Gastroenterology and Hepatology*, vol. 5, no. 11, pp. 1261–1267, 2007.

[9] V. Becker, T. Vercauteren, C. H. von Weyhern, C. Prinz, R. M. Schmid, and A. Meining, "High-resolution miniprobe-based confocal microscopy in combination with video mosaicing (with video)," *Gastrointestinal Endoscopy*, vol. 66, no. 5, pp. 1001–1007, 2007.

[10] M. B. Wallace, A. Meining, M. I. Canto et al., "The safety of intravenous fluorescein for confocal laser endomicroscopy in the gastrointestinal tract," *Alimentary Pharmacology and Therapeutics*, vol. 31, no. 5, pp. 548–552, 2010.

[11] I. Smith, P. E. Kline, M. Gaidhane, and M. Kahaleh, "A review on the use of confocal laser endomicroscopy in the bile duct," *Gastroenterology Research and Practice*, vol. 2012, Article ID 454717, 5 pages, 2012.

[12] A. Meining, E. Frimberger, V. Becker et al., "Detection of cholangiocarcinoma in vivo using miniprobe-based confocal fluorescence microscopy," *Clinical Gastroenterology and Hepatology*, vol. 6, no. 9, pp. 1057–1060, 2008.

[13] F. K. Shieh, H. Drumm, M. H. Nathanson, and P. A. Jamidar, "High-definition confocal endomicroscopy of the common bile duct," *Journal of Clinical Gastroenterology*, vol. 46, no. 5, pp. 401–406, 2012.

[14] C. S. Loeser, M. E. Robert, A. Mennone, M. H. Nathanson, and P. Jamidar, "Confocal endomicroscopic examination of malignant biliary strictures and histologic correlation with lymphatics," *Journal of Clinical Gastroenterology*, vol. 45, no. 3, pp. 246–252, 2011.

[15] M. Giovannini, E. Bories, G. Monges, C. Pesenti, F. Caillol, and J. R. Delpero, "Results of a phase I-II study on intraductal confocal microscopy (IDCM) in patients with common bile duct (CBD) stenosis," *Surgical Endoscopy*, vol. 25, no. 7, pp. 2247–2253, 2011.

[16] M. O. Othman and M. B. Wallace, "Confocal laser endomicroscopy: is it prime time?" *Journal of Clinical Gastroenterology*, vol. 45, no. 3, pp. 205–206, 2011.

[17] M. Wallace, G. Y. Lauwers, Y. Chen et al., "Miami classification for probe-based confocal laser endomicroscopy," *Endoscopy*, vol. 43, no. 10, pp. 882–891, 2011.

[18] A. Meining, R. J. Shah, A. Slivka et al., "Classification of probe-based confocal laser endomicroscopy findings in pancreaticobiliary strictures," *Endoscopy*, vol. 44, no. 3, pp. 251–257, 2012.

[19] A. Meining, Y. K. Chen, D. Pleskow et al., "Direct visualization of indeterminate pancreaticobiliary strictures with probe-based confocal laser endomicroscopy: a multicenter experience," *Gastrointestinal Endoscopy*, vol. 74, no. 5, pp. 961–968, 2011.

[20] J. P. Talreja, A. Sethi, P. A. Jamidar et al., "Interpretation of probe-based confocal laser endomicroscopy of indeterminate biliary strictures: is there any interobserver agreement?" *Digestive Diseases and Sciences*, vol. 57, no. 12, pp. 3299–3302, 2012.

[21] P. L. Hsiung, J. Hardy, S. Friedland et al., "Detection of colonic dysplasia in vivo using a targeted heptapeptide and confocal microendoscopy," *Nature Medicine*, vol. 14, no. 5, pp. 454–458, 2008.

Research Article

Endomicroscopic Imaging of COX-2 Activity in Murine Sporadic and Colitis-Associated Colorectal Cancer

Sebastian Foersch, Clemens Neufert, Markus F. Neurath, and Maximilian J. Waldner

Department of Medicine 1, University of Erlangen-Nuremberg, Ulmenweg 18, 91054 Erlangen, Germany

Correspondence should be addressed to Maximilian J. Waldner; maximilian.waldner@uk-erlangen.de

Although several studies propose a chemopreventive effect of aspirin for colorectal cancer (CRC) development, the general use of aspirin cannot be recommended due to its adverse side effects. As the protective effect of aspirin has been associated with an increased expression of COX-2, molecular imaging of COX-2, for instance, during confocal endomicroscopy could enable the identification of patients who would possibly benefit from aspirin treatment. In this pilot trial, we used a COX-2-specific fluorescent probe for detection of colitis-associated and sporadic CRC in mice using confocal microscopy. Following the injection of the COX-2 probe into tumor-bearing APCmin mice or mice exposed to the AOM + DSS model of colitis-associated cancer, the tumor-specific upregulation of COX-2 could be validated with in vivo fluorescence imaging. Subsequent confocal imaging of tumor tissue showed an increased number of COX-2 expressing cells when compared to the normal mucosa of healthy controls. COX-2-expression was detectable with subcellular resolution in tumor cells and infiltrating stroma cells. These findings pose a proof of concept and suggest the use of CLE for the detection of COX-2 expression during colorectal cancer surveillance endoscopy. This could improve early detection and stratification of chemoprevention in patients with CRC.

1. Introduction

A growing amount of evidence highlights the role of the acetylsalicylate aspirin for the chemoprevention of sporadic colorectal cancer (CRC) [1–4]. Similarly, aminosalicylates such as sulfasalazine, mesalazine, and others have been shown to reduce the risk for colitis-associated colorectal cancer (CAC) in patients with inflammatory bowel disease [5]. In addition, recent data also propose an improved outcome for patients treated with aspirin following the diagnosis of CRC [6]. This is of great importance, as colorectal neoplasia remains one of the leading causes of cancer-related morbidity and mortality in industrialized countries [7].

The effects of aspirin and aminosalicylates are largely attributed to the inhibition of cyclooxygenase-1 (COX-1) and -2. These enzymes convert arachidonic acid to prostaglandin PGH_2, a precursor molecule for various proinflammatory prostaglandins and eicosanoids. Especially COX-2 has been shown to be responsible for the tumor promoting effects, whereas COX-1 is involved in tissue homeostasis and platelet function [8]. In fact, COX-2 expression is elevated in almost

up to 90 percent of sporadic carcinomas and also 40 percent of colonic adenomas, while expression in healthy colonic epithelium remains low [9]. This was also confirmed in experimentally induced colon tumors in rodents [10].

These data propose the use of COX-inhibiting agents for the prevention of sporadic CRC and CAC. It can be achieved by reversible inhibition or irreversible acetylation of COX-1 and/or COX-2. However, the inhibition of COX enzymes is associated with severe side effects in treated patients [11]. In this regard, it would be helpful to quantify COX-2 activity in healthy, inflamed, or dysplastic colonic tissue in order to identify patients that could benefit from the treatment with COX inhibitors as a preventive or therapeutic strategy.

Today, surveillance endoscopy is the gold standard for the prevention of CRC. In addition to conventional endoscopy, technologic advances, such as confocal laser-scanning endomicroscopy (CLE), have recently equipped the gastroenterologist with the astounding possibility of histologic imaging of healthy and altered mucosa during ongoing examination [12, 13]. Importantly, several studies have proposed that CLE can be used for molecular imaging

(a)

(b)
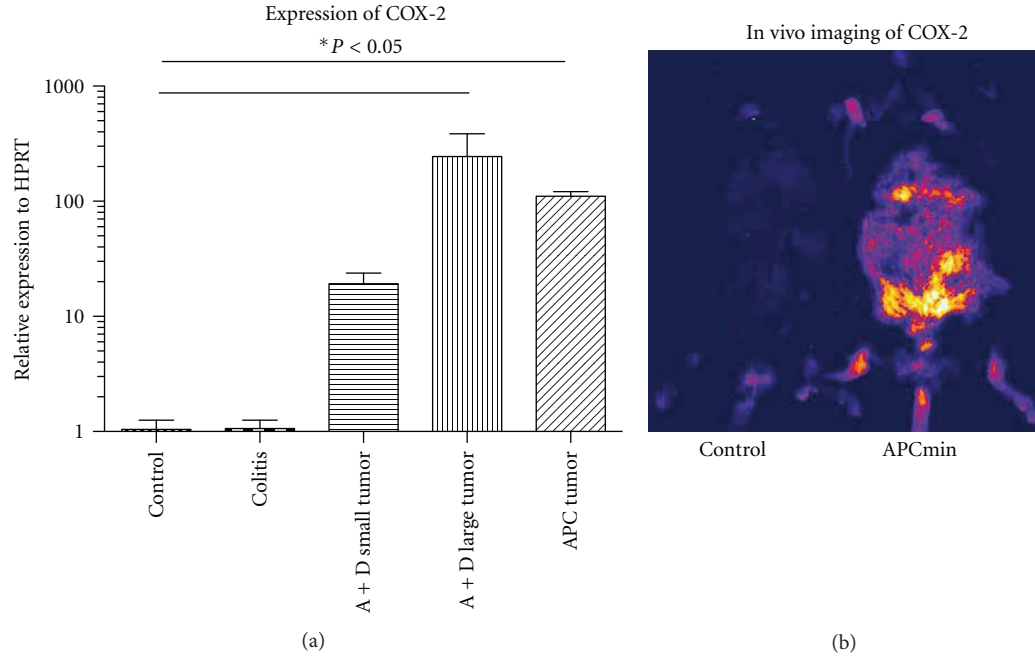
FIGURE 1: Expression of COX-2 in murine models of colitis, sporadic, and colitis-associated colorectal cancer. (a) Quantitative real-time PCR of COX-2 mRNA levels in control and inflamed colon tissue, small and large AOM + DSS induced tumors, and tumors of APCmin mice. Data are mean SEM. $N = 3$–5 per group. (b) Multispectral in vivo fluorescence imaging following the injection of a COX-2-specific fluorescence probe. One representative image of an APCmin mouse in comparison to a control animal is shown.

of the large intestine through the use of molecular-targeted fluorescence markers [14, 15]. As the selective visualization of COX-2 expression has recently been explored using a fluorescent probe [16], endomicroscopy of COX-2 expression seems to be a feasible approach.

In this first report, we evaluated the possibility of molecular targeted confocal imaging of COX-2 expression in murine models of colitis-associated and sporadic CRC. This was achieved after systemic injection of a fluorescent COX-2 probe, subsequent in vivo full-body fluorescence imaging and confocal microscopy of unprocessed tissue specimens. In correlation with COX-2 mRNA expression, in-vivo fluorescence imaging, and confocal microscopy showed a strong and specific signal of COX-2 in sporadic and colitis-associated CRC models. As the confocal imaging technique used in this study is also available for endomicroscopy of patients, the analysis of COX-2 expression during CLE could be an applicable and helpful tool for clinical decision-making.

2. Materials and Methods

2.1. Animals and Models of Sporadic CRC and CAC. Specific pathogen-free C57Bl/6 mice (8–12 weeks old) and APCmin mice were kept in individually ventilated cages and had free access to pellet food and tap-water. CAC was induced in C57Bl/6 mice as previously described [17]. In short, mice were injected with a single dose of the mutagenic agent azoxymethane (AOM) i.p. (7.5 mg/kg bodyweight), followed by three cycles of 2.0% dextran sodium sulfate (DSS) in drinking water and normal drinking water for 1 week. COX-2 expression was analyzed 9 weeks after AOM injection in

these animals and at the age of 10 weeks in untreated APCmin mice. These experiments were approved by the State Government of Middle Franconia and conducted according to institutional guidelines.

2.2. Imaging of COX-2 Activity. Untreated control mice, AOM + DSS treated mice, and APCmin mice were injected i.p. with a commercially available COX-2 probe (XenoLight RediJect COX-2 probe, Caliper) according to manufacturer guidelines. In vivo full body fluorescence imaging was performed 3 hours following the injection of the probe with a multispectral fluorescence-imaging device (Maestro, Caliper). 4 hours after the injection of the COX-2 probe, mice were sacrificed and healthy, inflamed or tumor tissue was dissected and kept in PBS for immediate confocal imaging without fixation of the tissue. Confocal imaging was performed with a commercial microscopy system (SP5, Leica) equipped with a 20x objective. Excitation of the fluorophore was achieved at 561 nm (DPSS laser), and emission was detected from 600 to 700 nm.

2.3. Quantitative Analysis of Gene Expression. Total RNA was isolated from healthy and inflamed colon tissue, APCmin, and AOM + DSS tumors using RNeasy columns (Qiagen). cDNA was generated with the iScript cDNA synthesis kit (Bio-Rad Laboratories). Quantitative real-time PCR analysis for COX-2 and HPRT was conducted with QuantiTect Primer assays (Qiagen) and QuantiTect Sybr Green (Qiagen). Gene expression was calculated relative to the house-keeping gene HPRT using the $\Delta\Delta Ct$ algorithm.

Unstained control | AOM + DSS colitis | APC tumor

(a) (b) (c)

Colon | AOM + DSS tumor | APC tumor magnification

(d) (e) (f)
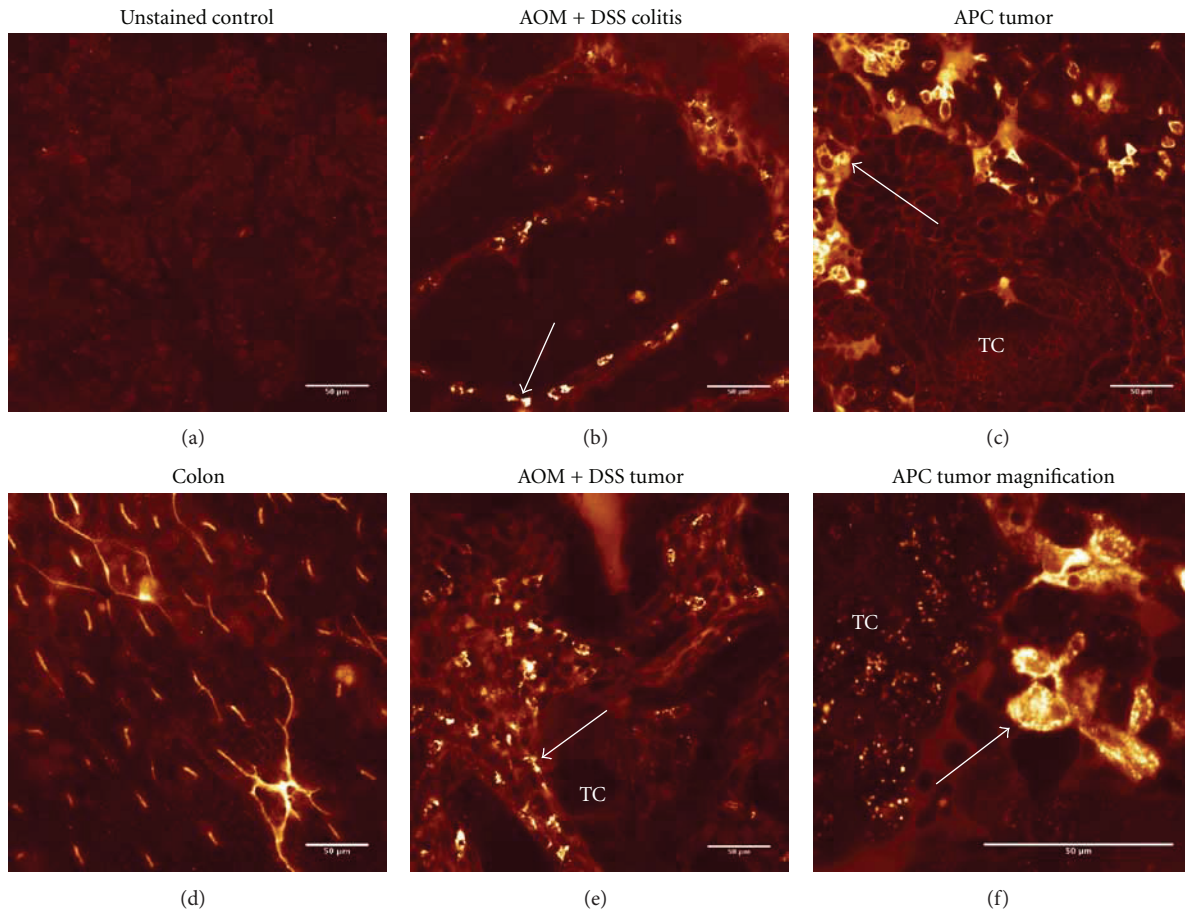
FIGURE 2: Confocal imaging of COX-2 expression. Confocal microscopy of COX-2 expression in unprocessed tissue specimens including healthy control tissue, inflamed colon tissue from AOM + DSS-treated animals and tumor tissue from AOM + DSS-treated animals and APCmin mice. The white bar represents 50 μm. The white arrows indicate individual cells in the stroma of inflamed colon or tumor tissue with high COX-2 expression. TC: tumor cells.

2.4. Statistical Analysis. Data from qPCR analysis were compared with the Kruskal-Wallis test followed by Dunn's test for nonparametric samples with GraphPad Prism v 5.00.

3. Results

In line with data from the literature, COX-2 expression was significantly increased in large tumors of AOM + DSS-treated mice or APC mice (Figure 1(a)). In contrast, COX-2 mRNA levels in the inflamed colon tissue of AOM + DSS-treated animals were comparable to control tissues.

In vivo full body fluorescence imaging of tumor-bearing mice following the injection of the COX-2 probe revealed a strong fluorescence in the lower abdominal region of these animals corresponding to the location of intestinal tumors of these mice (Figure 1(b)). Multispectral analysis of this signal verified the specific detection of the probe in comparison to autofluorescence.

Confocal imaging showed large amounts of infiltrating cells in the tumor stroma or at the tumor margin with a high COX-2 expression (Figure 2). Whereas nearly no COX-2 expressing cells were visible in healthy colon specimens, some COX-2 positive cells could be detected in the lamina propria of inflamed non-neoplastic colon tissue of AOM + DSS-treated mice. Interestingly, higher resolution imaging of tumor samples showed a weak expression of COX-2 in tumors epithelial cells in addition to the strong signal in stroma cells.

4. Discussion

Molecular imaging holds fascinating opportunities for the selective detection of specific cells and tissues by targeting unique markers of a particular disease of interest, such as inflammation or cancer. A potential target—in line with this basic concept—is COX-2 with a specific upregulation in premalignant and tumorous tissue and only very low expression in normal mucosa. In this preliminary, study we were able to specifically visualize high levels of COX-2 activity in mouse models of colitis-associated and sporadic CRC using confocal microscopy. Images obtained were comparable with immunohistology providing a subcellular resolution of COX-2 expression. Since endomicroscopy with similar scanners is already available for clinical application [18], molecular-targeted imaging of COX-2 could potentially be transferred into endoscopic routine.

In this regard, the endomicroscopic detection of COX-2 could serve two targets: (1) *the early detection of intestinal neoplasia and* (2) *a decision for chemoprevention.*

(1) Regarding the early detection of intestinal neoplasia, the molecular detection of COX-2 expression could be a helpful marker during endoscopy. Due to the specific upregulation of COX-2 in tumor tissue [9], targeted biopsies could be taken in areas that show an increased number of COX-2 positive cells. In fact, COX-2 expression has been shown to be upregulated not only in colorectal carcinoma, but also in early dysplastic lesions such as aberrant crypt foci or sporadic polyps [19–21]. Therefore, the analysis of COX-2 mRNA levels in feces has previously been proposed as a screening test for CRC [22]. However, large clinical trials further supporting the analysis of COX-2 expression as a predictive marker for CRC are missing so far. Of note, some subtypes of CRC, such as CRC with a defective mismatch repair (MMR) system, are not associated with an increased COX-2 expression and could be missed with COX-2-dependent screening tests [23].

(2) Despite the growing evidence supporting a chemopreventive effect of aspirin against CRC development, the general use of this therapeutic cannot be recommended due to the known side effects as discussed above. Interestingly, Chan et al. could show in a landmark study that the preventive effect of aspirin is only evident in patients that have an increased COX-2 expression [24]. Therefore, the endomicroscopic detection of COX-2 overexpression during surveillance endoscopy could identify patients with an increased risk for colorectal cancer development that could benefit from aspirin intake. As we have shown the technical feasibility for this approach in this paper, it would be interesting to evaluate this approach in a clinical study.

5. Conclusions

The data of this study clearly propose that molecular imaging of COX-2 expression in sporadic and colitis-associated cancer is possible with CLE. This technique could improve the detection of preneoplastic lesions during surveillance endoscopy or enable the identification of patients that would benefit from aspirin treatment as a preventive strategy against CRC development.

Acknowledgments

References

[1] J. A. Baron, B. F. Cole, R. S. Sandler et al., "A randomized trial of aspirin to prevent colorectal adenomas," *New England Journal of Medicine*, vol. 348, no. 10, pp. 891–899, 2003.

[2] J. A. Baron, "Aspirin and cancer: trials and observational studies," *Journal of the National Cancer Institute*, vol. 104, pp. 1199–1200, 2012.

[3] P. M. Rothwell, F. G. R. Fowkes, J. F. Belch, H. Ogawa, C. P. Warlow, and T. W. Meade, "Effect of daily aspirin on long-term risk of death due to cancer: analysis of individual patient data from randomised trials," *The Lancet*, vol. 377, no. 9759, pp. 31–41, 2011.

[4] P. A. Janne and R. J. Mayer, "Chemoprevention of colorectal cancer," *New England Journal of Medicine*, vol. 342, pp. 1960–1968, 2000.

[5] M. J. Waldner and M. F. Neurath, "Potential avenues for immunotherapy of colitis-associated neoplasia," *Immunotherapy*, vol. 4, pp. 397–405, 2012.

[6] E. Bastiaannet, K. Sampieri, O. M. Dekkers, A. J. de Craen, M. P. van Herk-Sukel, and V. Lemmens, "Use of aspirin postdiagnosis improves survival for colon cancer patients," *British Journal of Cancer*, vol. 106, pp. 1564–1570, 2012.

[7] R. Siegel, D. Naishadham, and A. Jemal, "Cancer statistics," *CA: A Cancer Journal for Clinicians*, vol. 62, pp. 10–29, 2012.

[8] S. D. Markowitz, "Aspirin and colon cancer—targeting prevention?" *New England Journal of Medicine*, vol. 356, no. 21, pp. 2195–2198, 2007.

[9] C. E. Eberhart, R. J. Coffey, A. Radhika, F. M. Giardiello, S. Ferrenbach, and R. N. Dubois, "Up-regulation of cyclooxygenase 2 gene expression in human colorectal adenomas and adenocarcinomas," *Gastroenterology*, vol. 107, no. 4, pp. 1183–1188, 1994.

[10] C. S. Williams, C. Luongo, A. Radhika et al., "Elevated cyclooxygenase-2 levels in Min mouse adenomas," *Gastroenterology*, vol. 111, no. 4, pp. 1134–1140, 1996.

[11] J. Cuzick, F. Otto, J. A. Baron et al., "Aspirin and nonsteroidal anti-inflammatory drugs for cancer prevention: an international consensus statement," *The Lancet Oncology*, vol. 10, no. 5, pp. 501–507, 2009.

[12] M. Goetz and R. Kiesslich, "Advances of endomicroscopy for gastrointestinal physiology and diseases," *American Journal of Physiology*, vol. 298, no. 6, pp. G797–G806, 2010.

[13] H. Neumann, R. Kiesslich, M. B. Wallace, and M. F. Neurath, "Confocal laser endomicroscopy: technical advances and clinical applications," *Gastroenterology*, vol. 139, no. 2, pp. 388–392, 2010.

[14] M. Goetz, A. Ziebart, S. Foersch et al., "In vivo molecular imaging of colorectal cancer with confocal endomicroscopy by targeting epidermal growth factor receptor," *Gastroenterology*, vol. 138, no. 2, pp. 435–446, 2010.

[15] S. Foersch, R. Kiesslich, M. J. Waldner, P. Delaney, P. R. Galle, and M. F. Neurath, "Molecular imaging of VEGF in gastrointestinal cancer in vivo using confocal laser endomicroscopy," *Gut*, vol. 59, pp. 1046–1055, 2010.

[16] M. J. Uddin, B. C. Crews, A. L. Blobaum et al., "Selective visualization of cyclooxygenase-2 in inflammation and cancer by targeted fluorescent imaging agents," *Cancer Research*, vol. 70, no. 9, pp. 3618–3627, 2010.

[17] C. Neufert, C. Becker, and M. F. Neurath, "An inducible mouse model of colon carcinogenesis for the analysis of sporadic and inflammation-driven tumor progression," *Nature Protocols*, vol. 2, no. 8, pp. 1998–2004, 2007.

[18] M. Goetz and T. D. Wang, "Molecular imaging in gastrointestinal endoscopy," *Gastroenterology*, vol. 138, no. 3, pp. 828–833, 2010.

[19] F. Mariani, P. Sena, L. Marzona et al., "Cyclooxygenase-2 and Hypoxia-Inducible Factor-1α protein expression is related to inflammation, and up-regulated since the early steps of colorectal carcinogenesis," *Cancer Letters*, vol. 279, no. 2, pp. 221–229, 2009.

[20] K. Tatsu, S. Hayashi, I. Shimada, and K. Matsui, "Cyclo-oxygenase-2 in sporadic colorectal polyps: immunohisto-chemical study and its importance in the early stages of colorectal tumorigenesis," *Pathology Research and Practice*, vol. 201, no. 6, pp. 427–433, 2005.

[21] K. M. Sheehan, F. O'Connell, A. O'Grady et al., "The relation-ship between cyclooxygenase-2 expression and characteristic of malignant transformation in human colorectal adenomas," *European Journal of Gastroenterology and Hepatology*, vol. 16, no. 6, pp. 619–625, 2004.

[22] S. Kanaoka, K. I. Yoshida, N. Miura, H. Sugimura, and M. Kajimura, "Potential usefulness of detecting cyclooxygenase 2 messenger RNA in feces for colorectal cancer screening," *Gastroenterology*, vol. 127, no. 2, pp. 422–427, 2004.

[23] A. Castells, A. Payá, C. Alenda et al., "Cyclooxygenase 2 expres-sion in colorectal cancer with DNA mismatch repair deficiency," *Clinical Cancer Research*, vol. 12, no. 6, pp. 1686–1692, 2006.

[24] A. T. Chan, S. Ogino, and C. S. Fuchs, "Aspirin and the risk of colorectal cancer in relation to the expression of COX-2," *New England Journal of Medicine*, vol. 356, no. 21, pp. 2131–2142, 2007.

Review Article

NBI and NBI Combined with Magnifying Colonoscopy

Mineo Iwatate,[1] Taro Ikumoto,[1] Santa Hattori,[1] Wataru Sano,[1] Yasushi Sano,[1] and Takahiro Fujimori[2]

[1] *Gastrointestinal Center, Sano Hospital, Kobe 655-0031, Japan*
[2] *Department of Surgical and Molecular Pathology, Dokkyo University School of Medicine, Tochigi, Japan*

Correspondence should be addressed to Mineo Iwatate, m.iwatate15@gmail.com

Although magnifying chromoendoscopy had been a reliable diagnostic tool, narrow-band imaging (NBI) has been developed in Japan since 1999 and has now replaced the major role of chromoendoscopy because of its convenience and simplicity. In this paper, we principally describe the efficacy of magnifying chromoendoscopy and magnifying colonoscopy with NBI for detection, histological prediction, estimation of the depth of early colorectal cancer, and future prospects. Although some meta-analyses have concluded that NBI is not superior to white light imaging for detection of adenomatous polyps in screening colonoscopy, NBI with magnification colonoscopy is useful for histological prediction, or for estimating the depth of invasion. To standardize these diagnostic strategies, we will focus on the NBI International Colorectal Endoscopic (NICE) classification proposed for use by endoscopists with or without a magnifying endoscope. However, more prospective research is needed to prove that this classification can be applied with satisfactory availability, feasibility, and reliability. In the future, NBI might contribute to the evaluation of real-time histological prediction during colonoscopy, which has substantial benefits for both reducing the risk of polypectomy and saving the cost of histological evaluation by resecting and discarding diminutive adenomatous polyps (resect and discard strategy).

1. Introduction

Narrow-band imaging (NBI) is a technique by which spectral features are modified by narrowing the band width of spectral transmittance using filters adjusted to the characteristics of hemoglobin absorption [1–3]. Diagnosis based on angiogenesis or vascular morphological change can be ideal for early detection and diagnosis of neoplastic lesions, as angiogenesis plays a critical role in the transition of premalignant lesions in a hyperproliferative state to a malignant phenotype [4–6]. By simply operating a button on the control panel of the endoscope, NBI yields a unique image that emphasizes the pattern of capillaries (vessels), as well as the surface of mucosal tissues. Because of its similarity to chromoendoscopy, NBI can be referred to as "optical/digital chromoendoscopy." The utility of NBI is enhanced when it is employed with a magnifying endoscope providing low- to high-power magnification (×80–100 maximum) utilizing a one-touch electrical power system [7].

This paper highlights the efficacy of magnifying chromoendoscopy and NBI colonoscopy with/without optical zoom magnification for diagnosis of colorectal lesions and discusses future perspectives.

2. Magnifying Chromoendoscopy

2.1. When and How to Use Magnifying Chromoendoscopy. Colorectal lesions are initially diagnosed by conventional-view colonoscopy, and then, if possible, by magnifying view and/or chromoendoscopy using indigo carmine. We routinely use a magnifying colonoscope because the insertion technique and manipulation are similar to those for an ordinary colonoscope [8]. In a prospective study, Konishi and colleagues reported that insertion of a magnifying colonoscope into the cecum was achieved successfully in 97% of cases, and that there were no significant differences in the average time taken to reach the cecum or the average total procedure time [9]. It might be argued that magnifying endoscopy is difficult to learn, and in fact Togashi et al. have reported that examination of 200 polyps was necessary in order to achieve a sensitivity rate of 90% for neoplastic lesions [10]. In 2012, Olympus Corp. produced a new
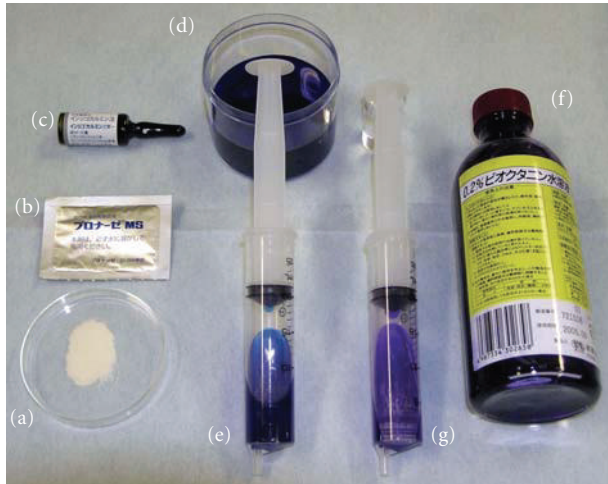
FIGURE 1: Preparations for magnifying observation. (a, b) Pronase MS. Washing of the target lesion surface can be done with 500 cc of lukewarm water containing a packet of Pronase MS (20000 U). (c) Indigo carmine (Daiichi Pharmaceutical Corp., Tokyo, Japan). (d) The dye is a blue stain that accentuates the contours of a lesion, providing a detailed view of its border and shape. The dye is used as a 0.1–0.4% aqueous solution. (e) This solution is flushed through the biopsy channel of the scope using a 20-cc syringe. Generally, 3–5 cc is delivered in 5 s along with 15 cc of air. (f) Crystal violet (Honzo Pharmaceutical Corp., Nagoya, Japan). The dye is a vital stain and is preferentially taken up by the Lieberkuhn gland openings (crypts), which appear as dots or pits. (g) A few small drops of crystal violet in 0.05% solution are applied using a nontraumatic catheter (Olympus 6233064; Olympus Optical Co., Ltd., Tokyo, Japan).

dual-focus endoscope capable of providing low- and medium-power optical magnification views (×45 maximum) automatically. It is anticipated that this endoscope will considerably shorten the learning period for magnifying endoscopy.

When a colonoscopist intends to perform chromoendoscopy, 3–5 mL of an aqueous solution of dye is sprayed onto the mucosa via the biopsy channel, along with 15 mL of air, using a 20-cc syringe. Common dyes used for characterization of the colorectum are indigo carmine as a contrast stain (0.1–0.4%), and crystal violet (0.05%) and methylene blue (0.1%) as absorptive stains. Although indigo carmine and methylene blue are often used to screen for sporadic adenoma, crystal violet, as an absorptive stain, offers advantages for patients with early invasive cancer or for detailed observation using a nontraumatic catheter after washing the lesion with lukewarm water containing pronase (Pronase MS) (Figures 1 and 2) [11].

Is it advisable to spray dye over the whole of the colon and rectum to identify significant lesions? When should magnification be employed? Certainly, pan-mucosal chromoendoscopy significantly increases the rate of detection of small neoplastic and flat lesions, but this technique requires an excessive volume of dye and a significantly prolonged procedure [12–16]. Therefore, colonoscopists use "selective" chromoendoscopy only for further examination of any subtle
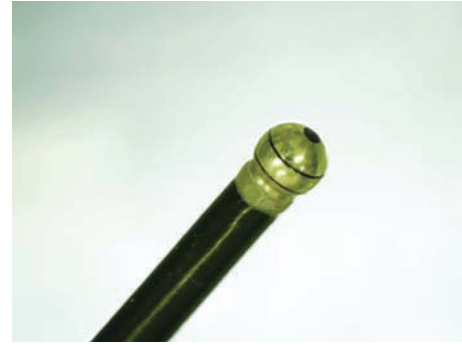
FIGURE 2: Nontraumatic, globular-tip catheter. This catheter is used to remove mucus and to drop crystal violet solution onto the lesion. Better positioning for magnifying observation can be obtained by pushing and holding the surrounding mucosa.

mucosal irregularity detected during standard colonoscopy. After a mucosal abnormality has been detected, target chromoendoscopy with magnification is indispensable for confirming the surface structure, perimeter shape, and mucosal crypt (pit) pattern of the lesion in detail (Figure 3).

2.2. Classification and Clinical Usefulness of Magnifying Chromoendoscopy. Kudo has proposed a gross classification of pit patterns into 7 types. It has been suggested that type I and II pit patterns are characteristic of nonneoplastic lesions such as normal mucosa or hyperplastic polyps. However, most lesions showing pattern types IIIS, IIIL, IV, and a subset of VI are intramucosal neoplastic lesions such as adenoma or intramucosal carcinoma. Lesions with a type VN pattern and a subset of type VI suggest deep invasive carcinoma (Figure 4) [7]. Because pit pattern classification is complicated for nonskilled endoscopists, Fujii et al. have modified it to a simpler form for clinical use. This clinical classification of pit patterns includes 3 types (nonneoplastic, noninvasive, and invasive) for which corresponding treatments are required (no treatment, endoscopic resection, and surgery, resp.) (Figure 5) [11, 17]. The precise definitions of these clinical pit patterns are as follows.

(1) *Invasive pattern*: irregular and distorted crypts in a demarcated area, as is evident in Kudo's type VN and selected cases of VI (e.g., deep submucosal invasive cancer).

(2) *Noninvasive pattern*: regular crypts with or without a demarcated area, or irregular pits without a demarcated area, as is evident in Kudo's type IIIS, IIIL, or IV, or selected cases of VI (e.g., adenomatous polyps and superficial submucosal invasive cancers).

(3) *Nonneoplastic pattern*: normal mucosa and star-shaped crypts, as is evident in Kudo's type I or II, respectively (e.g., hyperplastic, juvenile, and inflammatory polyps).

We have conducted a prospective study to examine whether magnification and/or indigo carmine dye-spraying is more reliable than the conventional view for distinguishing

(a)

(b)

(c)

(d)
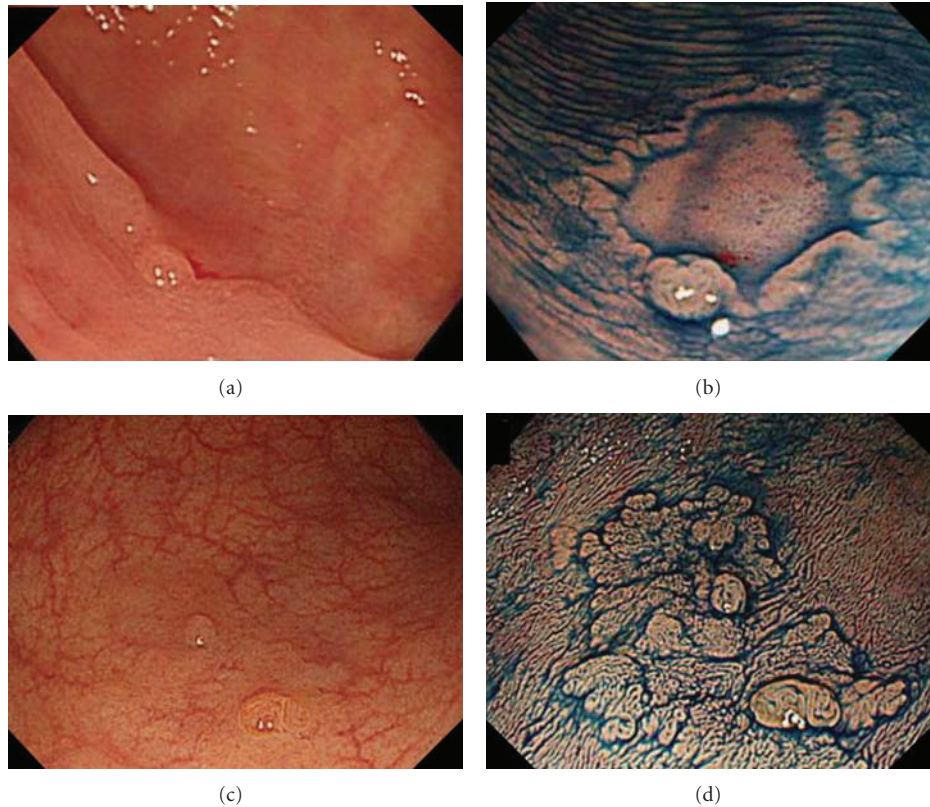
FIGURE 3: Usefulness of indigo carmine. (a) Disruption of the mucosal fold and a slightly reddish area are observed, but the whole lesion is unclear. (b) After spraying with indigo carmine dye, a 7 mm depressed lesion (0–II c) is identified clearly. (c) A slightly elevated lesion with an obscure superficial vascular component is evident, but the whole lesion is not recognized. (d) A slightly elevated lesion measuring 18 mm is obviously detected using indigo carmine.

nonneoplastic from neoplastic lesions of the colon and rectum [18]. The overall diagnostic accuracy of magnification in addition to chromoendoscopy using indigo carmine was 95.6%, being 10% and 5% more reliable than conventional endoscopy and chromoendoscopy, respectively. In addition, this method was significantly superior to conventional endoscopy and chromoendoscopy ($P < 0.0001$ and $P = 0.0152$).

Also, our recent large prospective series has demonstrated that the clinical classification of pit patterns (as invasive or noninvasive) is effective for differentiating intramucosal or sm superficial invasion ($<1000\,\mu$m) from sm deep invasion ($\geq 1000\,\mu$m). In that study, histopathology confirmed epithelial neoplasia in 99.4% of 4037 lesions with a noninvasive pattern, and confirmed deep sm invasion in 86.5% of 178 lesions with an invasive pattern [19]. Furthermore, the calculated sensitivity, specificity, positive predictive value, negative predictive value, and accuracy were 85.6%, 99.4%, 86.5%, 99.4%, and 98.8%, respectively.
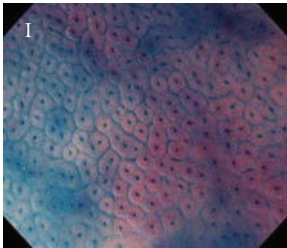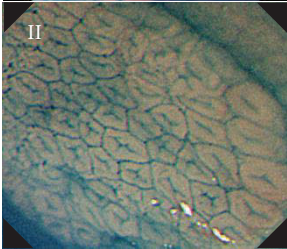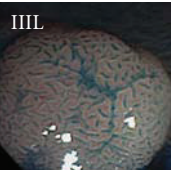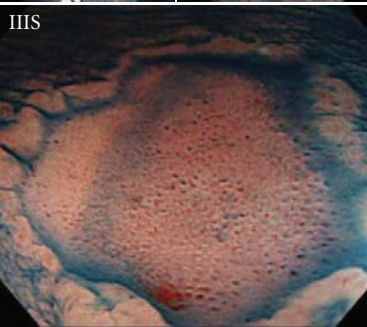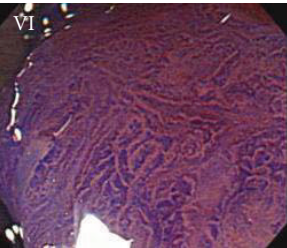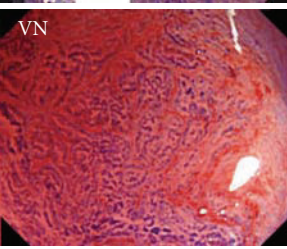
Therefore, based on these results, we are able to conclude that at present, a combination of magnifying colonoscopy and chromoendoscopy is the one of the most reliable methods for distinguishing nonneoplastic from neoplastic lesions, as well as for estimating the depth of early colorectal cancer.

3. Narrow-Band Imaging (NBI)

3.1. Detection. The colon and rectum are sites where neoplastic lesions occur most frequently. The National Polyp Study Group in the USA has reported that resection of all neoplastic polyps led to a 76–90% reduction in the incidence of colorectal cancer and a subsequent 53% reduction in mortality [22, 23]. Therefore, for prevention of colorectal cancer, it is important to find and resect neoplastic lesions as accurately as possible.

Neoplastic lesions are recognizable as a brownish area using NBI without magnification, which emphasizes neoplastic angiogenesis. Is NBI without magnification more useful for detecting neoplastic lesion than white light imaging (WLI)? Uraoka et al. have reported that NBI is superior to WLI ($P = 0.046$) for detection of flat and diminutive lesions [24]. However, Rex and Helbig have reported that there is no significant difference in the detection rate between NBI and WLI (65% versus 67% $P = 0.61$) [25]. Previous studies of the adenoma detection rate (ADR) have yielded conflicting results. Recently, to evaluate the ADR, Ikematsu et al. conducted a multicenter prospective trial in which 813 patients were randomized to a primary NBI group (NBI-WLI) and a primary WLI group (WLI-NBI) in the right-sided colon

	Clinical classification		
	Nonneoplastic pattern	Noninvasive pattern	Invasive pattern
Kudo's classification	I · II	IIIL · IIIS · IV · (part of VI)	VI · VN
Endoscopic findings			
Histology	Normal hyperplastic polyp	Adenoma *m **sm-slight	#sm-deep
Treatment	No treatment	Endoscopic treatment (polypectomy or EMR)	Surgical treatment

*Intramucosal cancer, **sm superficial invasion (<1000 μm), #sm deep invasion ($\geq$1000 μm).

FIGURE 4: Pit pattern classification and invasive pattern.

using the tandem method [26]. They found that the ADR for primary NBI and WLI was 42.3% and 42.5%, respectively, and the difference was not significant. Furthermore, three recent meta-analyses have concluded that NBI has no superiority to WLI in terms of ADR [27–29]. Therefore it can be concluded that the ADR for NBI is equivalent to that for WLI, and that both can be used equally effectively for screening colonoscopy.

3.2. Histological Prediction. In accordance with our previous investigations, the microvascular architecture (capillary pattern: CP) was classified into three types (CP types I, II, and III), and CP type III lesions were further classified into two groups: types IIIA and IIIB (Figure 6) [30–33]. Our observations demonstrated that assessment of CP by magnifying NBI is useful for differentiating small colorectal nonneoplastic from neoplastic polyps (accuracy 95.3%, sensitivity 96.4%, specificity 92.3%) and is highly accurate for distinguishing low-grade dysplasia from high-grade dysplasia/invasive cancer (accuracy 95.5%, sensitivity 90.3%, specificity 97.1%), and can thus be used to predict the histopathology of colorectal neoplasia [31, 32]. Because magnifying colonoscopy with NBI is convenient to use and as accurate as magnifying colonoscopy, we principally use only magnifying colonoscopy with NBI, and not chromoendoscopy, to distinguish neoplastic from nonneoplastic polyps during routine colonoscopy [34].

3.3. Estimation of the Depth of Early Colorectal Cancer. In Japan, there is growing evidence to support the theory that lesions with submucosal invasion limited to <1000 μm without lymphovascular involvement and a poorly differentiated component lack LN metastases [35–38] and can be cured by endoscopic resection alone. The Paris endoscopic classification of superficial neoplastic lesions has also determined 1000 μm to be the cutoff limit between sm1 and sm2 [39]. It is important to determine the vertical depth of invasion of submucosal colorectal cancers prior to endoscopic resection, because endoscopic resection of early colorectal cancer with massive submucosal invasion carries a high risk of bleeding and perforation.

Ikematsu and colleagues conducted a prospective study to determine whether CP type IIIA/IIIB identified by magnifying NBI was effective for estimating the depth of invasion in 130 early colorectal neoplasms [33]. These included 15 adenomas, 66 intramucosal cancers (pM), and 49 submucosal cancers (pSM): 16 pSM superficial (pSM1) and 33 pSM deep (pSM2-3) cancers. The sensitivity, specificity, and diagnostic accuracy of CP type III for differentiating pM-ca or pSM1 (<1000 μm) from pSM2-3 ($\geq$1000 μm) were 84.8%, 88.7%, and 87.7%, respectively. The accuracy of CP type IIIA (NPV) was 94.5% (86/91), and that for lesions of CP type IIIB (PPV) was 71.8% (29/39). In their study, the rate of diagnostic agreement among the three observers was good, without
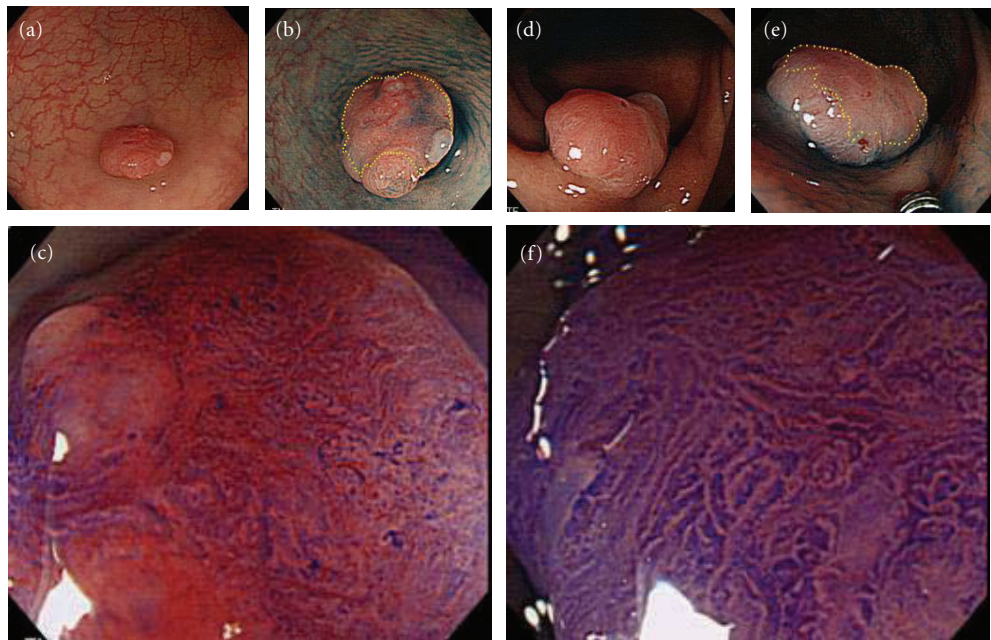
FIGURE 5: Cases of invasive pattern. (a) Endoscopic examination demonstrates a small (7 mm) flat elevated lesion in the sigmoid colon. (b) Chromoscopy with indigo carmine demonstrates a definite central depression. (c) Magnification with crystal violet staining demonstrates an invasive pattern in a demarcated area. Based on these findings, the tumor was diagnosed as an early colon cancer with deep submucosal invasion, and surgical resection was recommended. Histopathological examination of the resected specimen demonstrated well differentiated adenocarcinoma, invasive to the submucosa (sm deep; 4000 μm). (d) A sessile lesion Is(+IIc), 15 mm in diameter, identified in the upper rectum. (e) Chromoscopy with indigo carmine: reddish change and slight depression are observed on the surface of the tumor. (f) Magnification with crystal violet staining demonstrates an invasive pattern. Histopathological examination of the resected specimen demonstrated well differentiated adenocarcinoma (sm deep; 4500 μm).

Capillary pattern	Accuracy	Sensitivity	Specificity	PPV	NPV
Type I versus II [29]	95.3%	96.4%	92.3%	97.3%	90%
Type II versus III [30]	95.5%	90.3%	97.1%	90.3%	97.1%
Type IIIA versus IIIB [31]	87.7%	84.8%	88.7%	71.8%	94.5%
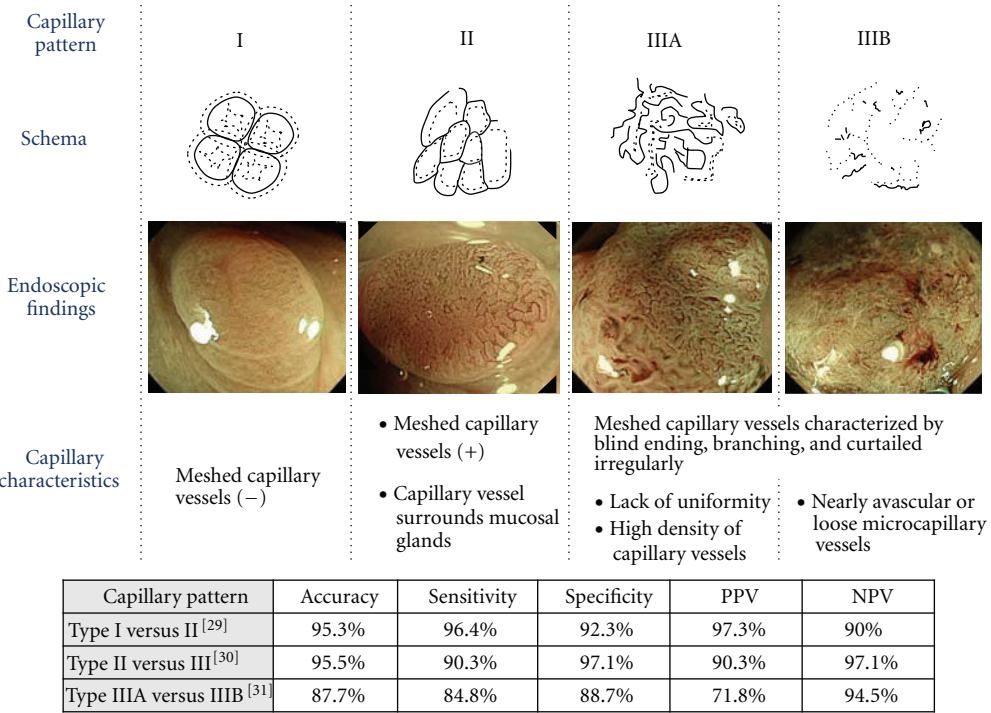
FIGURE 6: Capillary pattern (CP) classification and diagnostic ability (published data).

TABLE 1: Comparison of endoscopic diagnosis of the depth of submucosal deeply invasive colon cancer.

Diagnostic method	Number of adenoma, m-ca[#] sm-slight-ca[##]	Number of sm deep-ca[###]	Overall accuracy (%)	Sensitivity (%)	Specificity (%)	PPV (%)	NPV (%)
Magnifying chromoendoscopy (Invasive pattern)	4035	180	98.8	85.6	99.4	86.5	99.4
NBI with magnifying colonoscopy (capillary pattern classification)	97	33	87.7	84.8	88.7	71.8	94.5
Nonlifting sign	245	26	94.8	61.5	98.4	80.0	96.0

[#] Intramucosal cancer.
[##] sm slight invasive ($<1000\,\mu m$) cancer.
[###] sm deep invasive ($\geq 1000\,\mu m$) cancer.
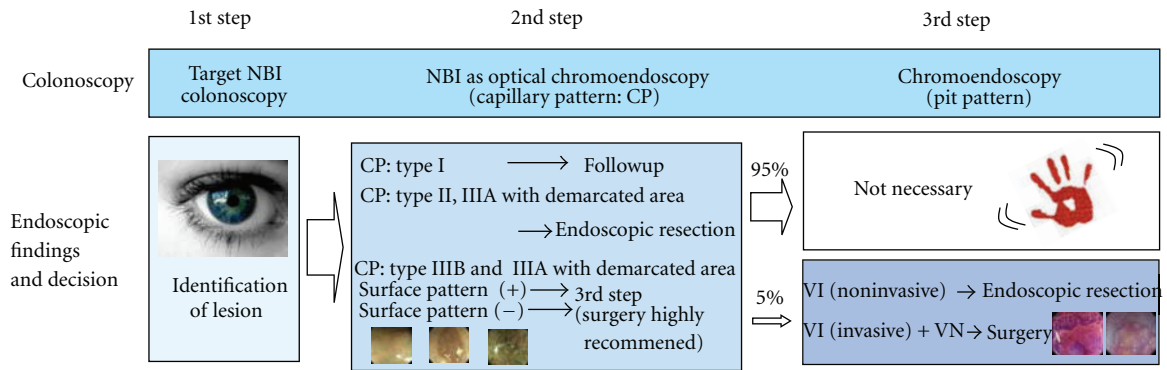
FIGURE 7: Modified 3-step strategy of NBI colonoscopy.

significant variability (interobserver variability: $\kappa = 0.68$, 0.67, 0.72; intraobserver agreement: $\kappa = 0.79, 0.76, 0.75$).

Submucosal saline injection is another useful method for estimating the depth of tumor invasion, not only when used for endoscopic mucosal resection (EMR) but also as a simple diagnostic tool for deeply invasive cancers. In Japan, Uno and Munakata were the first to propose the "nonlifting sign" in 1994, and considered it to be positive in cases where the surrounding mucosa, but not the lesion, was elevated [40]. Although adenoma and intramucosal cancer are easily lifted by submucosal injection of saline, deeply invasive cancer is not lifted because of the presence of a desmoplastic reaction and the invasive nature of the lesion (Table 1).

Considering the available evidence, we have suggested a three-step strategy for management of colorectal lesions using conventional colonoscopy, NBI colonoscopy, and chromoendoscopy (Figure 7). Chromoendoscopy is necessary in cases where deep invasion of the lesion into the submucosal layer is suspected, accounting for only 5% of all neoplastic lesions.

3.4. International Collaboration on NBI Observation of Colorectal Tumors: NBI International Colorectal Endoscopic (NICE) Classification. In 2011, we proposed an international classification system for conventional endoscopic observation assisted by NBI, and for applying this system to NBI magnifying observation (Table 2, Figure 8) [41]. When closely observing a colorectal lesion with the latest high-resolution electronic endoscope, the pit-like pattern on the surface is visible without the use of magnifying endoscopy. The use of NBI allows enhanced structural visualization, and hence the microvessels on the tumor surface can be observed in addition to the pit-like pattern. In Western countries, the magnifying endoscope is not widely used in clinical practice [42]. Even in Japan, use of the magnifying colonoscope in daily practice is still insufficiently widespread. Against this background, we have devised a simple system for categorical classification of colorectal tumors on the basis of NBI observation either with or without use of a magnifying endoscope (NBI International Colorectal Endoscopic [NICE] classification). We, along with endoscopists from Western countries, have reviewed the NICE classification system, and in 2012 some of our combined results were published in *Gastroenterology*, [43]. The NICE classification system is a simple categorical classification consisting of types 1–3 and based on three characteristics: (i) lesion color; (ii) microvascular architecture; and (iii) surface pattern. Type 1 is considered an index for hyperplastic lesions, type 2 an index for adenoma or mucosal/SM scanty invasive carcinoma, and type 3 an index for deeply SM-invasive carcinoma. To objectively verify the clinical usefulness of the NICE classification, an international collaborative effort has been launched by the Colon Tumor NBI Interest Group (CTNIG), whose members include Yasushi Sano (Japan), Shinji Tanaka (Japan), Douglas K. Rex (USA), Roy M. Soetikno (USA), Thierry Ponchon (France), and Brian P. Saunders (UK). The key advantage of

TABLE 2: NICE classification.

	Type 1	Type 2	Type 3
Color	Same or lighter than background	Browner relative to background (verify color arises from vessels)	Brown to dark brown relative to background; sometimes patchy whiter areas
Vessels	None, or isolated lacy vessels may be present coursing across the lesion	Brown vessels surrounding white structures**	Has area(s) of disrupted or missing vessels
Surface pattern	Dark or white spots of uniform size, or homogeneous absence of pattern	Oval, tubular or branched white structures** surrounded by brown vessels	Amorphous or absent surface pattern
Most likely pathology	Hyperplastic	Adenoma***	Deep submucosalinvasive cancer
Treatment	Followup	Polypectomy/EMR/ESD	Surgery

*Can be applied using colonoscopes with/without optical (zoom) magnification.
**These structures (regular or irregular) may represent the pits and the epithelium of the crypt opening.
***Type 2 consists of Vienna classification types 3, 4 and superficial 5 (all adenomas with either low or high grade dysplasia, or with superficial submucosal carcinoma). The presence of high grade dysplasia or superficial submucosal carcinoma may be suggested by an irregular vessel or surface pattern, and is often associated with atypical morphology (e.g., depressed area).

Typical endoscopic findings of NICE classification
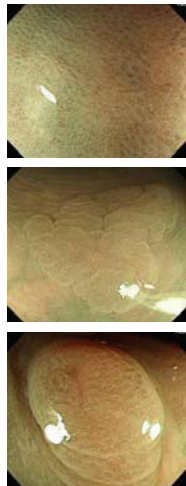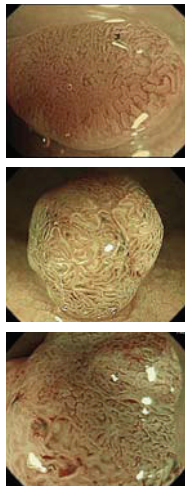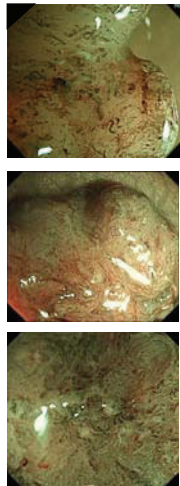
FIGURE 8: Figures to illustrate the NBI International Colorectal Endoscopic (NICE) classification.

the NICE classification is that it can be used by endoscopists without a magnifying endoscope. Some validation studies of the NICE classification have already been performed. Hewett et al. have reported that nonneoplastic and neoplastic lesions (NICE1 and NICE2) can be diagnostically differentiated in real time with high confidence by skilled endoscopists, achieving an accuracy of 89%, a sensitivity of 98%, and a negative predictive value of 95% [41]. In a study employing an endoscopic image library assessed by medical students, Nakayama et al. have confirmed that the NICE classification is valid for prediction of deep submucosal invasive carcinoma (NICE2 and NICE3). Diagnoses after teaching achieved an overall accuracy of 84.3% and an accuracy of 90.0%, high confidence being achieved for half of all cases examined [42].

Table 3 shows the relationship between the NICE classification and major NBI magnifying classifications used in Japan (Uraoka et al. [44, 45]/Hirata et al. [46]/Wada et al. [47] classification). As can be seen, the NICE classification has potential for use as a basic categorical classification of lesions demonstrated by NBI magnifying endoscopy. As a next step, we consider that it would be valuable to subclassify NICE type 2 lesions on the basis of features revealed by magnifying endoscopy to allow more detailed characterization of colorectal intramucosal tumors and scantily invasive carcinomas.

3.5. Resect and Discard Strategy. Resection of all adenomatous polyps during colonoscopy has been the world standard treatment since the National Polyp Study demonstrated that colonoscopic resection of all adenomatous polyps reduced both the incidence of and mortality due to colorectal cancer [22, 23]. Up to now, all polyps have been routinely retrieved

TABLE 3: NICE classification and Each NBI magnifying classification in Japan.

NICE clasification	Type 1	Type 2	Type 3
Sano classification	Type I	Type II~IIIA	Type IIIB
Hiroshima classification	Type A	Type B~C2	Type C3
Showa classification	Faint pattern	Dens/Network pattern irregular pattern	Sparse pattern

TABLE 4: Performance of NBI without magnification for real-time assessment with high diagnostic confidence.

HC rate	Accuracy	Sensitivity	Specificity	PPV	NPV
78%	92%	93%	88%	93%	82%
80%	95%	91%	93%	91%	95%

and submitted to pathology in view of the limited accuracy of conventional white light colonoscopy (59–84%) for differentiating neoplastic from nonneoplastic polyps [18, 34, 48–51]. Although magnifying chromoendoscopy using the pit pattern allows higher accuracy (85–96%) than conventional endoscopy or chromoendoscopy for differentiating polyps, the availability of both magnifying endoscopy and chromoendoscopy is unfortunately limited outside of Japan [18, 20, 50–52]. If it were possible to determine colorectal polyp pathology by endoscopy alone, recto-sigmoid hyperplastic polyps would be left *in situ* to reduce the risk of polypectomy, and small adenomas would be resected and then discarded to save the costs of histological evaluation. This concept, proposed in the UK and US, has been referred to as the "resect and discard" strategy, and has been limited to both diminutive (1–5 mm: US, UK) or small (6–9 mm: UK) polyps that appear histologically to have no malignant features and can be differentiated clinically with a high degree of confidence [21, 53]. Polyps for which diagnostic confidence is low are resected and sent for pathologic examination. The "resect and discard" strategy has considerable merits in terms of histology cost-saving and is thus expected to spread worldwide. However, discarding polyps without any histologic examination have an attendant risk of missing small invasive colorectal cancers that would normally be treated surgically. Kudo et al. reported that the frequency of small invasive cancers among all diminutive polyps (≤5 mm) was 0.16% (24/14892), and that macroscopically most of them were of the depressed type (22/24: 92%) [54]. Although such small invasive cancers are infrequent, they would be fatal if overlooked. Figure 9 shows two cases of small invasive colorectal cancer. In order to find small invasive cancers, it is important to detect any depressed area present in a lesion.

Currently, many endoscopic modalities are available, including NBI, autofluence imaging, Fuji Intelligent Chromo Endoscopy, i-scan, and so on. What kind of modality can best determine colorectal polyp pathology endoscopically? The American Society for Gastrointestinal Endoscopy (ASGE) has suggested that the necessary thresholds of endoscopic technology for accurate assessment of histology are >90% agreement in determining postpolypectomy surveillance intervals and a negative predictive value of ≥90% (when used with high confidence) for recto-sigmoid polyps with adenomatous histology [55]. Table 4 demonstrates the performance of NBI without magnification for real-time

assessment with high diagnostic confidence in the USA and UK [21, 53]. Both studies found that the accuracy was over 90%, but the the negative predictive value was 82% (<90%) in the UK and 95% in the USA. The lower negative predictive value in the UK study was explained by histological misclassification and loss or damage to polyps before histology. In both studies, the level of agreement in determining postpolypectomy surveillance intervals was over 90%. NBI might therefore become a useful modality for real-time assessment of the histology of diminutive polyps. Recently, Hewett et al. reported that use of NBI together with the NICE classification might also be useful, as the accuracy was 89% and the negative predictive value was 95% with high predictive value in real-time assessment [43]. However, more prospective research is needed to prove that this classification can be applied with satisfactory availability, feasibility, and reliability.

4. Summary

NBI with magnification colonoscopy is useful for histological prediction, and for estimating the depth of invasion of colorectal cancer. To standardize the diagnostic strategies currently available, the NICE classification would be helpful for endoscopists irrespective of whether they have access to magnifying endoscopy. However, more prospective research is needed to prove that this international classification can be applied with satisfactory availability, feasibility, and reliability. In the near future, NBI might make a valuable contribution to real-time histological prediction during colonoscopy, which would have substantial benefits for reducing both the risk of polypectomy and the costs of histological evaluation by allowing adenomatous polyps to be resected and discarded.

Conflict of Interests

The authors declare that they have no conflict of interests.

Disclosure

All authors have contributed significantly and are in agreement with the content of this paper.
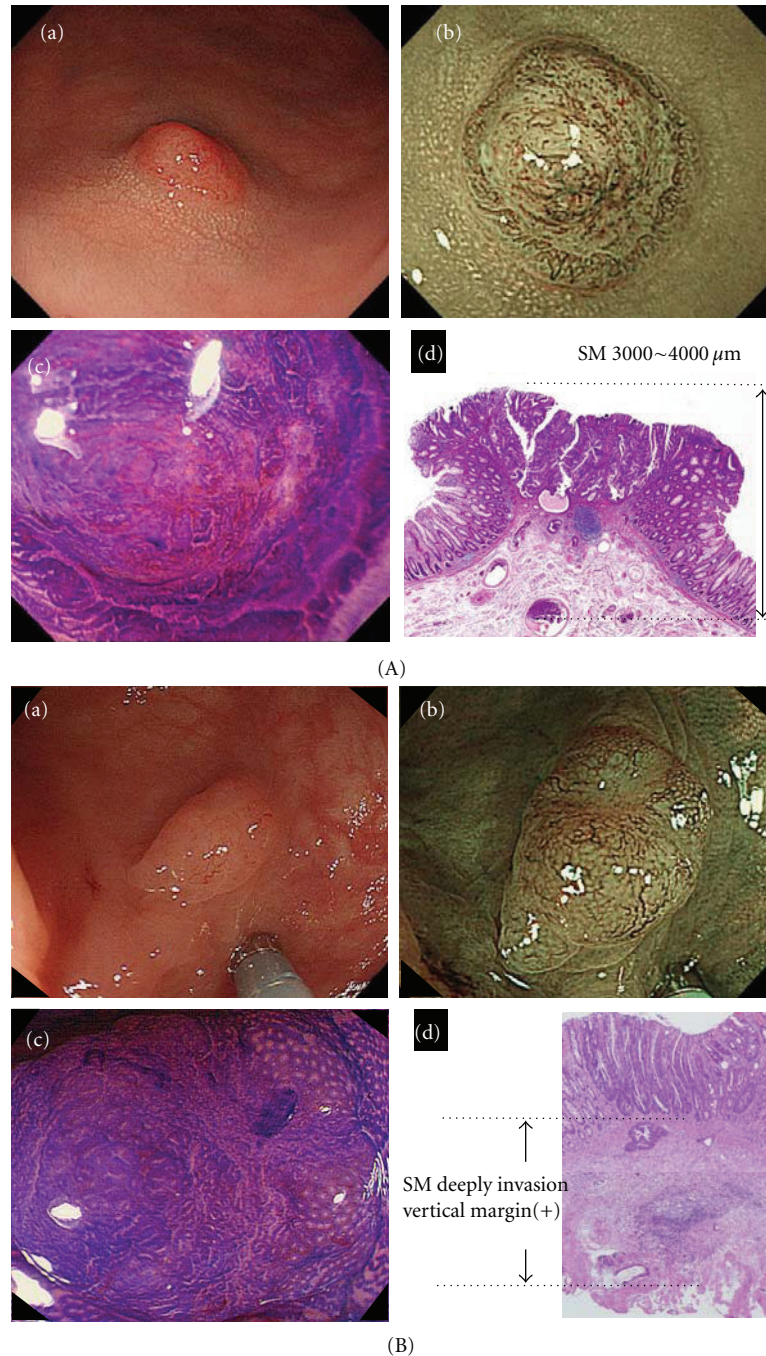
FIGURE 9: Two typical cases of small invasive colorectal cancer (≤5 mm). (A): (a) Conventional view: There is a small polyp (lesion size: 4 mm) located in the sigmoid colon. It is rather difficult to visualize any depressed area in this lesion. (b) NBI view: Magnification with NBI clearly demarcates the margin of the depressed area. The vascular pattern is capillary pattern Type III_B of the Sano classification, indicative of deep invasion into the submucosa. The center of the depressed area has a dome-like appearance, and the macroscopic type is "0-I s + II c", which requires attention in view of its frequent deep invasion into the submucosa. (c) Crystal violet view: magnification with crystal violet staining also demonstrates an invasive pattern and V_N pits, strongly indicative of deep submucosal invasion. We decided to treat this lesion surgically without endoscopic resection. (d) Pathological findings: well to moderately differentiated adenocarcinoma, pSM (3000–4000 μm), ly(+), v(-), pN0. (B): (a) Conventional view: there is a small polyp (lesion size: 5 mm) located in the descending colon. It is difficult to visualize any depressed area in this lesion. (b) NBI view: magnification with NBI clearly demonstrates a depressed area in the center of this lesion. The vascular pattern in the lesion center is capillary pattern Type III_B by the Sano classification, suggesting the possibility of invasive cancer. Crystal violet staining is therefore required. (c) Crystal violet view: magnification with crystal violet staining demonstrates an invasive pattern. Invasive cancer cannot be predicted with high confidence because the depressed area is small. This lesion was treated by endoscopic mucosal resection for initial diagnosis, and later the patient underwent surgery. (d) Pathological findings: well differentiated adenocarcinoma with scirrhous growth, pSM massive, VM(+), ly(+), EMR.

References

[1] Y. Sano, M. Kobayashi, Y. Hamamoto et al., "New diagnostic method based on color imaging using narrow band imaging (NBI) system for gastrointestinal tract," *Gastrointestinal Endoscopy*, vol. 53, p. AB125, 2001.

[2] K. Gono, K. Yamazaki, N. Doguchi et al., "Endoscopic observation of tissue by narrow-band illumination," *Optical Review*, vol. 10, pp. 1–5, 2003.

[3] K. Gono, T. Obi, M. Yamaguchi et al., "Appearance of enhanced tissue features in narrow-band endoscopic imaging," *Journal of Biomedical Optics*, vol. 9, no. 3, pp. 568–577, 2004.

[4] J. Folkman, "Tumor angiogenesis: therapeutic implications," *The New England Journal of Medicine*, vol. 285, no. 21, pp. 1182–1186, 1971.

[5] J. Folkman, K. Watson, D. Ingber, and D. Hanahan, "Induction of angiogenesis during the transition from hyperplasia to neoplasia," *Nature*, vol. 339, no. 6219, pp. 58–61, 1989.

[6] T. Aotake, C. D. Lu, Y. Chiba, R. Muraoka, and N. Tanigawa, "Changes of angiogenesis and tumor cell apoptosis during colorectal carcinogenesis," *Clinical Cancer Research*, vol. 5, no. 1, pp. 135–142, 1999.

[7] S. E. Kudo, S. Tamura, T. Nakajima, H. O. Yamano, H. Kusaka, and H. Watanabe, "Diagnosis of colorectal tumorous lesions by magnifying endoscopy," *Gastrointestinal Endoscopy*, vol. 44, no. 1, pp. 8–14, 1996.

[8] T. Tonooka, Y. Sano, T. Fujii et al., "Adenocarcinoma in solitary large hyperplastic polyp diagnosed by magnifying colonoscope: report of a case," *Diseases of the Colon and Rectum*, vol. 45, no. 10, pp. 1407–1411, 2002.

[9] K. Konishi, K. Kaneko, T. Kurahashi et al., "A comparison of magnifying and nonmagnifying colonoscopy for diagnosis of colorectal polyps: a prospective study," *Gastrointestinal Endoscopy*, vol. 57, no. 1, pp. 48–53, 2003.

[10] K. Togashi, F. Konishi, T. Ishizuka, T. Sato, S. Senba, and K. Kanazawa, "Efficacy of magnifying endoscopy in the differential diagnosis of neoplastic and non-neoplastic polyps of the large bowel," *Diseases of the Colon and Rectum*, vol. 42, no. 12, pp. 1602–1608, 1999.

[11] T. Fujii, R. T. Hasegawa, Y. Saitoh et al., "Chromoscopy during colonoscopy," *Endoscopy*, vol. 33, no. 12, pp. 1036–1041, 2001.

[12] A. Trecca, F. Gai, G. P. Di Lorenzo et al., "Conventional colonoscopy versus chromoendoscopy and magnifying endoscopy for the diagnosis of colorectal lesions: a comparative prospective study in 995 patients," *Chirurgia Italiana*, vol. 56, no. 1, pp. 31–36, 2004.

[13] R. Kiesslich, M. Von Bergh, M. Hahn, G. Hermann, and M. Jung, "Chromoendoscopy with indigocarmine improves the detection of adenomatous and nonadenomatous lesions in the colon," *Endoscopy*, vol. 33, no. 12, pp. 1001–1006, 2001.

[14] D. P. Hurlstone, S. S. Cross, R. Slater, D. S. Sanders, and S. Brown, "Detecting diminutive colorectal lesions at colonoscopy: a randomised controlled trial of pan-colonic versus targeted chromoscopy," *Gut*, vol. 53, no. 3, pp. 376–380, 2004.

[15] J. C. Brooker, B. P. Saunders, S. G. Shah et al., "Total colonic dye-spray increases the detection of diminutive adenomas during routine colonoscopy: a randomized controlled trial," *Gastrointestinal Endoscopy*, vol. 56, no. 3, pp. 333–338, 2002.

[16] H. Mitooka, T. Fujimori, S. Maeda, and K. Nagasako, "Minute flat depressed neoplastic lesions of the colon detected by contrast chromoscopy using an indigo carmine capsule," *Gastrointestinal Endoscopy*, vol. 41, no. 5, pp. 453–459, 1995.

[17] Y. Saito, F. Emura, T. Matsuda et al., "Letter to the editor: invasive pattern is an indication for surgical treatment," *Gut Letters*, March 2004.

[18] K. I. Fu, Y. Sano, S. Kato et al., "Chromoendoscopy using indigo carmine dye spraying with magnifying observation is the most reliable method for differential diagnosis between non-neoplastic and neoplastic colorectal lesions: a prospective study," *Endoscopy*, vol. 36, no. 12, pp. 1089–1093, 2004.

[19] T. Matsuda, T. Fujii, Y. Saito et al., "Efficacy of the invasive/non-invasive pattern by magnifying chromoendoscopy to estimate the depth of invasion of early colorectal neoplasms," *American Journal of Gastroenterology*, vol. 103, no. 11, pp. 2700–2706, 2008.

[20] K. Togashi and F. Konishi, "Magnification chromo-colonoscopy," *ANZ Journal of Surgery*, vol. 76, no. 12, pp. 1101–1105, 2006.

[21] A. Ignjatovic, J. E. East, N. Suzuki, M. Vance, T. Guenther, and B. P. Saunders, "Optical diagnosis of small colorectal polyps at routine colonoscopy (Detect InSpect ChAracterise Resect and Discard; DISCARD trial): a prospective cohort study," *The Lancet Oncology*, vol. 10, no. 12, pp. 1171–1178, 2009.

[22] S. J. Winawer, A. G. Zauber, M. N. Ho et al., "Prevention of colorectal cancer by colonoscopic polypectomy. The National Polyp Study Workgroup," *The New England Journal of Medicine*, vol. 329, pp. 1977–1981, 1993.

[23] A. G. Zauber, S. J. Winawer, M. J. O'Brien et al., "Colonoscopic polypectomy and long-term prevention of colorectal-cancer deaths," *The New England Journal of Medicine*, vol. 366, pp. 687–696, 2012.

[24] T. Uraoka, Y. Saito, T. Matsuda et al., "Detectability of colorectal neoplastic lesions using a narrow-band imaging system: a pilot study," *Journal of Gastroenterology and Hepatology*, vol. 23, no. 12, pp. 1810–1815, 2008.

[25] D. K. Rex and C. C. Helbig, "High yields of small and flat adenomas with high-definition colonoscopes using either white light or narrow band imaging," *Gastroenterology*, vol. 133, no. 1, pp. 42–47, 2007.

[26] H. Ikematsu, Y. Saito, K. Kaneko et al., "The impact of narrow band imaging for colon polyp detection: a multicenter randomized controlled trial by tandem colonoscopy," *Journal of Gastroenterology*, vol. 47, no. 10, pp. 1099–1107, 2012.

[27] L. C. Sabbagh, L. Reveiz, S. de Aguiar et al., "Narrow-band imaging does not improve detection of colorectal polyps when compared to conventional colonoscopy: a randomized controlled trial and meta-analysis of published studies," *BMC Gastroenterology*, vol. 11, p. 100, 2011.

[28] S. F. Pasha, J. A. Leighton, V. K. Sharma et al., "Comparison of the yield and miss rate of narrow band imaging and white light endoscopy in patients undergoing screening or suveillance colonoscopy: a meta-analysis," *The American Journal of Gastroenterology*, vol. 107, pp. 363–370, 2012.

[29] A. Nagorni, G. Bjelakovic, and B. Petrovic, "Narrow band imaging versus conventional white light colonoscopy for the detection of colorectal polyps," *Cochrane Database of Systematic Reviews*. In press.

[30] Y. Sano, F. Emura, and H. Ikematsu, "Narrow band imaging," in *Colonoscopy: Principles and Practice*, J. Waye, D. Rex, and C. Williams, Eds., pp. 514–526, Blackwell, Oxford, UK, 2009.

[31] Y. Sano, H. Ikematsu, K. I. Fu et al., "Meshed capillary vessels by use of narrow-band imaging for differential diagnosis of small colorectal polyps," *Gastrointestinal Endoscopy*, vol. 69, no. 2, pp. 278–283, 2009.

[32] A. Katagiri, K. I. Fu, Y. Sano et al., "Narrow band imaging with magnifying colonoscopy as diagnostic tool for predicting histology of early colorectal neoplasia," *Alimentary Pharmacology and Therapeutics*, vol. 27, no. 12, pp. 1269–1274, 2008.

[33] H. Ikematsu, T. Matsuda, F. Emura et al., "Efficacy of capillary pattern type IIIA/IIIB by magnifying narrow band imaging for

estimating depth of invasion of early colorectal neoplasms," *BMC Gastroenterology*, vol. 10, p. 33, 2010.

[34] H. Machida, Y. Sano, Y. Hamamoto et al., "Narrow-band imaging in the diagnosis of colorectal mucosal lesions: a pilot study," *Endoscopy*, vol. 36, no. 12, pp. 1094–1098, 2004.

[35] S. Tanaka, K. Haruma, C. R. Teixeira et al., "Endoscopic treatment of submucosal invasive colorectal carcinoma with special reference to risk factors for lymph node metastasis," *Journal of Gastroenterology*, vol. 30, no. 6, pp. 710–717, 1995.

[36] O. Tsuruta, A. Toyonaga, H. Ikeda, K. Tanikawa, and M. Morimatsu, "Clinicopathological study of superficial-type invasive carcinoma of the colorectum: special reference to lymph node metastasis," *International Journal of Oncology*, vol. 10, no. 5, pp. 1003–1008, 1997.

[37] M. Nishi and F. Moriyasu, "Clinicopathological study for reevaluation of the depth of submucosal invasion and histological classification of early colorectal cancer," *Japanese Journal of Gastroenterology*, vol. 99, no. 7, pp. 769–778, 2002.

[38] K. Kitajima, T. Fujimori, S. Fuji et al., "Correlations between lymph node metastasis and depth of submucosal invasion in submucosal invasive colorectal carcinoma: a Japanese collaborative study," *Journal of Gastroenterology*, vol. 39, no. 6, pp. 534–543, 2004.

[39] Participants in the Paris Workshop, "The Paris endoscopic classification of superficial neoplastic lesions: esophagus, stomach, and colon," *Gastrointestinal Endoscopy*, vol. 58, supplement 6, pp. S3–S43, 2002.

[40] Y. Uno and A. Munakata, "The non-lifting sign of invasive colon cancer," *Gastrointestinal Endoscopy*, vol. 40, no. 4, pp. 485–489, 1994.

[41] S. Tanaka and Y. Sano, "Aim to unify the narrow band imaging (NBI) magnifying classification for colorectal tumors: current status in Japan from a summary of the consensus symposium in the 79th annual meeting of the Japan gastroenterological endoscopy society," *Digestive Endoscopy*, vol. 23, supplement 1, pp. 131–139, 2011.

[42] Z. H. Henry, P. Yeaton, V. M. Shami et al., "Meshed capillary vessels found on narrow-band imaging without optical magnification effectively identifies colorectal neoplasia: a North American validation of the Japanese experience," *Gastrointestinal Endoscopy*, vol. 72, no. 1, pp. 118–126, 2010.

[43] D. G. Hewett, T. Kaltenbach, D. K. Rex et al., "Validation of a simple classification system for endoscopic diagnosis of small colorectal polyps using narrow-band imaging," *Gastroenterology*, vol. 143, no. 3, pp. 599–607, 2012.

[44] T. Uraoka, Y. Saito, H. Ikematsu, K. Yamamoto, and Y. Sano, "Sano's capillary pattern classification for narrow-band imaging of early colorectal lesions," *Digestive Endoscopy*, vol. 23, supplement 1, pp. 112–115, 2011.

[45] N. Kobayashi, Y. Saito, Y. Sano et al., "Determining the treatment strategy for colorectal neoplastic lesions: endoscopic assessment or the non-lifting sign for diagnosing invasion depth?" *Endoscopy*, vol. 39, no. 8, pp. 701–705, 2007.

[46] M. Hirata, S. Tanaka, S. Oka et al., "Evaluation of microvessels in colorectal tumors by narrow band imaging magnification," *Gastrointestinal Endoscopy*, vol. 66, no. 5, pp. 945–952, 2007.

[47] Y. Wada, S. E. Kudo, H. Kashida et al., "Diagnosis of colorectal lesions with the magnifying narrow-band imaging system," *Gastrointestinal Endoscopy*, vol. 70, no. 3, pp. 522–531, 2009.

[48] M. Y. Su, C. M. Hsu, Y. P. Ho, P. C. Chen, C. J. Lin, and C. T. Chiu, "Comparative study of conventional colonoscopy, chromoendoscopy, and narrow-band imaging systems in differential diagnosis of neoplastic and nonneoplastic colonic polyps," *American Journal of Gastroenterology*, vol. 101, no. 12, pp. 2711–2716, 2006.

[49] D. Apel, R. Jakobs, D. Schilling et al., "Accuracy of high-resolution chromoendoscopy in prediction of histologic findings in diminutive lesions of the rectosigmoid," *Gastrointestinal Endoscopy*, vol. 63, no. 6, pp. 824–828, 2006.

[50] J. J. W. Tischendorf, H. E. Wasmuth, A. Koch, H. Hecker, C. Trautwein, and R. Winograd, "Value of magnifying chromoendoscopy and narrow band imaging (NBI) in classifying colorectal polyps: a prospective controlled study," *Endoscopy*, vol. 39, no. 12, pp. 1092–1096, 2007.

[51] G. D. De Palma, M. Rega, S. Masone et al., "Conventional colonoscopy and magnified chromoendoscopy for the endoscopic histological prediction of diminutive colorectal polyps: a single operator study," *World Journal of Gastroenterology*, vol. 12, no. 15, pp. 2402–2405, 2006.

[52] K. Konishi, K. Kaneko, T. Kurahashi et al., "A comparison of magnifying and nonmagnifying colonoscopy for diagnosis of colorectal polyps: a prospective study," *Gastrointestinal Endoscopy*, vol. 57, no. 1, pp. 48–53, 2003.

[53] D. K. Rex, "Narrow-band imaging without optical magnification for histologic analysis of colorectal polyps," *Gastroenterology*, vol. 136, no. 4, pp. 1174–1181, 2009.

[54] S. Kudo, R. Lambert, P. D. Hurlstone et al., "Nonpolypoid neoplastic lesions of the colorectal mucosa," *Gastrointestinal Endoscopy*, vol. 68, pp. S3–S47, 2008.

[55] D. K. Rex, C. Kahi, M. O'Brien et al., "The American Society for Gastrointestinal Endoscopy PIVI (Preservation and Incorporation of Valuable Endoscopic Innovations) on real-time endoscopic assessment of the histology of diminutive colorectal polyps," *Gastrointestinal Endoscopy*, vol. 73, no. 3, pp. 419–422, 2011.

Clinical Study

Use of i-scan Endoscopic Image Enhancement Technology in Clinical Practice to Assist in Diagnostic and Therapeutic Endoscopy: A Case Series and Review of the Literature

Shawn Hancock,[1] Erik Bowman,[1] Jyothiprashanth Prabakaran,[1] Mark Benson,[1] Rashmi Agni,[2] Patrick Pfau,[1] Mark Reichelderfer,[1] Jennifer Weiss,[1] and Deepak Gopal[1]

[1] *Division of Gastroenterology and Hepatology, School of Medicine and Public Health, University of Wisconsin, 4th Floor, UWMF Centennial Building, 1685 Highland Avenue, Suite 4000, Madison, WI 53705-2281, USA*
[2] *Department of Pathology and Laboratory Medicine, School of Medicine and Public Health, University of Wisconsin, Madison, WI 53705, USA*

Correspondence should be addressed to Deepak Gopal, dvg@medicine.wisc.edu

Background. i-scan is a software-driven technology that allows modifications of sharpness, hue, and contrast to enhance mucosal imaging. It uses postimage acquisition software with real-time mapping technology embedded in the endoscopic processor. *Aims*. To review applications of i-scan technology in clinical endoscopic practice. *Methods*. This is a case series of 20 consecutive patients who underwent endoscopic procedures where i-scan image enhancement algorithms were applied. The main outcome measures were to compare mucosal lesions with high-definition white light endoscopy (HD-WLE) and i-scan image enhancement for the application of diagnostic sampling and therapy. *Results*. 13 cases involving the upper GI tract and 7 cases of the lower GI tract are included. For upper GI tract pathology i-scan assisted in diagnosis or therapy of Barrett's esophagus with dysplasia, esophageal adenocarcinoma, HSV esophagitis, gastric MALT lymphoma, gastric antral intestinal metaplasia with dysplasia, duodenal follicular lymphoma, and a flat duodenal adenoma. For lower GI tract pathology i-scan assisted in diagnosis or therapy of right-sided serrated adenomas, flat tubular adenoma, rectal adenocarcinoma, anal squamous cell cancer, solitary rectal ulcer, and radiation proctitis. *Conclusions*. i-scan imaging provides detailed topography of mucosal surfaces and delineates lesion edges, which can directly impact endoscopic management.

1. Introduction

As the field of gastrointestinal endoscopy continues to advance, various methods to enhance mucosal imaging continue to be developed and applied. Besides the progression from fiber optic endoscopes to standard resolution video endoscopes to high-resolution video endoscopes, several other techniques and technologies for enhancing mucosal imaging have been introduced and used. The most widely studied method is dye-based chromoendoscopy. Dye-based chromoendoscopy involves application of dyes or contrast stains directly to the mucosa and is often untidy and time consuming. Potential alternatives to chromoendoscopy involve mucosal enhancing technologies such as Olympus narrow band imaging (NBI), PENTAX i-scan, and FUJI Fice. PENTAX i-scan is a software-driven technology that allows for per pixel modifications of sharpness, hue, and contrast to modify and enhance mucosal imaging.

2. Background

i-scan uses postimage acquisition software with real time mapping technology embedded in the endoscopic processor (EPKi). The computer-controlled digital processing provides

resolution of 1.25 megapixels per image, which allows for analysis and modification of the per pixel luminosity data. It does so by using various combinations of three software algorithms: surface enhancement (SE), contrast enhancement (CE), and tone enhancement (TE). Surface enhancement improves light/dark contrast, making dark areas appear darker and light areas appear lighter to better delineate edges and lesion borders. Contrast enhancement slightly suppresses red and green wavelength components of the white light image, while adding a minute blue hue to darker or more depressed areas of mucosa to allow for detailed observation of subtle mucosal irregularities. This helps define "peaks and valleys" within the mucosal surface, resulting in a more detailed topography of the mucosal surface. Tone enhancement analyzes all three components (red, blue, and green) of the white light image, and then dissects out and suppresses most of the dominant red, creating an image with an elevated blue/green contrast for detecting more subtle mucosal abnormalities (Figure 1).

i-scan incorporates these three software algorithms into three distinct modes for the endoscopist: i-scan mode 1, i-scan mode 2, and i-scan mode 3. Each mode can be accessed or changed by a one button press on the endoscope. i-scan 1, designed as a surveillance mode uses SE and CE to provide more detailed topography of the mucosal surface and delineation of lesion edges without altering color. i-scan 2 and 3 also use SE and CE, but adds in TE to dissect out the dominant red and leave an elevated blue/green contrast (i-scan 2 darker contrast compared to i-scan 3). TE enhances vessel structures and minute mucosal structures to further pronounce margins of identified lesions.

We report a series of 20 cases from a single academic tertiary care hospital where i-scan technology significantly impacted the management of patients in a wide variety of clinical scenarios.

3. Methods

Consecutive cases were selected from our institution's endoscopy archive. Approval to review and report the selected cases was obtained from the University of Wisconsin Health Sciences Institutional Review Board. Informed consent was obtained from all participating patients. Data was collected on location of lesion (upper versus lower GI tract), diagnosis, i-scan mode, mucosal image detected, and impact on management. We compared and contrasted mucosal lesions detected with high-definition white light endoscopy (HD-WLE) versus i-scan image enhancement and the application on diagnostic sampling and therapy.

4. Results

i-scan image enhancement technology was used to diagnose and treat endoscopic findings and pathology in 13 cases involving the upper GI tract and 7 cases of the lower GI tract. Of the upper GI tract pathology, endoscopic image enhancement assisted in diagnosis, and/or therapy of 5 cases of Barrett's esophagus (BE) with dysplasia, 1 case each of T1 esophageal adenocarcinoma, HSV ulcerative esophagitis,

gastric MALT lymphoma, distal gastric antral intestinal metaplasia with dysplasia, a flat duodenal adenoma with high grade dysplasia, and 3 cases of duodenal follicular lymphoma. Lower GI tract findings and pathology detected by i-scan imaging included 2 right-sided serrated polyps >1 cm, 1 case each of flat tubular adenoma, T1N0 rectal adenocarcinoma, T1N0 anal squamous cell cancer, solitary rectal ulcer, and radiation proctitis (Table 1).

4.1. Upper GI Tract. The following clinical scenarios illustrate the diverse utility of i-scan in detecting several different types of upper GI tract mucosal abnormalities including neoplasms with dysplasia and those with malignant and infectious etiologies.

4.1.1. Esophageal Dysplasia. A 67-year-old man with long-standing GERD was referred for evaluation of short segment Barrett's esophagus with high-grade dysplasia. An endoscopic ultrasound (EUS) was performed and confirmed there was no invading submucosal lesions. EGD with HD-WLE demonstrated 2 cm of Barrett's mucosa (Figure 2(a)). With i-scan activated an erythematous area of nodularity within the Barrett's was better defined (Figures 2(b), 2(c), and 2(d)). This area was then removed in an overlapping fashion using the endoscopic mucosal resection (EMR) band ligation device. Histopathology of the EMR specimen demonstrated high-grade dysplasia (HGD) within the central nodule and surrounding low-grade dysplasia (Figure 2(e)). He subsequently returned two months later and underwent endoscopic radiofrequency ablation therapy (RFA). Followup surveillance endoscopy performed every 3 months for one year duration has not demonstrated recurrence of dysplasia or Barrett's esophagus.

A 71-year-old man with previously diagnosed Barrett's esophagus with low-grade dysplasia (LGD) was referred for possible RFA of the Barrett's. EGD was performed and revealed a 5 cm segment of Barrett's esophagus. WLE revealed a possible small nodule within the segment of Barrett's. i-scan modes 1 and 2 were turned on which clearly defined a nodule within the Barrett's. This allowed for targeted resection via EMR. Pathology from the EMR revealed HGD. He returned for EGD 2 months later and no further nodules were present. The remainder of his Barrett's was successfully treated with endoscopic RFA.

Three additional cases of Barrett's with esophageal nodularity and HGD were seen. The first was a 66-year-old female with known 4 cm, long segment Barrett's with HGD. Repeat EGD with i-scan modes 1–3 highlighted nodular areas in her distal esophagus which aided in targeted EMR of those areas. Next, a 78-year-old man with Barrett's with HGD underwent EGD with planned RFA. Upon initial evaluation with WLE a 4 cm tongue of Barrett's was noted. Visualization using i-scan modes 1 and 2 highlighted 2 focal nodules that were removed with targeted EMR prior to RFA. Pathology from the nodule resections showed intestinal metaplasia with very high-grade dysplasia and submucosal telangiectasia. Subsequent EGD's have shown reduction in the extent of his Barrett's. Lastly, a 54-year-old man with known Barrett's with high-grade dysplasia and normal EUS had a repeat EGD which showed

Principles of tone enhancement
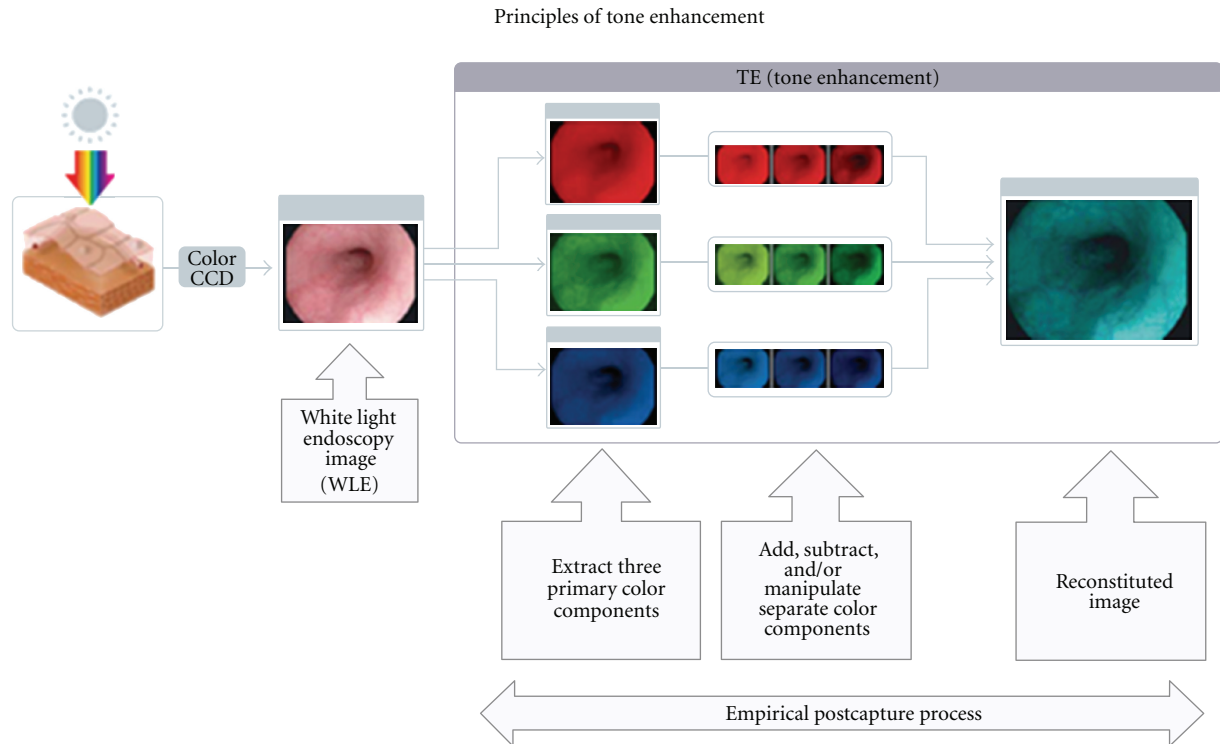
FIGURE 1: Principles of tone enhancement used by the postimage acquisition software in the endoscopic processor in i-scan technology. (Courtesy of Pentax Imaging, Pentax of America Montvale, NJ, USA).

irregular nodular mucosa in scattered islands. i-scan modes 2 and 3 were used to accentuate the abnormal areas to allow for optimal EMR.

4.1.2. Esophageal Cancer. A 73-year-old man with a 10 year history of GERD was referred for EGD and EUS for long segment Barrett's esophagus with nodularity. On EGD the patient had 7 cm segment of Barrett's esophagus, with a single are of nodularity as seen on HD-WLE endoscopy image (**Figure 3(a)**). i-scan Modes 1, 2, and 3 (Figures 3(b), 3(c), and 3(d)) demonstrated the surface enhancement and margins of the nodule, thus targeting EMR. The nodule was removed with EMR technique and completely excised. Pathology demonstrated Adenocarcinoma confined to the muscularis propria layer with the resection margins free of any cancer or high-grade dysplasia. The patient then followedup 2 months later to begin treatment with RFA for the remaining Barrett's.

4.1.3. Infectious Esophagitis. An 80-year-old man with history of orthotopic heart transplant presented with progressive dysphagia and odynophagia. Initial EGD demonstrated with WLE alone and biopsy sampling suggested mild, superficial candida esophagitis. He was treated appropriately with a 14-day course of fluconazole. However, his dysphagia and odynophagia persisted. After 10 days of antifungal therapy as an inpatient, a followup EGD was requested. Areas of mucosal irregularity and mild ulceration were visualized with WLE. Further examination with i-scan modes 1–3 showed severe distal esophagitis, with deep ulcerations,

which allowed for guided biopsies to be taken for viral culture and staining. Pathology revealed positive immunostaining for HSV I and II. He was started on treatment dose acyclovir and transitioned to valacyclovir prophylaxis with no recurrence of his esophagitis to date and marked improvement in symptoms.

4.1.4. Gastric Neoplasia. A 64-year-old man was referred for epigastric pain, nausea, bloating, and dyspepsia. He denied constitutional symptoms of weight loss, fevers, chills, or rigors. Physical examination findings and index laboratory testing were within normal limits. A two-week trial of PPI prescribed by his primary care physician did not relieve his symptoms. He was referred for an EGD. On EGD, in the body and fundus of the stomach, WLE demonstrated pale, atrophic-appearing mucosa that could be consistent with gastritis or gastropathy (Figure 4(a)). i-scan was activated and demonstrated a patch of pale yellow mucosa with surrounding nodular, edematous gastric folds (Figures 4(b) and 4(c)). The nodular folds were apparent and prominent using i-scan imaging and allowed for targeted biopsies to be taken. The histopathology demonstrated low-grade mucosa associated lymphoid tissue (MALT) lymphoma (Figure 4(d)). He underwent a two-week course of therapy for H. pylori eradication. Subsequently he also had a limited course of chemotherapy. Surveillance endoscopy using i-scan was initially performed at 3 month and then 6 month intervals over the following 2 years. Additional biopsies have found no recurrence of the MALT lymphoma.

Table 1: Cases in which i-scan imaging highlighted mucosal abnormalities not as clearly seen with white light endoscopy and subsequently affected management.

Case no.	Diagnosis	i-scan mode	Mucosal image	Impact on management
Esophagus				
(1)	BE with HGD	1, 3	Nodule of HGD	Targeted EMR
(2)	BE with LGD	1, 2	Nodule of LGD	Targeted EMR
(3)	BE with HGD	1, 2, 3	Nodularity with HGD	Targeted EMR
(4)	BE with HGD	1, 2	Nodularity with HGD	Targeted EMR
(5)	BE with HGD	1, 2, 3	Nodularity with HGD	Targeted EMR
(6)	Esophageal cancer	1, 2, 3	Accentuated abnormal tissue	Targeted EMR
(7)	HSV esophagitis	1, 2, 3	Deep ulcerations	Targeted biopsy
Stomach				
(8)	Gastric MALT lymphoma	1, 3	Gastric folds mucosal abnormality	Targeted EMR
(9)	CAG with intestinal metaplasia and dysplasia	1, 2, 3	Highlighted gastric thickening and nodularity	Subtotal gastrectomy
Small intestine				
(10)	Periampullary follicular lymphoma	1, 2	Identified extent of involvement	Prevented unnecessary ampullectomy
(11)	Duodenal adenoma with dysplasia	1, 2, 3	Highlighted flat polyp margins	Complete EMR
(12)	Grade 1-2 submucosal follicular lymphoma	1, 2	Highlighted lymphoid appearance	Targeted EMR and prevention of surgical excision
(13)	Low-grade follicular lymphoma	1, 2	Highlighted nodular area	Targeted biopsy
Colon and rectum				
(14)	Serrated adenoma	1, 2	Margins of polyp	Polyp detection and polypectomy
(15)	Serrated adenoma	2	Accentuated borders of right-sided polyp	Complete polypectomy
(16)	Tubular adenoma	1, 2	Detailed border of polyp on fold	R hemicolectomy
(17)	Anal SCCa T1N0	1, 2	Identified mucosal abnormality in anal canal	Targeted Bx
(18)	Rectal adenocarcinoma T1N0	1, 2, 3	Identified borders of flat "depressed" rectal polyp	Targeted complete polypectomy
(19)	Radiation proctitis	1	Identified extent of involvement	Allowed for more diffuse APC
(20)	Solitary rectal ulcer	1, 2	Accentuated subtle ulcer	Targeted Bx

Abbreviations: BE: Barrett's esophagus, LGD: low-grade dysplasia, HGD: high-grade dysplasia, EMR: endoscopic mucosal resection, HSV: herpes simplex virus, MALT: mucosa-associated lymphoid tissue, CAG: chronic active gastritis, SCCa: squamous cell carcinoma, and APC: argon plasma coagulation.

A 77-year-old female with history of previous gastric antral intestinal metaplasia with tubulovillous adenoma presented for followup EGD. Initially, WLE showed friable, nodular, and heterogeneous mucosa along the greater curvature of the stomach. i-scan modes 1–3 showed more pronounced involvement of the antrum in an irregular circumferential manner with mucosa that appeared somewhat fibrotic. Biopsies of the abnormal area showed chronic active gastritis with areas of intestinal metaplasia and dysplasia. The patient was then referred for surgical evaluation and is awaiting a subtotal gastrectomy.

4.1.5. Small Intestinal Neoplasia. A 60-year-old woman was referred for EGD for symptoms of atypical, noncardiac chest pain. She also had been experiencing profound weakness without any other specific symptoms. On EGD, she was found to have a normal esophagus and stomach. Incidentally, she had an abnormal appearing polyp in the second portion of the duodenum. She was referred for possible ampullectomy. Upon repeat EGD, there was evidence of not only a large, irregular appearing periampullary polyp, but also multiple small satellite lesions. i-scan modes 1 and 2 were turned on and revealed more widespread distinct lesions. Directed biopsies of these lesions revealed grade 1 follicular lymphoma. The patient was referred to hematology. Staging CT of her chest, abdomen, and pelvis, as well as a bone marrow biopsy, revealed no other evidence of lymphoma. She has not required treatment and has been followed closely with observation and serial EGDs and CT scans.

A 52-year-old man with history of alcohol abuse and past pulmonary embolism in the setting of positive lupus anticoagulant underwent EGD for evaluation of dyspepsia.

(a)

(b)

(c)

(d)

(e)
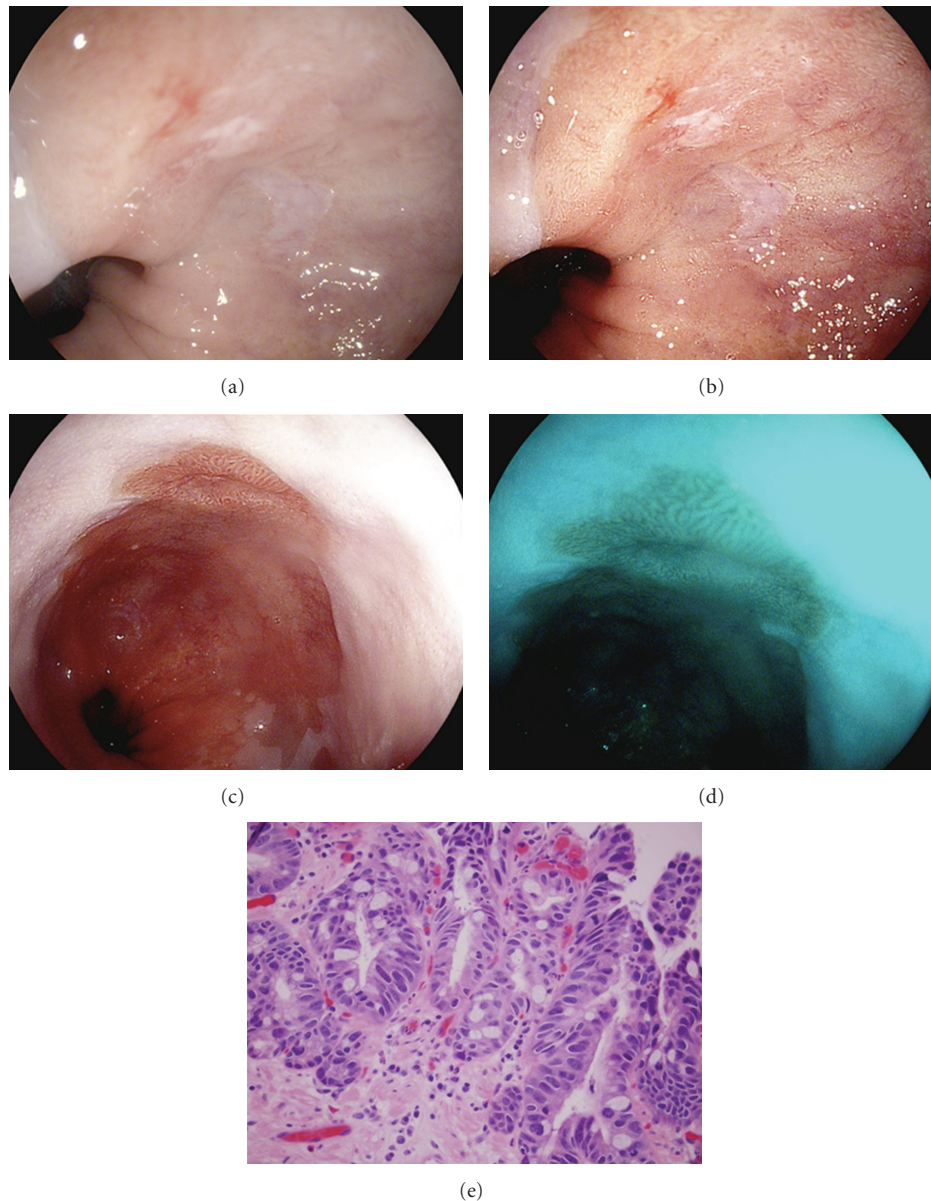
Figure 2: Barrett's esophagus with nodularity and high-grade dysplasia (HGD) visualized with HD-WLE (a), i-scan mode 1 (b) and (c), and i-scan mode 3 (d). Histopathology of EMR specimen showing Barrett's esophagus with HGD, H&E stain, and 400x magnification (e).

EGD showed erosive esophagitis without Barrett's and a normal stomach. Inspection of the duodenum showed an area of mucosal irregularity with WLE and further visualization with i-scan modes 1–3 showed a sessile polyp that was removed and found to be an adenoma. Follow-up EGD showed a postpolypectomy scar and some areas of nodularity in the duodenum but biopsies obtained were normal.

Two additional cases of follicular lymphoma highlighted by i-scan were discovered. First, a 72-year-old man with abdominal pain and a known pancreas head mass was evaluated with EGD and EUS for further diagnosis of the mass. EGD with WLE showed mild gastritis and a hiatal hernia with nodular mucosa in the second portion of the duodenum. i-scan modes 1 and 2 showed additional focal areas of nodularity that upon biopsy revealed grade 1-2

follicular lymphoma. EUS biopsy of the pancreas mass also showed lymphoma. The patient followed up locally for treatment of his lymphoma. Second, a 60-year-old female underwent interval surveillance EGD to monitor her known focal low-grade follicular lymphoma (staging CT and bone marrow biopsy were negative for involvement). Using i-scan modes 1 and 2 slight regression of the burden of lymphoma was seen. The patient has active hematology followup and surveillance with EGD and CT.

4.2. Lower GI Tract. The following collection of clinical scenarios represent i-scan's varied utility in detecting lower GI tract pathology. The cases range from detection of colonic polyps to that of anorectal malignancies and nonmalignant anorectal pathology.

(a)

(b)

(c)

(d)

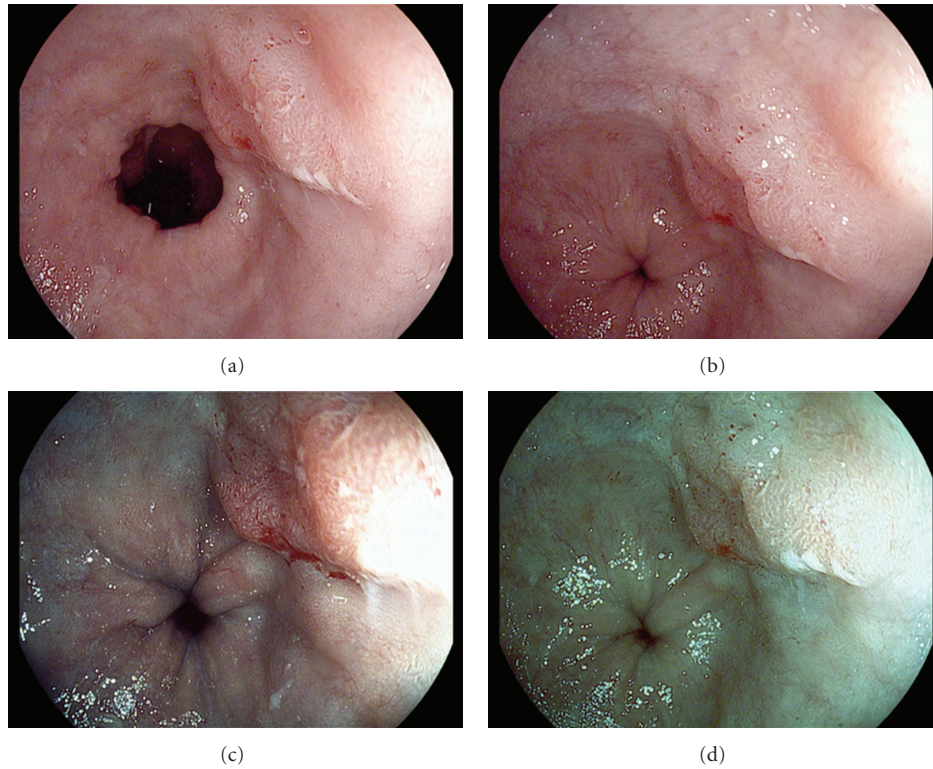FIGURE 3: Raised nodule of adenocarcinoma within a segment of Barrett's esophagus as seen with HD-WLE (a), i-scan mode 1 (b), i-scan mode 2 (c), and i-scan mode 3 (d).
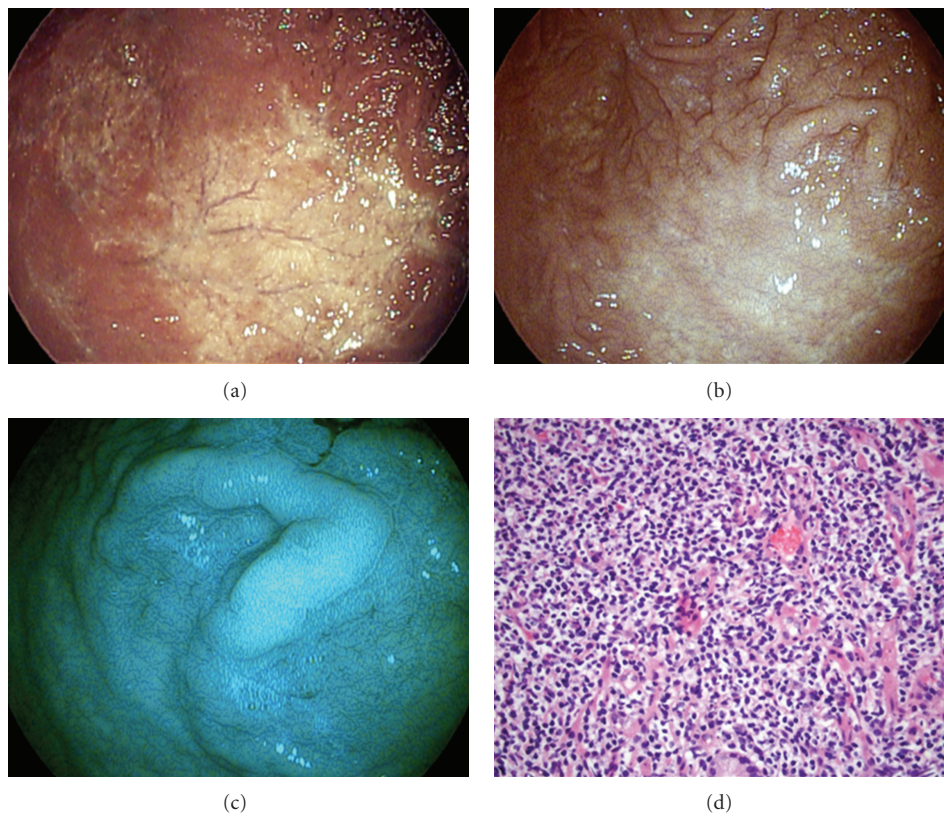

(a)

(b)

(c)

(d)

FIGURE 4: Gastric mucosa associated lymphoid tissue (MALT) lymphoma visualized with HD-WLE (a), i-scan mode 1 (b), and i-scan mode 3 (c). Histopathology showing MALT lymphoma, H&E stain, and 400x magnification (d).

4.2.1. Colonic Polyps. A 66-year-old asymptomatic, average risk woman was referred for a screening colonoscopy. In the ascending colon there was a large sessile polyp visualized under HD-WLE. i-scan mode 1 more clearly visualized the borders of the polyp. The polyp was lifted with injection of 3 mL of saline and was then removed in piecemeal fashion with hot snare polypectomy. i-scan allowed for improved visualization to ensure the polyp was completely removed. The area was then tattooed for future surveillance. Histopathology revealed a serrated polyp. Surveillance colonoscopy 6 months later revealed no residual polyp tissue.

A 45-year-old man with no family history of colorectal cancer was referred for colonoscopy due to a change in bowel pattern. A minimally erythematous flat mucosal abnormality was noted in the ascending colon with WLE (Figure 5(a)). Further characterization with i-scan mode 2 showed a 7 mm polyp that was removed with hot snare (Figure 5(b)). Pathology revealed a sessile serrated polyp. He will have a repeat colonoscopy in 5 years.

A 64-year-old average risk man underwent routine colonoscopy for colorectal cancer screening. Near the ileo-cecal junction a fold appeared slightly prominent on WLE. Upon visualization with i-scan modes 1 and 2 a 2 cm sessile polyp was highlighted. Attempts to lift the polyp via saline injection for safe polypectomy were unsuccessful. The polyp was then biopsied and tattooed. An additional 6 mm sigmoid polyp was found and removed. Pathology showed tubular adenoma in both polyps. The patient underwent laparoscopic right hemicolectomy for the cecal adenoma and no higher grade lesions were discovered.

4.2.2. Anorectal Malignancy. A 69-year-old man was referred for routine surveillance colonoscopy. He had a colonoscopy 5 years prior with a single tubular adenoma. Surveillance colonoscopy was normal throughout, including a retroflexed view in the rectum. Upon withdrawal of the scope, there was an area of mucosal irregularity noted at the dentate line. i-scan mode 1 was activated and revealed a small erythematous, friable, ulcerated nodular lesion in the distal anorectum in the posterior wall. This area was targeted for biopsy and the histopathology revealed squamous cell cancer of the anal canal. The patient had a rectal ultrasound which revealed a T1N0 lesion. He was referred to oncology and started on a combined chemotherapy and radiation regimen.

A 50-year-old asymptomatic, average risk woman underwent a screening virtual-CT colonography. An 8 mm polyp was seen in the sigmoid colon. She was referred for same day colonoscopy with polypectomy and the 8 mm polyp was removed. Upon retroflexion in the rectum, another 2 cm sessile polyp was seen (Figure 6(a)). i-scan modes 1, 2, and 3 were turned on and more clearly visualized the extent and borders of this large polyp and defined the lesion edges (Figures 6(b), 6(c), and 6(d)). The polyp was injected with saline and was removed completely in a piecemeal fashion using i-scan images to assess for completeness of resection. Pathology revealed tubulovillous adenoma and infiltrating well-differentiated adenocarcinoma extending to the cauterized margin. The patient was referred to colorectal surgery and underwent a transanal excision. Final surgical pathology revealed no residual carcinoma.

4.2.3. Nonmalignant Anorectal Disease. An 81-year-old man with a history of prostate cancer treated with radiation was referred for a colonoscopy for evaluation of hematochezia. His screening colonoscopy five years earlier was normal. A colonoscopy was performed and revealed no polyps, tumors, or evidence of inflammatory bowel disease or ischemic colitis. In the distal rectum, there was the appearance of radiation proctitis seen on initial WLE which suggested the degree of proctitis was mild, encompassing approximately 25% of the surface area. However, i-scan mode 1 was turned on and revealed extensive radiation proctitis involving approximately 60% of the lumen surface area in the anterolateral wall in a semicircumferential fashion. This allowed for better targeting of therapy with argon plasma coagulation (APC). His symptoms of hematochezia improved. Two months later, he returned for one more follow-up flexible sigmoidoscopy with additional APC therapy of the radiation proctitis, which had significantly improved since the first colonoscopy. After followup one year later, he has had no further hematochezia.

Finally, a 64-year-old female with history of diarrhea and rectal bleeding was evaluated with colonoscopy. The colon was normal outside of some scattered diverticula and a couple of diminutive polyps. Further evaluation of her rectum with i-scan modes 1 and 2 showed a 6 mm solitary rectal ulcer. Biopsy of the ulcer edge showed benign squamous and columnar mucosa with focal neutrophilic infiltrates.

5. Discussion

There is an increasing demand for improving mucosal imaging as a means to identify pathology and target diagnostic sampling and guide endoscopic therapy. This has resulted in the development of technology-based methods for enhancing mucosal imaging. Digital filter technologies, such as i-scan, are becoming one of the more common and practical technologies to achieve this goal. We have presented a series of cases that illustrates the applicability of this technology across a broad spectrum of clinical scenarios.

Digital filter-based technologies like i-scan were developed out of the concept of dye-based chromoendoscopy. Dye-based chromoendoscopy involves manually applying dye or contrast directly to the mucosa to better delineate normal from pathologic mucosa. It can be done in either an untargeted fashion across the entire mucosal surface, or in a targeted fashion at specific lesions. Dye-based chromoendoscopy leads to improved visualization of mucosal irregularities and has been studied in various situations ranging from screening colonoscopy to ulcerative colitis and Barrett's surveillance [1–3]. However, while it still useful in some situations, dye-based chromoendoscopy can be cumbersome and increase procedure times. Also, following initially promising studies on dye-based chromoendoscopy, no further studies have been conducted and the data remains descriptive [4, 5].

(a)

(b)
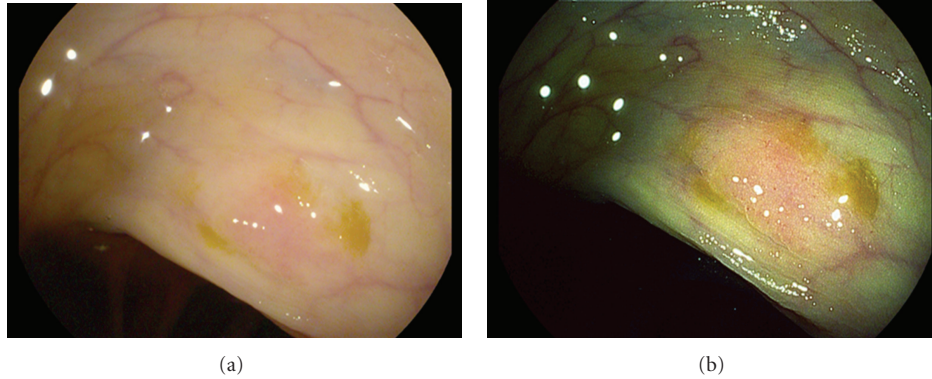
FIGURE 5: Sessile serrated polyp visualized under HD-WLE (a) and with i-scan mode 2 (b).

(a)

(b)

(c)

(d)
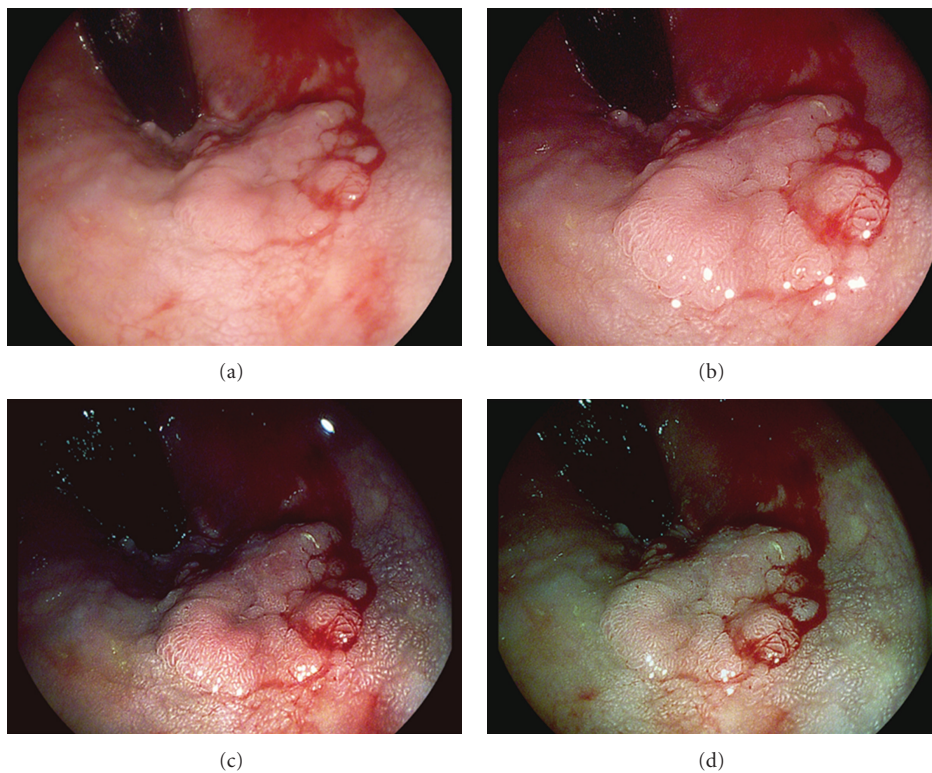
FIGURE 6: Large rectal polyp with focus of adenocarcinoma, visualized with HD-WLE (a), i-scan mode 1 (b), i-scan mode 2 (c), and i-scan mode 3 (d).

There are several optical and digital filter techniques that have been developed to enhance mucosal imaging without manually applying contrast to the mucosa. Narrow band imaging (NBI) uses optical light filters in front of the light source to narrow the bandwidth of the projected light. This produces a colored image on the screen with enhanced contrast. NBI has not been shown to improve adenoma detection rates [6], but has been shown to improve discrimination of hyperplastic from adenomatous polyps [7]. When compared to standard WLE, NBI improves diagnostic yield in detecting dysplasia in Barrett's esophagus by detecting more dysplasia from fewer, more targeted biopsies [8].

As opposed to using filters at the light source as in NBI, newer proprietary technologies such as Fuji Intelligent

Chromoendoscopy (FICE) (Fuji) and i-scan (Pentax) use postimage acquisition software to modify the images seen. FICE has been shown to be as good as dye chromoendoscopy in detecting colonic adenomas [9, 10]. FICE is also superior to conventional WLE, but equal to dye chromoendoscopy, in differentiating neoplastic from nonneoplastic colon polyps [11]. FICE can diagnose Barrett's esophagus with the ability to clearly demarcate between Barrett's mucosa and gastric mucosa [12]. FICE has also been shown to be equivalent to conventional chromoendoscopy with acetic acid in detecting neoplasia in Barrett's esophagus [13]. i-scan has been shown to significantly increase the detection of small colon polyps sized 5 mm or less [14]. i-scan in combination with high-definition colonoscopy has also been shown to improve

overall adenoma detection compared to standard white light colonoscopy alone [15]. In the esophagus, i-scan can help identify reflux-associated mucosal breaks, but it has not been extensively studied in the setting of Barrett's esophagus [16].

We have illustrated a variety of cases where i-scan technology can be clinically useful and directly impact management of patients. i-scan was able to better detect and enhance mucosal abnormalities throughout the gastrointestinal tract compared to HD-WLE. Lesions that were highlighted ranged from Barrett's esophagus and gastric MALT lymphoma to duodenal follicular lymphoma and rectal adenocarcinoma. In general i-scan allowed for more precise delineation of lesion borders to allow for more complete mucosal resection and/or biopsy. In several of the cases there were significant changes in outcomes that may have been missed if WLE was used alone. Specifically, in the case involving the periampullary follicular lymphoma i-scan was able to further delineate the extent of a duodenal lymphoma, preventing unnecessary ampullectomy with its potential morbidities.

This case series adds to the growing body of literature supporting the clinical utility of enhanced mucosal imaging. The main limitations of this series are that the experiences were limited to a single center and a few endoscopists experienced in the use of i-scan. The validity of i-scan to more readily detect mucosal abnormalities compared to current WLE will need to be addressed in more detail by prospective multicenter studies. Currently there are only single institution studies reported in the literature [14, 15, 17, 18].

i-scan technology shows promise as a useful modality in a wide array of clinical scenarios throughout the gastrointestinal tract to better detect and treat mucosal abnormalities. It can provide more detailed topography of the mucosal surface and delineate lesion edges by enhancing vessel and minute mucosal structures. Utilizing i-scan endoscopic image enhancement may directly impact the management of patients.

Disclosure

None of the authors have received funding for this study or have conflict of interests to disclose.

References

[1] B. J. Rembacken, T. Fujii, A. Cairns et al., "Flat and depressed colonic neoplasms: a prospective study of 1000 colonoscopies in the UK," *The Lancet*, vol. 355, no. 9211, pp. 1211–1214, 2000.

[2] R. Kiesslich, M. Von Bergh, M. Hahn, G. Hermann, and M. Jung, "Chromoendoscopy with indigocarmine improves the detection of adenomatous and nonadenomatous lesions in the colon," *Endoscopy*, vol. 33, no. 12, pp. 1001–1006, 2001.

[3] S. H. Itzkowitz, D. H. Present, V. Binder et al., "Consensus conference: colorectal cancer screening and surveillance in inflammatory bowel disease," *Inflammatory Bowel Diseases*, vol. 11, no. 3, pp. 314–321, 2005.

[4] S. K. Amateau and M. I. Canto, "Enhanced mucosal imaging," *Current Opinion in Gastroenterology*, vol. 26, no. 5, pp. 445–452, 2010.

[5] M. Goetz and R. Kiesslich, "Advanced imaging of the gastrointestinal tract: research versus clinical tools?" *Current Opinion in Gastroenterology*, vol. 25, no. 5, pp. 412–421, 2009.

[6] D. K. Rex and C. C. Helbig, "High yields of small and flat adenomas with high-definition colonoscopes using either white light or narrow band imaging," *Gastroenterology*, vol. 133, no. 1, pp. 42–47, 2007.

[7] A. Rastogi, J. Keighley, V. Singh et al., "High accuracy of narrow band imaging without magnification for the real-time characterization of polyp histology and its comparison with high-definition white light colonoscopy: a prospective study," *American Journal of Gastroenterology*, vol. 104, no. 10, pp. 2422–2430, 2009.

[8] H. C. Wolfsen, J. E. Crook, M. Krishna et al., "Prospective, controlled tandem endoscopy study of narrow band imaging for dysplasia detection in Barrett's Esophagus," *Gastroenterology*, vol. 135, no. 1, pp. 24–31, 2008.

[9] J. Pohl, E. Lotterer, C. Balzer et al., "Computed virtual chromoendoscopy versus standard colonoscopy with targeted indigocarmine chromoscopy: a randomised multicentre trial," *Gut*, vol. 58, no. 1, pp. 73–78, 2009.

[10] C. E. O. Dos Santos, J. C. P. Lima, C. V. Lopes et al., "Computerized virtual chromoendoscopy versus indigo carmine chromoendoscopy combined with magnification for diagnosis of small colorectal lesions: a randomized and prospective study," *European Journal of Gastroenterology and Hepatology*, vol. 22, no. 11, pp. 1364–1371, 2010.

[11] K. Togashi, H. Osawa, K. Koinuma et al., "A comparison of conventional endoscopy, chromoendoscopy, and the optimal-band imaging system for the differentiation of neoplastic and non-neoplastic colonic polyps," *Gastrointestinal Endoscopy*, vol. 69, no. 3, pp. 734–741, 2009.

[12] H. Osawa, H. Yamamoto, N. Yamada et al., "Diagnosis of endoscopic Barrett's esophagus by transnasal flexible spectral imaging color enhancement," *Journal of Gastroenterology*, vol. 44, no. 11, pp. 1125–1132, 2009.

[13] J. Pohl, A. May, T. Rabenstein et al., "Comparison of computed virtual chromoendoscopy and conventional chromoendoscopy with acetic acid for detection of neoplasia in Barrett's esophagus," *Endoscopy*, vol. 39, no. 7, pp. 594–598, 2007.

[14] A. Hoffman, C. Kagel, M. Goetz et al., "Recognition and characterization of small colonic neoplasia with high-definition colonoscopy using i-Scan is as precise as chromoendoscopy," *Digestive and Liver Disease*, vol. 42, no. 1, pp. 45–50, 2010.

[15] A. Hoffman, F. Sar, M. Goetz et al., "High definition colonoscopy combined with i-Scan is superior in the detection of colorectal neoplasias compared with standard video colonoscopy: a prospective randomized controlled trial," *Endoscopy*, vol. 42, no. 10, pp. 827–833, 2010.

[16] A. Hoffman, N. Basting, M. Goetz et al., "High-definition endoscopy with i-Scan and Lugol's solution for more precise detection of mucosal breaks in patients with reflux symptoms," *Endoscopy*, vol. 41, no. 2, pp. 107–112, 2009.

[17] C. K. Lee, S. H. Lee, and Y. Hwangbo, "Narrow-band imaging versus I-Scan for the real-time histological prediction of diminutive colonic polyps: a prospective comparative study by using the simple unified endoscopic classification," *Gastrointestinal Endoscopy*, vol. 74, no. 3, pp. 603–609, 2011.

[18] S. N. Hong, W. H. Choe, J. H. Lee et al., "Prospective, randomized, back-to-back trial evaluating the usefulness of i-SCAN in screening colonoscopy," *Gastrointestinal Endoscopy*, vol. 75, no. 5, pp. 1011–1021, 2012.

Clinical Study

The Learning Curve of Gastric Intestinal Metaplasia Interpretation on the Images Obtained by Probe-Based Confocal Laser Endomicroscopy

**Rapat Pittayanon,[1] Rungsun Rerknimitr,[1] Naruemon Wisedopas,[2]
Suparat Khemnark,[1] Kessarin Thanapirom,[1] Pornpahn Thienchanachaiya,[1]
Nuttaporn Norrasetwanich,[1] Kriangsak Charoensuk,[1] Wiriyaporn Ridtitid,[1]
Sombat Treeprasertsuk,[1] Pradermchai Kongkam,[1] and Pinit Kullavanijaya[1]**

[1] *Division of Gastroenterology, Department of Medicine, Chulalongkorn University, Bangkok 10330, Thailand*
[2] *Department of Pathology, Chulalongkorn University, Bangkok 10330, Thailand*

Correspondence should be addressed to Rapat Pittayanon, rapat125@gmail.com

Background. Reading the results of gastric intestinal metaplasia (GIM) with probe-based confocal laser endomicroscopy (pCLE) by the expert was excellent. There is a lack of study on the learning curve for GIM interpretation. Therefore, we conducted a study to explore the learning curve in the beginners. *Material and Method*. Five GI fellows who had no experience in GIM interpretation had been trained with a set of 10 pCLE video clips of GIM and non-GIM until they were able to interpret correctly. Then they were asked to interpret another 80 video clips of GIM and non-GIM. The sensitivity, specificity, accuracy, PPV, NPV, and interobserver agreement on each session were analyzed. *Results*. Within 2 sessions, all beginners can achieve 80% accuracy with substantial to almost perfect level of interobserver agreement. The sensitivities and specificities among all interpreters were not different statistically. Four out of five interpreters can maintain their high quality of reading skill. *Conclusion*. After a short session of training on GIM interpretation of pCLE images, the beginners can achieve a high level of reading accuracy with at least substantial level of interobserver agreement. Once they achieve the high reading accuracy, almost all can maintain their high quality of reading skill.

1. Introduction

Gastric cancer is the second leading cause of cancer death worldwide [1], and gastric intestinal metaplasia (GIM) is the precancerous lesion for intestinal type gastric cancer [2, 3]. The strategies which can detect precancerous and/or early cancerous transformation are very beneficial because only early gastric cancer can potentially be cured by endoscopic treatment. Probe-based confocal laser endomicroscope or pCLE is one of the useful equipments for GIM detection. The endoscopic criteria for GIM reading by pCLE were (1) villous-like gastric epithelium and (2) dark (no fluorescein uptake) goblet cells in the gastric columnar epithelium [4]. Previously our group reported the results of GIM detection

and interpretation by pCLE as 94% in sensitivity, 85% in specificity, and 89% in accuracy [4]. However, these excellent results in pCLE interpretation were established by the expert. The study on learning curve by the beginners for the new type of image reading including GIM interpretation by pCLE is important for community practice. Therefore, we conducted a study to explore the learning curve pattern by the beginners.

2. Material and Method

2.1. Procedure and Data Collection. This study was conducted at the Division of Gastroenterology, Department of medicine, Chulalongkorn University. The protocol study

was registered through ClinicalTrials.gov (NCT01491724) and approved by the Chulalongkorn University Institutional Review Board. Fifty patients with previous histologies confirmed as GIM underwent a surveillance gastroscopy with pCLE (Mauna Kea Technologies, Paris, France) performed by one endoscopist (RP) under a standard conscious sedation with intravenous midazolam (Cenexi SAS, Fontenay-sous-Bois, France) and meperidine (M&H manufacturing Co., Ltd., Samutprakarn, Thailand). For the best quality of pCLE images, 10 milligrams of hyoscine (Pharmaland (1982) Co., Ltd, Bangkok, Thailand) were given before the procedure to decrease the bowel movement.

After an intravenous injection of two and a half milliliter of 10% fluorescein (Novartis Pharmaceutical Corporation, Bangkok, Thailand), pCLE video clips in MPEG format with duration of 40–120 sec were obtained from GIM and non-GIM suspicious area. After histology confirmation of both GIM and non-GIM video clips, the experienced pCLE endoscopist (RP) selected 90 high quality pCLE video clips (clearly visualized gastric epithelium, vessel and goblet cell, and good image stability) for further interpretation by the beginners. Of those, 45 video clips corresponded to normal mucosa and the other 45 video clips represented GIM. All video clips were incorporated into a slideshow format (Microsoft PowerPoint 2003) with the play duration of 10–20 sec.

The beginners in this study were defined as first-year GI fellows who had no experience in pCLE images interpretation. Five eligible GI fellows (SK, KC, PT, NN, and KT) from Chulalongkorn University were recruited to the study. They were trained by the experienced endoscopist (RP) in the training class for 1 hour with an initial set of 10 pCLE video clips representing 5 GIM and 5 non-GIM. The criteria for GIM reading by pCLE were (1) villous-like gastric epithelium and (2) dark (no fluorescein uptake) goblet cells in the gastric columnar epithelium [4]. Then, they were provided with the same set of 10 video clips for self-practice until they were able to interpret all 10 video clips correctly. All video clips used for the learning set were not included in the study sets.

To assess the learning curve, the other 80 high quality pCLE video clips were divided into 4 sets of 20 video clips. All beginners interpreted the 4 sets of 20 pCLE video clips of GIM and non-GIM at 2-week interval. For each testing session, all interpreters were asked to sit in a class room and viewed the video clips displayed by a projector. Each video clip was played twice before the interpreters chose their answers (as GIM or non-GIM). After each session, their scores and the correct answers of video clips were not revealed to any readers.

2.2. Statistical Analysis. The outcome in GIM interpretation by pCLE of each beginner was assessed for the sensitivity, specificity, accuracy, positive predictive value (PPV), and negative predictive value (NPV). For numerical variables, the results were expressed as a mean $\pm$ SD whereas other quantitative variables were shown in percentage. Fleiss' kappa (κ) was used to analyze the interobserver agreement among 5 beginners on those captured pCLE images. The value of kappa (κ) for agreement was graded as poor for 0.01 to 0.20,
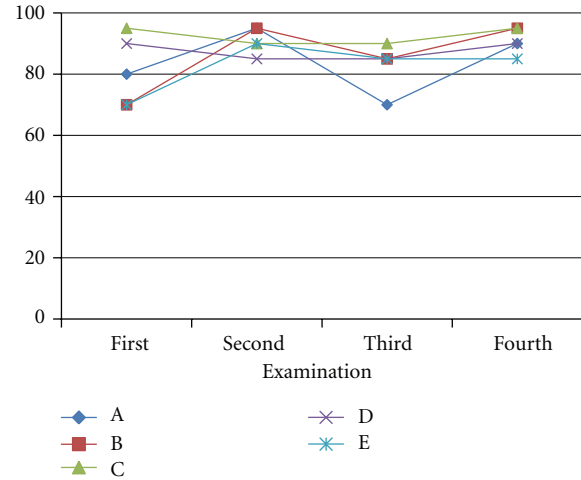
FIGURE 1: Accuracies of different beginners. A: beginner number 1, B: beginner number 2, C: beginner number 3, D: beginner number 4, E: beginner number 5.

fair for 0.21 to 0.40, moderate for 0.41 to 0.60, substantial for 0.61 to 0.80, and almost perfect for 0.81 to 1.00.

3. Results

From the first session, the overall sensitivity and specificity for GIM diagnosis of the 5 beginners were above 70% and gradually increased over time. The PPV was more than 90% on average, whereas NPV was lower at 75–85%. Among all interpreters, there were no differences in statistical analysis of all validity scores (Table 1). Additionally, one beginner achieved the 100% sensitivity, 91.6% specificity, and 95% accuracy within the first session. Within two sessions, all beginners were able to provide more than 80% in accuracy with substantial to almost perfect level of interobserver agreement (Table 2). Almost all of them (4 from 5) were able to maintain their good reading skill with 85–95% accuracy through the rest of study sessions (Figure 1).

4. Discussion

Confocal laser endomicroscope (CLE) is the latest novel endoscopic technology which has been commercially available since 2005 [9]. Currently, there are two types of CLE: (1) endoscopic-based or integrated confocal laser endomicroscope (eCLE or iCLE, Pentax, Tokyo, Japan) and (2) probe-based confocal laser endomicroscope (pCLE, Mauna Kea Technologies, Paris, France) [10, 11]. From various studies, CLE can provide real-time histology [12–19] and possibly dynamic cellular changing in gastrointestinal disease [20, 21]. Even though, the learning curve study in CLE is still limited.

To our knowledge, this is the first study of the learning curve of GIM interpretation by both iCLE and pCLE. The acceptance of all new technologies requires not only high validity scores and good accessibility but also a short learning curve to attract practicing users. The previous study revealed

Table 1: Representing sensitivity, specificity, accuracy, PPV, and NPV in each beginner.

	Beginner number 1	Beginner number 2	Beginner number 3	Beginner number 4	Beginner number 5	P value
Sensitivity (%) (range)	87.5 (75, 100)	87.5 (75, 100)	97.2 (88.8, 100)	89.5 (81.8, 100)	90.9 (75, 100)	0.53
Specificity (%) (range)	75.2 (45.5, 88.8)	79.9 (66.6, 91.6)	85.6 (77.7, 91.6)	86.3 (81.8, 91.6)	75.2 (66.6, 81.8)	0.52
Accuracy (%) (range)	83.7 (70, 95)	86.2 (70, 95)	91.2 (85, 95)	87.5 (85, 90)	82.5 (70, 90)	0.57
PPV (%) (range)	94.3 (83.3, 100)	94.6 (80, 100)	97.4 (90, 100)	90.5 (80, 100)	91.7 (80, 100)	0.64
NVP (%) (range)	75.6 (60, 91.7)	79.1 (60, 91.7)	85.3 (80, 88.9)	84.2 (80, 87.5)	75.0 (60, 84.6)	0.55

Table 2: Representing accuracy, sensitivity, specificity, and Fleiss' kappa in overall assessment by the beginners.

	First test	Second test	Third test	Fourth test
Sensitivity (%) (range)	83.3 (75, 100)	96.3 (81.8, 100)	93.2 (88.8, 100)	97.5 (87.5, 100)
Specificity (%) (range)	71.6 (66.6, 91.6)	84.3 (77.7, 88.8)	72.7 (45.4, 81.8)	86.6 (75.0, 91.6)
Accuracy (%) (range)	81 (70, 95)	91 (85, 95)	82 (70, 85)	91 (85, 95)
Agreement (Fleiss' kappa)	0.44 (moderate)	0.82 (Almost perfect)	0.52 (Substantial)	0.86 (Almost perfect)

the excellent sensitivity, specificity, and accuracy of a combination method with FICE and pCLE for GIM diagnosis at 94%, 85%, and 89%, respectively [4]. In addition, the other type of CLE called iCLE showed the near perfect sensitivity at 98% and specificity at 95% for GIM diagnosis based on the updated Sydney System's recommendation [22]. However, all interpretations of GIM by both CLE techniques were performed by skilful researchers. Lim et al. emphasized that experienced interpreters in iCLE reading can achieve greater validity score than the beginners in GIM diagnosis with the sensitivity of 95% versus 61% ($P = 0.39$) and specificity of 93% versus 62% ($P < 0.001$) [23]. Moreover, experienced iCLE interpretation provided almost perfect interobserver agreement ($\kappa = 0.89$), whereas the beginner showed only fair interobserver agreement ($\kappa = 0.28$) [23].

Because one of the important factors determining the good GIM reading outcome is the experience of interpreter, then it is important to study how difficult it is to train the beginners to become accurate in pCLE image interpretation. In our opinion, gaining the acceptable reading skill in GIM interpretation by pCLE is not too difficult because the endoscopic criteria for GIM reading are not complicate, and the goblet cells can be simply observed [22]. Our study confirmed this by showing that the interpretation of pCLE images in GIM can be learnt rapidly after a short training session and many of them achieved the high sensitivity of their interpretations within 2 sessions of the 4-session study format. Moreover, all of them can provide a very high PPV ($\geq 80\%$) since the first test. It is emphasizing that the beginners can interpret GIM images correctly only after a brief learning period. In addition, almost all of the beginners can maintain the high interpretation skill with substantial ($\kappa = 0.52$) to almost perfect interobserver agreement ($\kappa = 0.86$).

However, the pCLE reading skill is not representing the pCLE endoscopic skill which is important to obtain the high quality images for interpretation. Achieving the skill to perform pCLE with high quality output may not be easy and need longer time to practice because of certain reasons such as the unfamiliarity of small fragile devices that need a gentle handling and the shaking effect of the pCLE image due to the very fine examination in a small area. Although, there has been no report on the effect of GIM image quality on the accuracy in GIM detection, a study of pCLE used to detect colonic neoplasm showed that the suboptimal image quality on pCLE resulted in a lower sensitivity of colonic adenoma detection [24]. Moreover, another recent study revealed that the interobserver agreement, sensitivity, specificity, and accuracy of distinguishing between neoplastic colonic polyp and nonneoplastic colonic polyp by pCLE were increased from 0.55, 76%, 72%, and 75% to 0.83, 88%, 89%, and 88%, respectively, after considering only good and excellent quality video clips [25]. Therefore, we may extrapolate that the quality of GIM image may be an important confounding factor affecting the difficulty of image interpretation. In our study selected only high quality video clips before we provided those to our trainees. All video clips in this study were chosen by our experienced endoscopist (RP) by using the criteria as follows: clearly visualized gastric epithelium, vessels, and goblet cell with no shaking effect or significant artifact. Although hyoscine injection is required to decrease gastric movement, it is not easy to obtain a high quality image by putting a tiny pCLE probe in the stomach that always has a lot of peristalsis. In our anecdotal experience, a significant period of training to stabilize a scope embedded with a transparent cap is also important to qualify a good MPEG stream. The examples of high and poor quality GIM images by pCLE are displayed in Figure 2.

(a)   (b)
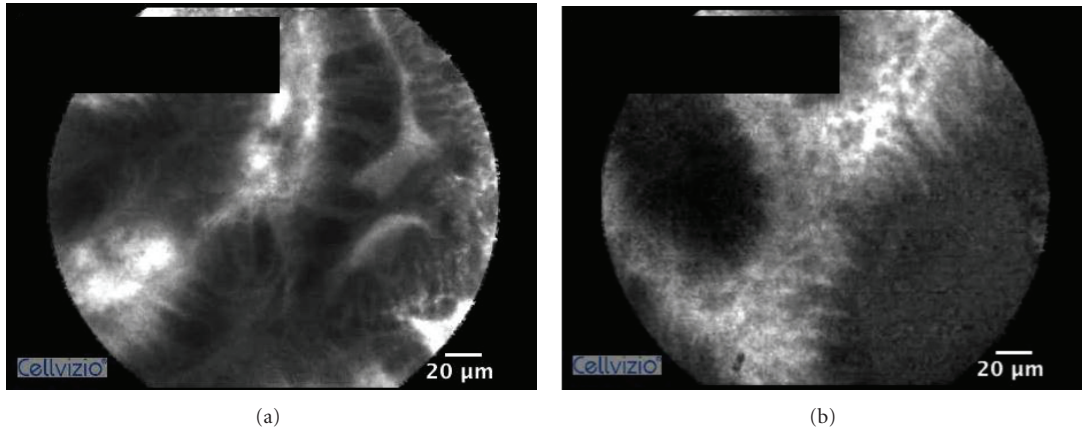
FIGURE 2: Comparing between high and poor quality pCLE imaging of gastric intestinal metaplasia. (a) High quality pCLE image shows clearly visualized epithelium and goblet cell. (b) Poor quality pCLE image shows unclear epithelial boarder and vessels.

TABLE 3: Comparing the learning curve of different studies of CLE in the GI tract.

	Present study	Kuiper et al. Gastrointest Endosc 2012 [5]	Buchner et al. Gastrointest Endosc 2011 [6]	Neumann et al. Histol Histopathol 2011 [7]	Gaddam et al. Am J Gastroenterol 2011 [8]
Type of confocal laser	pCLE	iCLE	pCLE	pCLE	pCLE
Tissue	Stomach (GIM)	Colonic polyp	Colonic polyp	Colon (IBD)	Esophagus (Barrett)
Number of reader	5	3	11	2	3
Number of center	1	1	3	1	1
Type of study	Offline study	Offline study	Offline study	Offline study	Offline study
Training duration	1 hr	N/A	2 hr	N/A	1 hr
Intraobserver agreement (κ)	N/A	Yes (0.68–0.84)	N/A	N/A	N/A
Interobserver agreement (κ)	Yes (0.52–0.86)	Yes (0.67–0.73)	N/A	N/A	Yes (0.48–0.68)
Conclusion	Easy to learn	Easy to learn	Easy to learn	Easy to learn	Short learning curve

pCLE: probe-based confocal laser endomicroscope, iCLE: integrated confocal laser endomicroscope, GIM: gastric intestinal metaplasia, IBD: inflammatory bowel disease, and N/A: no data.

To date there has been no study on the learning curve for GIM image interpretation by pCLE. However, there are a handful number on learning curve studies of CLE evaluating colonic polyp [5, 6] and inflammatory bowel disease (IBD) [7]. In those series, by post hoc assessment, they showed remarkable results. Kuiper et al. conducted a study to interpret 90 iCLE images of different colonic polyps including normal, regenerative, and neoplastic polyps. After a brief period of training session (30-image assessment), they found that the diagnostic accuracies by the 3 endoscopists were high (90%, 93%, and 93%, resp.). Moreover, the intra- and interobserver agreements were substantial ($\kappa = 0.67$ and 0.84, resp.) [5]. Additionally, Buchner et al. requested 11 endoscopists from different 3 centers to interpret the difference between 76 polyp images (neoplastic and non-neoplastic) obtained by pCLE. They found that the overall accuracy by 11 endoscopists was only 63% for the first 40 lesions; however, it gradually improved to 86% in the final 16 lesions. They concluded that accurate interpretation of pCLE images for predicting neoplastic colonic lesion can be learned rapidly by a wide range of GI specialists [6]. In the other aspect of colonic disease, Gaddam et al. showed the agreement in IBD mucosal readings between pCLE and histopathology improved over time with kappa values of 0.81 at the end of the study (twenty-six cases) [8]. Moreover, they collected the pCLE endoscopic skill information by using different performance parameters including total duration of the procedure, time to receive a pCLE image in focus, the ratio between total pCLE images obtained from each patient and the number of pCLE images in focus. They concluded that pCLE is easy to learn. However, the limitations of their study were only 2 blinded endoscopists included in the study and the absence of interobserver agreement analysis (Table 3). In addition, Gaddam et al. showed the substantial

interobserver agreement ($\kappa = 0.61$) in both experienced and nonexperienced observers for Barrett esophagus diagnosis by pCLE [8]. In their study, they gave 1 hr and 10 video clips to 3 beginners during the formal training session. Then, 75 high quality pCLE video clips of dysplasia and nondysplasia in Barrett esophagus were evaluated in 2 parts, starting with the initial 30 pCLE video clips evaluation and followed by the other 45 pCLE video clips after the feedback session. They showed that the accuracies of readings on the first 30 (83%) and the last 45 video clips (81%) were not statistically significant ($P = 0.51$).

There are certain limitations of the present study. The first was the lack of intraobserver agreement (test and retest validities on different beginners); therefore this study cannot show the consistency of each beginner for GIM evaluation by pCLE. Second, no external validation was assessed; therefore the result from this study may not be applicable to other centers that may have different types of beginners. Last, the result of this offline study cannot be extrapolated for the possible result of the real-time images interpretation.

In summary, the interpretation of GIM images obtained by pCLE can be learned rapidly after a short training period with at least substantial interobserver agreement. However, we cannot extrapolate the result of this study as pCLE examination for GIM diagnosis is easy to perform since the present study did not investigate the difficulty of pCLE scoping technique. And we also believe that skillful scoping technique is a requisite for the endoscopist to be able to obtain high quality pCLE images.

Acknowledgment

References

[1] J. Ferlay, H. R. Shin, F. Bray, D. Forman, C. Mathers, and D. M. Parkin, "Estimates of worldwide burden of cancer in 2008: GLOBOCAN 2008," *International Journal of Cancer*, vol. 127, no. 12, pp. 2893–2917, 2010.

[2] J. G. Fox and T. C. Wang, "Inflammation, atrophy, and gastric cancer," *Journal of Clinical Investigation*, vol. 117, no. 1, pp. 60–69, 2007.

[3] P. Correa, M. B. Piazuelo, and K. T. Wilson, "Pathology of gastric intestinal metaplasia: clinical implications," *The American Journal of Gastroenterology*, vol. 105, no. 3, pp. 493–498, 2010.

[4] R. Pittayanon, R. Rerknimitr, W. Ridtitid et al., "Magnified intelligence chromoendoscopy (FICE) plus probe-based confocal laser endomicroscopy (pCLE) for gastric intestinal metaplasia (GIM) diagnosis: a pilot feasibility trial," *Gastrointestinal Endoscopy*, vol. 73, no. 4, Article ID AB164, 2011.

[5] T. Kuiper, R. Kiesslich, C. Ponsioen, P. Fockens, and E. Dekker, "The learning curve, accuracy, and interobserver agreement of endoscope-based confocal laser endomicroscopy for the differentiation of colorectal lesions," *Gastrointestinal Endoscopy*, vol. 75, no. 6, pp. 1211–1217, 2012.

[6] A. M. Buchner, V. Gomez, M. G. Heckman et al., "The learning curve of in vivo probe-based confocal laser endomicroscopy for prediction of colorectal neoplasia," *Gastrointestinal Endoscopy*, vol. 73, no. 3, pp. 556–560, 2011.

[7] H. Neumann, M. Vieth, R. Atreya, M. F. Neurath, and J. Mudter, "Prospective evaluation of the learning curve of confocal laser endomicroscopy in patients with IBD," *Histology and Histopathology*, vol. 26, no. 7, pp. 867–872, 2011.

[8] S. Gaddam, S. C. Mathur, M. Singh et al., "Novel probe-based confocal laser endomicroscopy criteria and interobserver agreement for the detection of dysplasia in Barrett's esophagus," *The American Journal of Gastroenterology*, vol. 106, no. 11, pp. 1961–1969, 2011.

[9] R. Kiesslich, J. Burg, M. Vieth et al., "Confocal laser endoscopy for diagnosing intraepithelial neoplasias and colorectal cancer in vivo," *Gastroenterology*, vol. 127, no. 3, pp. 706–713, 2004.

[10] A. Meining, "Confocal endoscopy," *Gastrointestinal Endoscopy Clinics of North America*, vol. 19, no. 4, pp. 629–635, 2009.

[11] R. Kiesslich and M. I. Canto, "Confocal laser endomicroscopy," *Gastrointestinal Endoscopy Clinics of North America*, vol. 19, no. 2, pp. 261–272, 2009.

[12] A. L. Polglase, W. J. McLaren, S. A. Skinner, R. Kiesslich, M. F. Neurath, and P. M. Delaney, "A fluorescence confocal endomicroscope for in vivo microscopy of the upper- and the lower-GI tract," *Gastrointestinal Endoscopy*, vol. 62, no. 5, pp. 686–695, 2005.

[13] A. Hoffman, M. Goetz, M. Vieth, P. R. Galle, M. F. Neurath, and R. Klesslich, "Confocal laser endomicroscopy: technical status and current indications," *Endoscopy*, vol. 38, no. 12, pp. 1275–1283, 2006.

[14] N. Q. Nguyen and R. W. L. Leong, "Current application of confocal endomicroscopy in gastrointestinal disorders," *Journal of Gastroenterology and Hepatology*, vol. 23, no. 10, pp. 1483–1491, 2008.

[15] X. J. Xie, C. Q. Li, X. L. Zuo et al., "Differentiation of colonic polyps by confocal laser endomicroscopy," *Endoscopy*, vol. 43, no. 2, pp. 87–93, 2011.

[16] W. B. Li, X. L. Zuo, C. Q. Li et al., "Diagnostic value of confocal laser endomicroscopy for gastric superficial cancerous lesions," *Gut*, vol. 60, no. 3, pp. 299–306, 2011.

[17] K. B. Dunbar, P. Okolo III, E. Montgomery, and M. I. Canto, "Confocal laser endomicroscopy in Barrett's esophagus and endoscopically inapparent Barrett's neoplasia: a prospective, randomized, double-blind, controlled, crossover trial," *Gastrointestinal Endoscopy*, vol. 70, no. 4, pp. 645–654, 2009.

[18] A. Meining, Y. K. Chen, D. Pleskow et al., "Direct visualization of indeterminate pancreaticobiliary strictures with probe-based confocal laser endomicroscopy: a multicenter experience," *Gastrointestinal Endoscopy*, vol. 74, no. 5, pp. 961–968, 2011.

[19] K. B. Dunbar and M. I. Canto, "Confocal laser endomicroscopy in Barrett's esophagus and endoscopically inapparent Barrett's neoplasia: a prospective, randomized, double-blind, controlled, crossover trial," *Gastrointestinal Endoscopy*, vol. 72, no. 3, article 668, 2010.

[20] J. Humphris, D. Swartz, B. J. Egan, and R. W. Leong, "Status of confocal laser endomicroscopy in gastrointestinal disease," *Tropical Gastroenterology*, vol. 33, no. 1, pp. 9–20, 2012.

[21] E. Coron, J. F. Mosnier, A. Ahluwalia et al., "Colonic mucosal biopsies obtained during confocal endomicroscopy are prestained with fluorescein in vivo and are suitable for histologic evaluation," *Endoscopy*, vol. 44, no. 2, pp. 148–153, 2012.

[22] Y. T. Guo, Y. Q. Li, T. Yu et al., "Diagnosis of gastric intestinal metaplasia with confocal laser endomicroscopy in vivo: a prospective study," *Endoscopy*, vol. 40, no. 7, pp. 547–553, 2008.

[23] L. G. Lim, K. G. Yeoh, M. Salto-Tellez et al., "Experienced versus inexperienced confocal endoscopists in the diagnosis of gastric adenocarcinoma and intestinal metaplasia on confocal images," *Gastrointestinal Endoscopy*, vol. 73, no. 6, pp. 1141–1147, 2011.

[24] T. Kuiper, F. J. van den Broek, S. van Eeden, P. Fockens, and E. Dekker, "Feasibility and accuracy of confocal endomicroscopy in comparison with narrow-band imaging and chromoendoscopy for the differentiation of colorectal lesions," *The American Journal of Gastroenterology*, vol. 107, no. 4, pp. 543–550, 2012.

[25] V. Gómez, A. M. Buchner, E. Dekker et al., "Interobserver agreement and accuracy among international experts with probe-based confocal laser endomicroscopy in predicting colorectal neoplasia," *Endoscopy*, vol. 42, no. 4, pp. 286–291, 2010.

Review Article

A Review of Machine-Vision-Based Analysis of Wireless Capsule Endoscopy Video

Yingju Chen and Jeongkyu Lee

Department of Computer Science and Engineering, School of Engineering, University of Bridgeport, Bridgeport, CT 06604, USA

Correspondence should be addressed to Yingju Chen, yingjuc@bridgeport.edu

Wireless capsule endoscopy (WCE) enables a physician to diagnose a patient's digestive system without surgical procedures. However, it takes 1-2 hours for a gastroenterologist to examine the video. To speed up the review process, a number of analysis techniques based on machine vision have been proposed by computer science researchers. In order to train a machine to understand the semantics of an image, the image contents need to be translated into numerical form first. The numerical form of the image is known as *image abstraction*. The process of selecting relevant image features is often determined by the modality of medical images and the nature of the diagnoses. For example, there are radiographic projection-based images (e.g., X-rays and PET scans), tomography-based images (e.g., MRT and CT scans), and photography-based images (e.g., endoscopy, dermatology, and microscopic histology). Each modality imposes unique image-dependent restrictions for automatic and medically meaningful image abstraction processes. In this paper, we review the current development of machine-vision-based analysis of WCE video, focusing on the research that identifies specific gastrointestinal (GI) pathology and methods of shot boundary detection.

1. Introduction

Wireless capsule endoscopy (WCE) is a technology breakthrough that allows the noninvasive visualization of the entire small intestine. It was made possible because of the recent advances in low-power and low-cost of miniaturized image sensors, application-specific integrated circuits, wireless transmission technology, and light emitted diodes. This swallowable capsule technology enables the investigation of the small intestine without pain or need for sedation, thus encouraging patients to undergo GI track examinations. The first WCE was launched by Given Imaging (PillCam SB; Yokneam, Israel) in 2001. The successful launch of WCE encourages several other capsule manufacturers to develop their own products. Table 1 is a list of commercially available capsule specifications. According to Given Imaging, more than 1,200,000 patients worldwide have benefited from their PillCam endoscopy.

Although WCE allows access to the small intestine noninvasively, the average viewing time ranges between 1 and 2 hours, depending on the experience of the gastroenterologist. In order to assist the gastroenterologist to speed up the review session, machine vision researchers have proposed various systems, including automatic video summarization, general abnormality detection, specific pathology identification, shot boundary detection, and topographic video segmentation. In this paper, we review the current development of machine vision-based analysis of WCE video, focusing on the research of specific GI pathology detection and shot boundary detection. A review of current capsule endoscopy hardware development is available to the interested reader in [1]; the review of machine vision-based analysis for push enteroscopy, intraoperative enteroscopy, push-and-pull enteroscopy, and radiographic methods is beyond the scope of this paper.

2. Image Features for Abstraction

A color WCE image is a snapshot of the digestive tract at a given time. However, in a computer-aided diagnosis system, the image content semantics needs to be translated in numerical ways for interpretation. There are several ways to represent the numerical form of an image known as *image abstraction*. Among WCE applications, there are three

TABLE 1: Technical specifications of commercially available small intestine capsules.

Company	Given imaging Inc.	Olympus	IntroMedic	Jinshan
Capsule	PillCam SB/SB2	EndoCapsule	MiroCam	OMOM
Size (diameter × length)	11 mm × 26 mm	11 mm × 26 mm	11 mm × 24 mm	13 mm × 27.9 mm
Image Sensor	CMOS	CCD	CMOS	CCD
Resolution	256 × 256	NA	320×320	640 × 480
Field of View	140°/156°	145°	150∘	140 ± 10°
Image Capture Rate	2 fps	2 fps	3 fps	0.5–2 fps
Illumination	6 LEDs	6 LEDs	6 LEDs	6 LEDs
Battery Life	8 hr	8+ hr	11+ hr	8 ± 1 hr
Communication	RF	RF	HBC	RF
Approval	FDA 2001/2011	FDA 2007	FDA 2012	PRC FDA 2004

CMOS: complementary metal oxide semiconductor, CCD: charge-coupled device, LED: light-emitting diode, RF: radio frequency, HBC: human body communications, NA: not available.

(a) Esophagus (b) Stomach (c) Small Intestine (d) Colon
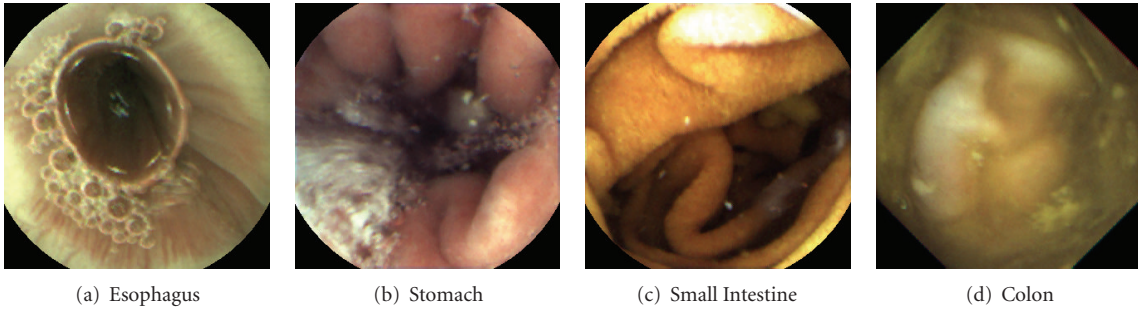
FIGURE 1: Typical images captured by WCE at different organs.

popular features for image abstraction: (1) *color*, (2) *texture*, and (3) *shape* features. Color images produced by WCE contain much useful color information and hence can be used as effective cue to suggest the topographic location of the current image.

Figure 1 shows typical images taken from each organ. In this figure, the stomach looks pinkish, the small intestine is yellowish due to the slightly straw-color of the bile, and the colon is often yellowish or greenish due to the contamination of the liquid form of faeces. Another popular image abstraction feature in medical-imaging-related applications is the texture feature [2]. In WCE applications, a unique texture pattern called "villi" can be used to distinguish the small intestine from other organs. In addition, abnormality in WCE video can be discriminated by comparing the texture patterns between normal and abnormal mucosa regions, making texture pattern a popular feature for image abstraction. Shape feature is another commonly used abstraction approach for machine vision applications. Object shapes provide strong clues to object identity, and humans can recognize objects solely on their shapes. In the following subsections, we provide a high level survey of these features along with some popular implementations.

2.1. Color. Color is a way the human visual system used to measure a range of the electromagnetic spectrum, which is approximately between 300 and 830 nm. The human visual system only recognizes certain combinations of the visible spectrum and associates these spectra into color. Today, a number of color models (e.g., RGB, HSI/HSV, CIE Lab, YUV, CMYK, and Luv) are available. Among all, the most popular color models in WCE applications are the RGB and HSI/HSV color models.

The RGB color model is probably best known. Most image-capturing devices use the RGB model, and the color images are stored in forms of two-dimensional array of triplets made of *red*, *blue*, and *green*. There are a couple of characteristics that make the RGB model the basic color space: (1) existing methods to calibrate the image capturing devices and (2) multiple ways to transform the RGB model into a linear, perceptually uniform color model. On the other hand, the main disadvantage of RGB-based natural images is the high degree of correlation between their components, meaning that if the intensity changes, all three components will change accordingly [5].

The HSI/HSV color model is another commonly used model in machine vision applications. Three components, *hue*, *saturation*, and *intensity* (or *value*), can be obtained through simple transformations of the RGB model. Hue specifies the base color, saturation specifies the purity of a color, and intensity shows how bright the color should be. Although the HSI/HSV model carries the same shortcomings as the RGB model, Gevers et al. show that HSI model is invariant to viewing orientation, illumination direction, and illumination intensity [23]. This outstanding property has

made HSI/HSV model much less sensitive to illumination changes, which is a common problem of the WCE image as the battery of the capsule weakens over time.

2.2. Texture. Texture is a fundamental property of surfaces. It can be seen almost anywhere (e.g., tree bark, grass, sand, wall, etc.). Some examples of texture analysis applications are industrial surface inspection, biomedical image analysis, and face and facial expression recognition. A common approach for discriminating WCE images is to extract mucosa texture and then classify the feature with trained classifiers. Texture feature extraction in WCE imaging is difficult because: (1) WCE images are taken by a miniature camera which has a limited range of luminance and hence suffer from illumination variations; (2) as a tiny capsule travels down the GI tract via digestive peristalsis, the moving or spinning motion of the capsule contributes to uneven illumination; (3) the battery life weakens over time; and (4) the uncertainty of a functioning digestive tract such as food residue, bubbles, faeces, and so forth is encountered. Because of these challenges, the most popular textural features are the multi-resolution and gray scale texture features.

In general, the characteristics of texture are measured by variations in the image's intensity or color. The differences between the gray level value of a reference pixel and its neighboring pixels have been used for analyzing textural properties. *Local Binary Pattern* (LBP) operator, proposed by Ojala et al. in [24], is one of the texture features that are invariant against gray scale transformation and rotation, yet computationally simple. In order to compute the texture model of a specific surface, an LBP code is computed for each pixel of this surface by comparing its gray level against those of its neighboring pixels. The final histogram of LBP codes is the texture model that represents this surface. Figure 2 is an example of a texture model that utilizes a joint LBP histogram to represent the mucosa of different organs.

Another well-known texture feature called *Gray Level Co-occurrence Matrices* (GLCM) was introduced by Haralick et al. in the 1970s [25, 26]. It belongs to the second-order statistics methods that describe spatial relationships between the reference and neighbor pixels within a local neighborhood. In this approach, texture is characterized by the spatial distribution of gray levels (or gray scale intensities) in a neighborhood. A cooccurrence matrix is defined to represent the distance and angular spatial relationship over subregion of a gray-scale image. It is calculated to show how often the pixel with gray level value occurs horizontally, vertically, or diagonally to adjacent pixels. Once the GLCMs are created, the similarity of texture pattern can be measured using the formulas as described in [25, 26].

As the size of lesion may vary in size, it is desirable to analyze the lesion and its mucosa in multiple resolutions. *Wavelet* theory has been commonly used in multiresolution analysis. In this method, an image is analyzed at various frequencies under various resolutions. Wavelet transform provides powerful insight to the spatial and frequency characterstics of an image. In image processing, the transform could be achieved using Discrete Wavelet Transform (DWT) by decomposing an image into four subbands: LL1, LH1,

HL1, and HH1 (Figure 3(a)). The LL1 subband is referred to as the *approximation component* while the remaining subbands are referred to as the *detail components*. Subband LL1 could be further decomposed to result in a two-level wavelet decomposition (Figure 3(b)). By repeating this process with subband LL2, we can obtain the three-level wavelet decomposition. This process can be repeated on the approximation component until the desired scale is reached. The coefficients in the approximation and detail components are the essential features for DWT based texture analysis and discrimination.

2.3. Shape. In WCE imaging, shape-based features are employed mostly in polyp and tumor detection. In this category, the most common process is to detect the edges first, followed by region segmentation. Geometric rules are applied to the segmented regions to construct the shape information of these regions. Although most of the objects in the real world are three-dimensional, image and video processing usually deals with two-dimensional projections of real world objects. Good descriptors should capture shape characteristics in a concise manner, and they should be invariant to scaling, rotation, translation, and various types of distortions. In addition, they should be able to handle nonrigid deformations caused by perspective transformation of two-dimensional shapes.

In machine vision, *moments* describe image content with respect to its axes. For example, the *width* of a set of points in one dimension or the *shape* of a cloud of points in a higher dimension can be measured by computing the second moment of these points. Since moments describe image content with respect to its axes, the global and detailed geometric information of an image can be captured by moments.

Gabor filters have been widely used for edge detection. Gabor filters are defined by harmonic functions modulated by a Gaussian distribution. Since *frequency* and *orientation* representations of Gabor filters are similar to those of the human visual system, a set of Gabor filters with different frequencies and orientations are found to be useful for texture-based region segmentation of an image [27]. In [28], Field introduces Log-Gabor filters and suggests that natural images are better coded by filters that have Gaussian transfer functions when viewed on the logarithmic frequency scale. Unlike Gabor filters that suffer from bandwidth limitation, Log-Gabor filters can be constructed with arbitrary bandwidth and hence can be optimized to produce a filter with minimal spatial extent.

3. Computer-Aided Diagnosis Systems

Figure 4 is an illustration of the general process flowchart of a typical WCE machine vision analysis system. It is a common practice that each image is preprocessed to enhance the accuracy of feature extraction, followed by feature refinement. The output of the feature refinement is a concise form of the image abstraction for the final classification, and the classifiers may be artificial intelligent based or rule based. In general, artificial-intelligent-based classifiers need to be trained

(a) Esophagus

(b) Stomach

(c) Small Intestine

(d) Colon
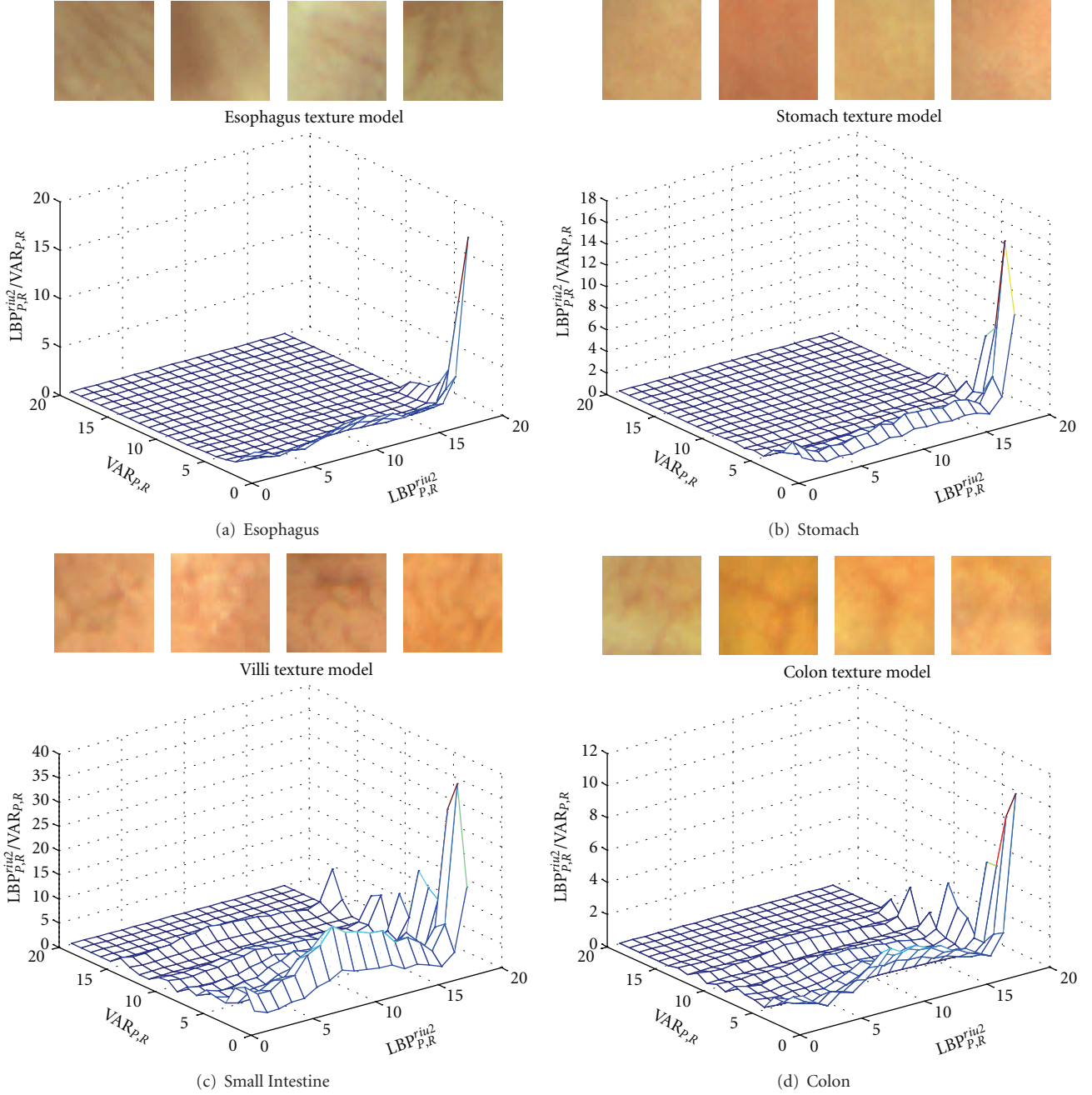
FIGURE 2: Mucosa representations based on a joint histogram of LBP operator ($LBP_{P,R}^{riu2}$) and local gray level variance ($VAR_{P,R}$).

before use, whereas rule-based classifiers utilize "*if... then...*" rules for classification which requires no training.

3.1. Shot Boundary Detection and Video Segmentation.

Temporal video segmentation is usually the first step towards automatic annotation of image sequences. It divides a video stream into a set of meaningful segments called *shots* for indexing. In conventional video segmentation, there are two types of shot transitions: *abrupt* and *gradual*. Abrupt transition is easier to detect because it occurs when the camera is stopped and restarted [29]; however, the detection of gradual transition is more difficult because it is caused by

camera operations such as zoom, tilt, and pan. Although there are algorithms for shot transition detection, these are not suitable for WCE. WCE video is created without any stops; therefore, these algorithms do not work well in WCE. Instead of modeling shot boundary detection by camera operations, it is preferred that shots are modeled by similar semantic content or by the digestive organ.

In order to provide the gastroenterologist with a quick glance of the video contents, WCE researchers utilize digestive peristalses and image analysis techniques for shot boundary detection and organ boundary detection. Vu et al. proposed a coherent three-stage procedure to detect

(a)

(b)

Figure 3: Image decomposition using DWT where (a) represents a one-level wavelet decomposition and (b) represents a two-level wavelet decomposition.

Figure 4: General steps involving in computer-aided diagnosis (CAD) system where gray boxes may be optional.

Figure 5: A shot detection scheme based on event boundary detection approach as described in [3].

vector to classify every 10th image of the video. The final classification result was assessed using a 4-state hidden Markov model for topographical segmentation. In [3], two color vectors that were created with hue and saturation components of HSI model were used to represent the entire video. Spectrum analysis was applied to detect sudden changes in the peristalsis pattern. Chen et al. assumed that each organ has a different peristalsis pattern and hence, any change in the pattern may suggest an event in which a gastroenterologist may be interested (see Figure 5). Energy and High Frequency Content (HFC) functions are used to identify such change while two other specialized features aim to enhance the detections of duodenum and cecum.

3.2. Significant Medical Event Detection. The primary use of capsule endoscopy is to find the source of bleeding and abnormality in the small intestine. Shot boundary detection may help to speed up the review by grouping images with similar semantics, but it may not detect medical significant events other than acute bleeding. A common trait of aforementioned algorithms is to group images by global features such as the distribution of color; however detail features such as patches of mucosa deficiency are often neglected. Most of medical significant events of WCE only account for a handful of images of the entire video, lesions in these images may not result in significant shifts in the global features and hence cannot be detected by shot boundary detection algorithms. Acute bleeding that lasts for several dozens of consecutive images may be bundled into one shot, since a vast amount

intestinal contractions in [30]. They utilized changes in intestinal edge structure of the intestinal folds for contraction assessment. The output is contraction-based shots. Another shot detection proposed by Iakovidis et al. was based on nonnegative matrix factorization (NMF) [31]. A full length of WCE video was uniformly sampled to generate consecutive nonoverlapping video segments followed by a dimensionality reduction algorithm. Fuzzy C-means was applied for extraction of most representative frames and the results were enhanced by applying symmetric NMF to the symmetric matrices. The final cluster indicators (or shots) were obtained using nonnegative Lagrangian relaxation. Another shot detection scheme based on organ was proposed by Mackiewicz et al. in [32]. The authors utilized three-dimension LBP operator, color histogram, and motion

(a)   (b)

FIGURE 6: A bleeding detection scheme as described in [3].

of fresh blood may cause noticeable shifts among the global feature distribution. In order to detect significant medical events that contain little or no temporal relationship with their consecutive image frames (e.g., ulcers, polyps, tumors, etc.), imagewise semantic analysis is inevitable. In this subsection, we 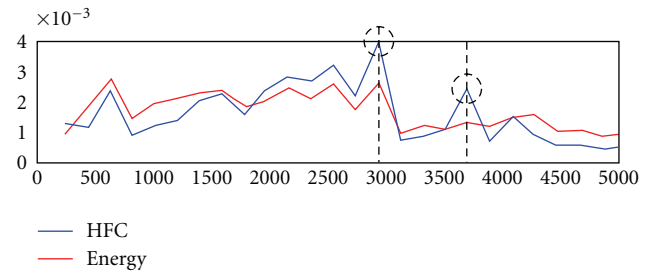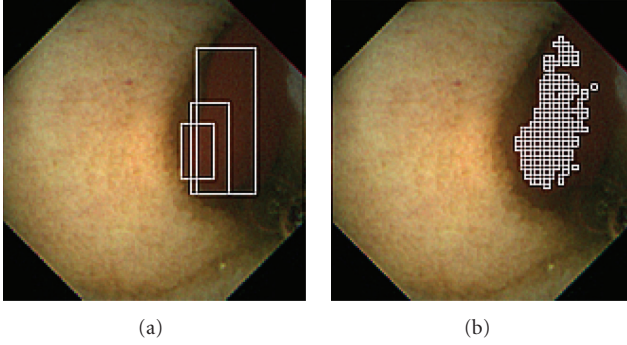review the machine vision analysis literature on specific GI pathology identification, namely, *bleeding*, *ulcer*, *polyp*, and *tumor*.

The visual appearance of bleeding images is bright red. However, depending on the lifetime of blood, it could be black or tarry. Lau and Correia proposed a two-step system that discriminates bleeding and nonbleeding images under the HSV color model [6]. The classification is rule-based with certain combinations between color luminance and saturation. Their system classifies images into one of the following categories: (1) nonbleeding, (2) low-intensity bleeding, (3) bleeding, and (4) high-intensity bleeding. Another system proposed by Liu and Yuan [7] uses *Support Vector Machines* (SVMs) to classify images using color features extracted in the RGB color model. In [9], Penna et al. utilize a Reed-Xiaoli detector for bleeding regions and normal mucosa region discrimination. Karargyris and Bourbakis [10] propose a mechanism that combines Karhunen-Loeve color transformation, fuzzy region segmentation, and local-global graphs. Li and Meng [11] adopt neural network classifiers for bleeding imaging classification. The feature vector consists of color texture feature and statistical measures. The color texture feature is obtained from chrominance moment, while the statistical measures were obtained from the uniform LBP histogram.

The physician usually observes GI bleeding based on a set of medical criteria such as potential causes or sources of bleeding, bleeding frequency, and amount of blood loss. To mimic this process, Chen et al. [3] use a macro-micro hybrid approach for bleeding detection (see Figure 6). Unlike a binary classification approach, their system shows a potential bleeding distribution. In the macroapproach, each potential bleeding area is extracted using pyramid segmentation. Depending on the angle of the hue component, each suspicious bleeding segment is assigned with various weights for bleeding assessment. In the microapproach, each image is divided into 7×7 blocks and each block is validated against specific ranges of hue and saturation components for bleeding detection. Each image is analyzed using the two

approaches and the final bleeding distribution is the average score of the two approaches.

With regard to polyp detection, Karargyris et al. [17] suggest a rule-based classification system that utilizes log Gabor filters and SUSAN edge detectors. In [18], Li and Meng conduct a comparative study between two-shape features, MPEG-7 region based shape descriptor and Zernik Moments. The classifier is based on multilayer perceptron (MLP) neural networks. The authors conclude that Zernik Moments are superior to MPEG-7 region based shape descriptors.

With regard to tumor detection, Karkanis et al. [21] utilize a texture feature for tumor discrimination and the classifier is a multilayer feed forward neural networks (MFNNs). In [22], Li and Meng propose a feature vector consisting of LBP and DWT. The experiment result shows that their proposed feature outperforms both original rotation invariant LBP and color wavelet covariance texture features.

For ulcer detection, Li and Meng [13, 14] propose a feature vector that consists of curvelet transformation and uniform LBP. However, this approach performs an exhaustive comparison regardless of the unique visual appearance of an ulcer and hence, the performance could be slow. On the other hand, Karargyris and Bourbakis [15] present a segmentation scheme utilizing log Gabor filters, color texture features, and an SVM classifier. Although the authors considered the unique visual appearance of ulcers, the HSV color model they chose suffers the same shortcoming as the RGB color model. Chen and Lee [4] propose a four-step detection scheme (see Figure 7). The first step is to create a saliency map emphasizing the ulcerated mucosa, followed by initial saliency segmentation. Second, Gabor filters are applied to find the contour for saliency region refinement. When the saliency region is refined and extracted, a feature vector is formed using LBP and six statistical measurements along the region contour. Finally, the feature vector is validated by an SVM classifier for ulcer detection.

4. Discussion

Human beings are capable of interpreting images at different levels. For example, we can interpret images based on low level features such as color, shape, texture, or based on high level semantics such as events or abstract objects. A computer only interprets images based on low level features and thus, choosing the right image feature becomes critical for computer-aided diagnosis systems. Generally, feature selection for image abstraction is modeled to mimic a human's understanding of visual content. For example, the dominant color of fresh blood is red, hence it is desirable to use the color feature for bleeding detection. The color and amount of blood are important cues for bleeding detection; however, color alone does not always discriminate images correctly. According to experiment results from [3, 6–9, 11, 12], the accuracy of bleeding detection ranges from the lower 70% to the upper 90%. Bleeding image detection based on predefined threshold values is especially difficult since the image quality is susceptible to illumination and camera

Saliency map

Edge detection with
Gabor filters

And

Saliency region

(1) Feature extraction along region contours

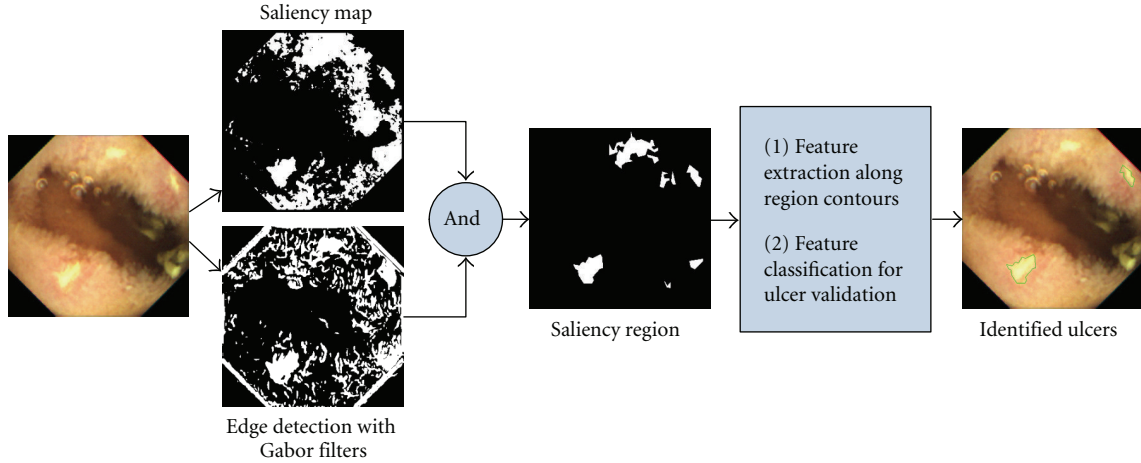(2) Feature classification for ulcer validation

Identified ulcers

FIGURE 7: Ulcer detection scheme described in [4].

motion and also due to the fact that visual color appearance of an organ varies from person to person.

Currently, detection rate for ulcer, polyp, and tumor is also not perfect. According to [12–15], the ulcer detection accuracy for image-based experiments ranges from 90% to 96%. The detection rate for polyp, as published in [16–18], ranges from 73% to 89%. As for tumor detection, the detection rate ranges from 96% to 98% [19–22]. Today, the image quality of WCE imaging is considered low when compared to conventional endoscopes. Commercially available WCEs have very limited flexibility in terms of capsule control. The hardware design limitation of WCE (e.g., battery life, no manual operation support, etc.) and uncertainty operating inside a functioning digestive tract (e.g., food residue, faeces, contraction, etc.) make developing an efficient computer aided diagnosis system a challenging task. Although innovative approaches are introduced to enhance the quality of WCE images, the accuracy of detection remains low when compared to other image processing applications such as motion detection in surveillance video or industrial surface inspection.

Meanwhile, the experimental results show a wide variance in accuracy, one possible cause could be the size of image collection. Although a full length WCE video contains at least 55,000 images, most of the experimental results that claim high accuracy were tested with less than 1,000 images (Table 2). Among the literature in this paper, only [3, 8, 32] used full-length videos, other works were validated against privately selected image set. The aforementioned hardware limitation of WCE coupled with the lack of publicly accessible WCE video database makes it difficult for researchers to measure their work against some baseline. In addition, the fact that only a handful of significant images observed in each video also makes it difficult to effectively characterize the visual appearance for pathology assessment.

The research of effective image retrieval from an image or video database has been active since 1970s. However, a robust image understanding at the machine level remains an open issue. In the 1970s, the most popular method was text-based search. In this approach, only images that are annotated with text are retrieved. If there were any error in the annotation, the result could be erroneous. In the 1990s, content-based image retrieval (CBIR) was introduced as an alternative to text search. Low level features such as color, texture, and shape features are extracted to search images with similar visual features. Although there are sophisticated algorithms to describe color, texture, and shape features, these low level features cannot be compared to the human cognitive concept of visual content. The gap between human and computational ability to recognize visual content has been termed the *semantic gap* [33]. Semantic-based image retrieval was introduced in 2000s to create semantic content representation for images. This method allows users to perform a text query based on the semantic they have in mind for image retrieval. However, to be able to describe an image in semantic terms as identified by users remains an open issue in the image processing world. In particular, we are yet to see any work that offers semantic-based image retrieval tool for physicians to query WCE videos.

5. Conclusion

WCE technology is fairly new and is originally intended for the detection of obscure GI bleeding. However, GI specialists are still uncovering other potential uses of WCE for abnormal indications. Nevertheless, the need for automatic GI pathology identification is in strong demand. In this paper, we reviewed a variety of works that are related to shot boundary detection and GI abnormality detection. The main image abstraction approaches for WCE video can be classified into three image features: color, texture, and shape features. Depending on the visual characteristics of each pathology targeted, a suitable feature form is selected for image abstraction. Currently, most bleeding-related applications utilize color-based features, while other GI disorders utilize texture and shape features. Among the surveyed literature, we focus on the research that identifies specific GI pathology. This way we can learn the relationships between GI pathology and machine vision. Despite the effort that researchers put for abnormality detection, it is almost impossible to

TABLE 2: Summary of abnormality types, features and claimed experimental results.

Paper	Pathology				Feature			Experiment results		
	Bleeding	Polyp	Tumor	Ulcer	Color	Texture	Shape	Image count	Sensitivity	Specificity
Chen et al. [3]	√				√			1,857,657	71.54%	N/A
Lau and Correia [6]	√				√			1,705	88.30%	N/A
Liu and Yuan [7]	√				√			800	99.73%	98.89%
Giritharan et al. [8]	√				√			275,000	83.1%	93.6%
Penna et al. [9]	√				√			1,111	92%	88%
Karargyris and Bourbakis [10]	√						√	N/A	N/A	N/A
Li and Meng [11, 12]	√			√	√			200	92.6%	91%
Li and Meng [13, 14]				√		√		100	93.28%	91.46%
Karargyris and Bourbakis [15]				√			√	50	100%	67.5%
Iakovidis et al. [16]		√				√		4,000	87.5%	N/A
Karargyris and Bourbakis [17]		√					√	50	75%	73.3%
Li et al. [18]		√					√	300	89.8%	82.5%
Barbosa et al. [19]			√			√		192	98.7%	96.6%
Barbosa et al. [20]			√			√		600	97.4%	97.5%
Karkanis et al. [21]			√			√		N/A	N/A	N/A
Li and Meng [22]			√			√		300	97.33%	96%

Sensitivity = Number of True Postives/(Number of True Postives + Number of False Negatives). Sensitivity of 100% means no positives are incorrectly marked as negative. In other words, the test recognizes all positives.
Specificity = Number of True Negatives/(Number of True Negatives + Number of False Postives). Specificity of 100% means no negatives are incorrectly marked as positive. In other words, the test recognizes all negatives.
N/A: data is not available.

compare the performance of different implementations due to the lack of a publicly accessible WCE video database. Consequently, machine vision researchers are forced to test their implementation against relatively small image sets and thus slows down the development of commercially available tools for WCE video review sessions.

Disclosure

The authors have no relevant financial or nonfinancial relationships to disclose.

References

[1] G. Ciuti, A. Menciassi, and P. Dario, "Capsule endoscopy: from current achievements to open challenges," *IEEE Reviews in Biomedical Engineering*, vol. 4, pp. 59–72, 2011.

[2] M. Tuceryan and A. K. Jain, *Texture Analysis, Handbook of Pattern Recognition & Computer Vision*, World Scientific Publishing, River Edge, NJ, USA, 2nd edition, 1999.

[3] Y. J. Chen, W. Yasen, J. Lee, D. Lee, and Y. Kim, "Developing assessment system for wireless capsule endoscopy videos based on event detection," in *Proceedings of the Medical Imaging: Computer-Aided Diagnosis*, vol. 7260 of *Proceedings of SPIE*, Orlando, Fla, USA, February 2009.

[4] Y. Chen and J. Lee, "Ulcer detection in wireless capsule endoscopy videos," in *Proceedings of the ACM Multimedia*, Nara, Japan, October 2012.

[5] M. Tkalcic and J. F. Tasic, "Colour spaces: perceptual, historical and applicational background," in *Proceedings of the The IEEE Region 8 EUROCON: Computer as a Tool*, vol. 1, pp. 304–308, 2003.

[6] P. Y. Lau and P. L. Correia, "Detection of bleeding patterns in wce video using multiple features," in *Proceedings of the Annual International Conference of the IEEE Engineering in Medicine and Biology Society*, pp. 5601–5604, 2007.

[7] J. Liu and X. Yuan, "Obscure bleeding detection in endoscopy images using support vector machines," *Optimization and Engineering*, vol. 10, no. 2, pp. 289–299, 2008.

[8] B. Giritharan, Y. Xiaohui, L. Jianguo, B. Buckles, O. JungHwan, and T. S. Jiang, "Bleeding detection from capsule endoscopy videos," in *Proceedings of the 30th Annual International Conference of the IEEE Engineering in Medicine and Biology Society (EMBS '08)*, pp. 4780–4783, August 2008.

[9] B. Penna, T. Tilloy, M. Grangettoz, E. Magli, and G. Olmo, "A technique for blood detection in wireless capsule endoscopy images," in *Proceedings of the 17th European Signal Processing Conference (EUSIPCO '09)*, pp. 1864–1868, Glasgow, UK, 2009.

[10] A. Karargyris and N. Bourbakis, "A methodology for detecting blood-based abnormalities in wireless capsule endoscopy videos," in *Proceedings of the 8th IEEE International Conference on BioInformatics and BioEngineering (BIBE '08)*, pp. 1–6, October 2008.

[11] B. Li and M. Q. H. Meng, "Computer-aided detection of bleeding regions for capsule endoscopy images," *IEEE Transactions on Biomedical Engineering*, vol. 56, no. 4, pp. 1032–1039, 2009.

[12] B. Li and M. Q. H. Meng, "Computer-based detection of bleeding and ulcer in wireless capsule endoscopy images by chromaticity moments," *Computers in Biology and Medicine*, vol. 39, no. 2, pp. 141–147, 2009.

[13] B. Li and M. Q. H. Meng, "Ulcer recognition in capsule endoscopy images by texture features," in *Proceedings of the 7th World Congress on Intelligent Control and Automation, (WCICA '08)*, pp. 234–239, June 2008.

[14] B. Li and M. Q. H. Meng, "Texture analysis for ulcer detection in capsule endoscopy images," *Image and Vision Computing*, vol. 27, no. 9, pp. 1336–1342, 2009.

[15] A. Karargyris and N. Bourbakis, "Identification of ulcers in wireless capsule endoscopy videos," in *Proceedings of the IEEE International Symposium on Biomedical Imaging: From Nano to Macro (ISBI '09)*, pp. 554–557, July 2009.

[16] D. K. Iakovidis, D. E. Maroulis, S. A. Karkanis, and A. Brokos, "A comparative study of texture features for the discrimination of gastric polyps in endoscopic video," in *Proceedings of the 18th IEEE Symposium on Computer-Based Medical Systems*, pp. 575–580, June 2005.

[17] A. Karargyris and N. Bourbakis, "Identification of polyps in wireless capsule endoscopy videos using Log Gabor filters," in *Proceedings of the IEEE/NIH Life Science Systems and Applications Workshop (LiSSA '09)*, pp. 143–147, April 2009.

[18] B. Li, M. Q. H. Meng, and L. Xu, "A comparative study of shape features for polyp detection in wireless capsule endoscopy images," in *Proceedings of the 31st Annual International Conference of the IEEE Engineering in Medicine and Biology Society (EMBC '09)*, pp. 3731–3734, September 2009.

[19] D. J. C. Barbosa, J. Ramos, and C. S. Lima, "Detection of small bowel tumors in capsule endoscopy frames using texture analysis based on the discrete wavelet transform," in *Proceedings of the 30th Annual International Conference of the IEEE Engineering in Medicine and Biology Society (EMBS '08)*, pp. 3012–3015, August 2008.

[20] D. J. C. Barbosa, J. Ramos, J. H. Correia, and C. S. Lima, "Automatic detection of small bowel tumors in capsule endoscopy based on color curvelet covariance statistical texture descriptors," in *Proceedings of the 31st Annual International Conference of the IEEE Engineering in Medicine and Biology Society (EMBC '09)*, pp. 6683–6686, September 2009.

[21] S. A. Karkanis, G. D. Magoulas, D. K. Iakovidis, D. E. Maroulis, and N. Theofanous, "Tumor recognition in endoscopic video images using artificial neural network architectures," in *Proceedings of the 26th EUROMICRO Conference*, pp. 423–429, 2000.

[22] B. Li and M. Q. H. Meng, "Small bowel tumor detection for wireless capsule endoscopy images using textural features and support vector machine," in *Proceedings of the IEEE/RSJ International Conference on Intelligent Robots and Systems (IROS '09)*, pp. 498–503, October 2009.

[23] J. V. D. W. T. Gevers and H. Stokman, *Color Feature Detection, Color Image Processing: Methods and Applications*, CRC/Taylor & Francis, Boca Raton, Fla, USA, 2007.

[24] T. Ojala, M. Pietikäinen, and T. Mäenpää, "Multiresolution gray-scale and rotation invariant texture classification with local binary patterns," *IEEE Transactions on Pattern Analysis and Machine Intelligence*, vol. 24, no. 7, pp. 971–987, 2002.

[25] R. M. Haralick, "Statistical and structural approaches to texture," *Proceedings of the IEEE*, vol. 67, no. 5, pp. 786–804, 1979.

[26] R. M. Haralick, K. Shanmugam, and I. Dinstein, "Textural features for image classification," *IEEE Transactions on Systems, Man and Cybernetics*, vol. 3, no. 6, pp. 610–621, 1973.

[27] J. G. Daugman, "Uncertainty relation for resolution in space, spatial frequency, and orientation optimized by two-dimensional visual cortical filters.," *Journal of the Optical Society of America A*, vol. 2, no. 7, pp. 1160–1169, 1985.

[28] D. J. Field, "Relations between the statistics of natural images and the response properties of cortical cells.," *Journal of the Optical Society of America A*, vol. 4, no. 12, pp. 2379–2394, 1987.

[29] I. Koprinska and S. Carrato, "Temporal video segmentation: a survey," *Signal Processing: Image Communication*, vol. 16, no. 5, pp. 477–500, 2001.

[30] H. Vu, T. Echigo, R. Sagawa et al., "Detection of contractions in adaptive transit time of the small bowel from wireless capsule endoscopy videos," *Computers in Biology and Medicine*, vol. 39, no. 1, pp. 16–26, 2009.

[31] D. K. Iakovidis, S. Tsevas, and A. Polydorou, "Reduction of capsule endoscopy reading times by unsupervised image mining," *Computerized Medical Imaging and Graphics*, vol. 34, no. 6, pp. 471–478, 2010.

[32] M. Mackiewicz, J. Berens, and M. Fisher, "Wireless capsule endoscopy color video segmentation," *IEEE Transactions on Medical Imaging*, vol. 27, no. 12, pp. 1769–1781, 2008.

[33] A. W. M. Smeulders, M. Worring, S. Santini, A. Gupta, and R. Jain, "Content-based image retrieval at the end of the early years," *IEEE Transactions on Pattern Analysis and Machine Intelligence*, vol. 22, no. 12, pp. 1349–1380, 2000.

Review Article

Contrast-Enhanced Harmonic Endoscopic Ultrasonography in Pancreatic Diseases

Can Xu,[1, 2] Zhaoshen Li,[2] and Michael Wallace[1]

[1] *Division of Gastroenterology and Hepatology, Mayo Clinic, Jacksonville, FL 32224, USA*
[2] *Department of Gastroenterology, Changhai Hospital, Second Military Medical University, Shanghai 200433, China*

Correspondence should be addressed to Michael Wallace, wallace.micheal@mayo.edu

Endoscopic ultrasonography (EUS) is the most sensitive imaging method for diagnosis of pancreatic tumors. However, it still has limits in the differentiation between pancreatic cancers and inflammatory tumor-like masses. A novel technology, contrast-enhanced harmonic EUS (CH-EUS), has been developed recently. It can visualize both parenchymal perfusion and microvasculature in pancreas without Doppler-related artifacts. Therefore, it is superior to EUS and CT in detecting small pancreatic masses and differential diagnosis of pancreatic masses. CH-EUS could be used for adequate sampling of pancreatic tumors and may predict the pathological features of the pancreatic solid lesions but still cannot replace EUS-FNA now.

1. Introduction

Pancreatic cancer is one of the most devastating diseases with long-term survival being still rare. Therefore, there is an urgent need to develop a method for diagnosing pancreatic cancer at an early curable stage. Endoscopic ultrasound (EUS) is considered to be the most sensitive technology in detecting small pancreatic tumors [1, 2]. However, the differentiation between pancreatic tumors and inflammatory tumor-like masses still remains difficult. The evaluation of vascularity using ultrasound contrast may assist the differentiation of cancers from benign tumors.

Contrast-enhanced harmonic endoscopic ultrasonography (CH-EUS) is a novel technology which observes both parenchymal perfusion and microvasculature in the pancreas and has been reported to improve characterization of pancreatic cancers from other pancreatic diseases [3, 4].

In this paper, we will describe the development of a new technology CH-EUS and will review the advantages and its value in clinical practice in pancreatic diseases [5].

2. Development of CH-EUS

Power-Doppler and color-Doppler have been used for contrast enhanced transabdominal US (CE-US) until recently. Although the contrast agent selectively enhances the useful signal, the main disadvantage of these techniques is the presence the inevitable artifacts such as blooming and overpainting [3].

CE harmonic US (CH-US) is a technique that is able to detect signals from microbubbles in vessels with very slow flow without Doppler-related artifacts [5].

CH-US is used to characterize tumor vascularity in liver and pancreas. It helps to differential diagnose of benign and malignant liver tumors mainly because of the dual blood supply of the liver via the arterial supply and liver-specific portal vessels. In contrast to liver, pancreas does not contain a dual vascular system. But, several studies showed promising results in differentiating malignant from benign pancreatic lesions in analyzing vascularity with CH-US [6, 7].

Recently, contrast-enhanced EUS with Doppler mode (CE-EUS) employing ultrasound contrast agents, which indicate vascularization in pancreatic lesions, has been found to be useful in the differential diagnosis of pancreatic tumors, especially small pancreatic tumors. Sakamoto et al. [8] compared CE-CT and CE-EUS by power Doppler mode using sonographic contrast agent Levovist for detection and differential diagnosis of pancreatic tumors in 156 consecutive patients with suspected pancreatic tumors. Thirty-six of 156 patients examined had tumors of ≤2 cm. The results

showed that EUS had significantly higher sensitivity (94.4%) for detection of pancreatic carcinomas of 2 cm or less in comparison to CE-CT (50%). For small pancreatic tumor of ≤ 2 cm, sensitivities for differentiating ductal carcinomas from other tumors were 50.0%, 11.0%, and 83.3% for CE-CT, Power Doppler or color Doppler mode EUS (PD-EUS) and CE-EUS. CE-EUS was significantly more sensitive than PD-EUS and CE-CT. CE-EUSs are more sensitive than CE-CT in the detection and the differentiation of small pancreatic tumors.

However, just like CE-US, CE-EUS has a couple of limitations such as blooming artifacts, poor spatial resolution, and low sensitivity to slow flow. Consequently, contrast-enhanced harmonic EUS (CH-EUS) with a second-generation ultrasound contrast agent was developed recently. The CH-EUS technique is expected to improve the differential diagnosis of pancreatic disease in the future [9].

In 2005, Dietrich et al. [10] first described this new method with a preliminary prototype in six patients by injection of the second generation of contrast agent Sonovue which is composed of microbubbles of sulfur hexafluoride. The technique was subsequently improved by Kitano and his study group in 2008 [11]. They reported their study with a dedicated contrast harmonic method by using a prototype echoendoscope with a broad-band transducer with Sonovue in patients with pancreatobiliary diseases, gastrointestinal stromal tumors, and lymph node metastases. This feasibility study showed that an optical mechanical index of 0.4 allowed successful visualization of parenchymal perfusion and microvasculature of the pancreas during real-time imaging. However, contrast-enhanced power-Doppler EUS (CE-EUS) failed to depict images of the fine vessels and parenchymal perfusion, whereas blooming artifacts of large vessels were observed. These indicated that the contrast harmonic method was superior to the CE-EUS and it could improve the accuracy in evaluate tissue vasculature with EUS imaging.

3. Endoscope Scope and Contrast Agents for CH-EUS

The CH-EUS endoscope has a broad-band transducer and a specified imaging mode. An echoendoscope which is developed for CH-EUS (GF-UCT260, Olympus medical systems, Tokyo, Japan) is now commercially available. The ultrasound image processor for CH-EUS is the Aloka ProSound SSD α-10 (Aloka, Tokyo, Japan). CH-EUS technology can detect signals from microbubbles in vessels with a very slow flow without Doppler-related artifacts and can be used to characterize parenchyma perfusion and the vascular structures of pancreatic lesions. Contrast agents are made of gas-filled microbubbles encapsuled by a phospholipid or albumin shell. They are categorized into first and second generation based on the capability for transpulmonary passage and the half-life in the human body. Sonovue and Sonazoid are the most commonly used second-generation contrast agents which produce harmonic signals at low acoustic powers and thus are suitable for EUS imaging at low acoustic

Table 1: Pancreatic lesions with different vascular patterns in CH-EUS.

Lesions	Vascular patterns
Pancreatic carcinomas	Hypovascular
Neuroendocrine tumors	Hypervascular
Benign lesions	Isovascular
IPMN	Exclude avascular regions (mural nodules with enhancement)

powers. Sonovue (Bracco imaging, Milan, Italy) is composed of microbubbles of sulfur hexafluoride within a phospholipid membrane. Sonazoid (Daiichi-Sankyo, Tokyo, Japan; GE Healthcare Milwaukee,WI) consists of perfluorobutane microbubbles with a diameter of 2-3 μm surrounded by a lipid membrane [5]. The clinically used contrast agents are safe and there were no severe long-lasting adverse effects observed.

4. CH-EUS in Pancreatic Diseases

Pancreatic solid masses are characterized according to the vascular patterns observed on CH-EUS images. The different lesions have different specialized vascular patterns (Table 1).

5. Is CH-EUS Superior to CT or MRI?

Computed tomography (CT) and magnetic resonance imaging (MRI) are also widely used in pancreatic diseases. Comparing with CT and MRI, EUS has been reported to have higher sensitivity and specificity in the diagnosis of pancreatic tumors for the ability to place the EUS transducer in direct proximity to the pancreas enables accurate preoperative staging of cancer [12].

Kitano et al. [2] reported that CH-EUS was superior to multidetector computed tomography (MDCT) in diagnosing small (≤ 2 cm) pancreatic carcinomas ($P < 0.05$). In all 12 neoplasms that MDCT failed to detect, 7 ductal carcinomas and 2 neuroendocrine tumors had hypoenhancement and hyperenhancement on CH-EUS, respectively. However, CH-EUS and MDCT did not differ significantly in diagnostic ability with regard to all pancreatic lesions. Michiko et al. [13] compared CH-EUS using Sonazoid as contrast agent with CT and MRI; he demonstrated that the vascular image on CH-EUS was more precise than CT and MRI. CH-EUS may become a new investigation of tumor vasculature, especially for evaluation of pancreatic mass lesions. Intraductal papillary mucinous neoplasms (IPMNs) are a unique entity of pancreatic tumor with a wide spectrum of histological differentiation from hyperplasia to invasive carcinoma. Ohno et al. [14] reported that only CE-EUS revealed mural nodules in 3 (27.3%) of the 11 patients with malignant IPMN treated with resection which were not detected by CT or MRI. Form all the above-reported results, we can see that CH-EUS is superior to CT and MRI scan in diagnosis of pancreatic tumors with higher sensitivity and specificity.

6. Is CH-EUS Better Than Conventional EUS?

CH-EUS is an EUS system with a broad-band transducer which enabled the visualization of microvessels and the parenchymal perfusion of the pancreas. It has been shown that most pancreatic cancers exhibit hypovascular heterogeneous enhancement with irregular network-like microvessels. Moreover, it can diagnose pancreatic cancers with a high sensitivity (89–92%) [15]. The same group also reported that CH-EUS is much better than conventional EUS in clearly depicting the outline of six pancreatic carcinomas [2]. A quantitative CH-EUS study showed that the size of the pancreatic mass was assessed significantly effectively by CH-EUS compared with conventional EUS [16]. Recently, Fusaroli et al. [17] reported that CH-EUS could overcome some of the limitations of the conventional EUS, such as confounding factors, biliary stents, and chronic pancreatitis, and could improve the diagnostic accuracy. In their study CH-EUS detected small hypoenhancing lesions clearly in 7 patients who had uncertain standard EUS findings because of biliary stents ($n = 5$) or diffuse chronic pancreatitis ($n = 2$). The final diagnosis was adenocarcinoma in all these patients. In this respect, CH-EUS provided an increase in diagnostic yield of pancreatic adenocarcinoma of almost 8%. Hypovascularity as a sign of malignancy in CH-EUS obtained 92% sensitivity and 100% specificity. A recent pilot study showed that the rated as undecided/indeterminate with EUS and CH-EUS was 13.3% versus 3.3% ($P = 0.35$), and CH-EUS adds minimal imaging time and is accurate, with small improvement over EUS [18].

EUS is probably the most useful method available for evaluating pancreatic cystic lesions, particularly intraductal papillary mucinous neoplasms (IPMN) [19]. Diagnosis of IPMN by EUS depends on whether a mural nodules are detected; moreover, the mural nodule including the size observed by EUS was a reliable preoperative diagnostic finding capable of distinguishing low-risk and high-risk IPMN [20]. However, it is sometimes very difficult to discriminate sludge or mucous clots from mural nodules by conventional EUS. Results showed that CH-EUS could exclude avascular regions (mucous clots), whereas it depicts the mural nodules with enhancement. Therefore, CH-EUS might improve the ability of EUS in depicting mural nodules of IPMN [11, 15].

7. Could CH-EUS Aid the Differential Diagnosis of Pancreatic Diseases?

Distinguishing pancreatic adenocarcinoma from other pancreatic masses remains challenging with current imaging techniques. So several study aimed to evaluate the accuracy of CH-EUS in differentiate diagnosis for pancreatic masses. Napoleon's pilot study [21] revealed that of all 18 lesions with a hypointense signal on CH-EUS, 16 were adenocarcinomas. The sensitivity, specificity, negative predictive value (NPV), positive predictive value (PPV), and accuracy of hypointensity for diagnosing pancreatic adenocarcinoma were 89%, 88%, 88%, 89%, and 88.5%, compared with corresponding values of 72%, 100%, 77%, 100%, and 86% for EUS-FNA. Therefore, they concluded that CH-EUS with the new Olympus prototype device successfully visualized the microvascular pattern in pancreatic solid lesions, and might be useful for distinguishing adenocarcinomas from other pancreatic masses.

The majority of cases of both pancreatic cancer and chronic pancreatitis were hypoenhanced and visual discrimination was not possible. A study about CH-EUS for the quantitative assessment of uptake after contrast injection showed that it can aid differentiation between benign and malignant masses. The therapeutic strategy has not been changed after contrast medium injection during CH-EUS [16]. Though the application of CH-EUS in the differential diagnosis of chronic pancreatitis and pancreatic cancer is promising, it still cannot replace the role of EUS-FNA nowadays.

8. Could CH-EUS Help Preoperative T-Staging?

In pancreaticobiliary cancers, preoperative T-staging is of great importance to guide the appropriate treatment. EUS has been widely used for local T-staging of pancreaticobiliary cancers. The accuracy of EUS for tumor staging has been shown in a lot of studies to be significantly better than that of any other imaging modalities. However, the precise preoperative T-staging still remains a challenge.

A Japanese study group compared the T-staging accuracy of CH-EUS with use of Sonazoid and conventional harmonic EUS (H-EUS). The results showed H-EUS misstaged the depth of invasion to pancreas (T3) as T2 in a case of ampulla cancer, and misdiagnosed T2 stage of gallbladder cancer as adenomyomatosis (T0) localized in the surface of gallbladder wall. Moreover, H-EUS overstaged two cases of pancreatic carcinoma (T2) and two cases of extrahepatic bile duct carcinoma (T3) without portal vein invasion as T3 and T4 with portal vein invasion, respectively. However, CH-EUS correctly staged all these 6 cases. The overall T-staging accuracy of CH-EUS was significantly higher than H-EUS at 92.4% (24/26) and 69.2% (18/26), respectively ($P < 0.05$). The specificity of CH-EUS in detection of portal vein involvement was relatively high compared to H-EUS (100% versus 82.6%). Therefore, The depth of invasion of biliary and ampulla cancer and vascular invasion of pancreatic and biliary cancer was demonstrated more clearly with CH-EUS compared to H-EUS. CH-EUS may improve the accuracy of preoperative T-staging of pancreaticobiliary cancer [22].

However, the results in another study that used quantitative CH-EUS for discrimination of solid pancreatic masses showed that the adenocarcinoma staging was not modified with application of CH-EUS technology compared with conventional EUS [16]. Until now it is still controversial if CH-EUS could help preoperative T-staging. Therefore, further study with more cases is needed to answer this question.

9. Could CH-EUS Replace EUS-Guided FNA (Avoid FNA)?

EUS-guided FNA is an accurate and safe technique to confirm the diagnosis of pancreatic cancer. The results of the EUS-FNA influenced the clinical management of the patients [23, 24]. A recent meta-analysis revealed that EUS-FNA has a high positive predictive value (99%) and a reasonable negative predictive value (64%). Because of the possible false-negative results, deciding the treatment strategy for patients with negative EUS-FNA findings still remains a challenge.

A pilot study of 35 patients compared CH-EUS and EUS-FNA for the identification of pancreatic carcinomas, the sensitivity of CH-EUS for carcinoma identification was higher than that of EUS-FNA, and four of the five carcinomas with false-negative findings at EUS-FNA had hypoenhancement at CH-EUS [21]. Interestingly, in another study, Kitano et al. [2] reported that CH-EUS was not superior to EUS-FNA for identification of pancreatic carcinomas. However, CH-EUS revealed all ductal carcinomas with false-negative EUS-FNA results had hypoenhancement. Combining CH-EUS with EUS-FNA improved the sensitivity with which EUS-FNA identified ductal carcinomas from 92.2 to 100%. Therefore, CH-EUS before EUS-FNA complements EUS-FNA in identifying ductal carcinomas. They recommended surgical resection or pathological reevaluation by EUS-FNA of the tumor when CH-EUS revealed a hypovascular pattern in a pancreatic tumor, even if the EUS-FNA findings were negative.

Seicean et al. [16] used quantitative CH-EUS for differentiate diagnosis of solid pancreatic masses and made a conclusion that it is helpful in differentiation but cannot replace EUS-FNA. CH-EUS can be used to identify the target for EUS-guided FNA by clearly depicting the outline of the lesions [25]. Another study of 84 sessions (2.2 ± 1.2 sessions per patient, 39 patients) with a hypoechoic solid lesion in the pancreas of FNA was performed and the results revealed that in the sites with heterogeneous enhancement ($n = 40$), 8 samples (20%) were inadequate for pathological diagnosis, while malignant cells were found in 73%. In the sites with homogeneous enhancement, all samples were available for pathological diagnosis. Thus, CH-EUS may predict the pathological features of the pancreatic solid lesions. Simultaneous imaging of vascularity by CH-EUS during EUS-FNA is helpful for adequate sampling of pancreatic tumors [26].

CH-EUS, as a new technology, can visualize both parenchymal perfusion and microvasculature in pancreas without artifacts. It is useful in both differentiate diagnosis of pancreatic masses and detecting small pancreatic masses. Although it helps identify the target for EUS FNA by clearly depicting the outline and may predict the pathological features of the pancreatic lesions, but it still cannot replace EUS-FNA now.

10. Conclusion

Though EUS is a highly sensitive modality for detection of small lesions in the pancreas, sometimes it is hard to differentiate between diagnosis of the malignant lesion from the benign lesions. Recently developed contrast-enhanced harmonic EUS can visualize both parenchymal perfusion and microvasculature in pancreas without Doppler-related artifacts. Studies show that it is superior to conventional EUS and CT in detecting small pancreatic masses and in differentiating diagnosis of pancreatic masses. It could be applied in adequate sampling of pancreatic tumors and it may help predict the pathological features of the pancreatic lesions, but it still cannot replace EUS-FNA nowadays.

References

[1] M. A. Khashab, E. Yong, A. M. Lennon et al., "EUS is still superior to multidetector computerized tomography for detection of pancreatic neuroendocrine tumors," *Gastrointestinal Endoscopy*, vol. 73, no. 4, pp. 691–696, 2011.

[2] M. Kitano, M. Kudo, K. Yamao et al., "Characterization of small solid tumors in the pancreas: the value of contrast-enhanced harmonic endoscopic ultrasonography," *American Journal of Gastroenterology*, vol. 107, no. 2, pp. 303–310, 2012.

[3] N. K. Reddy, A. M. Ioncică, A. Săftoiu, P. Vilmann, and M. S. Bhutani, "Contrast-enhanced endoscopic ultrasonography," *World Journal of Gastroenterology*, vol. 17, no. 1, pp. 42–48, 2011.

[4] H. Matsubara, A. Itoh, H. Kawashima et al., "Dynamic quantitative evaluation of contrast-enhanced endoscopic ultrasonography in the diagnosis of pancreatic diseases," *Pancreas*, vol. 40, no. 7, pp. 1073–1079, 2011.

[5] M. V. A. Sanchez, S. Varadarajulu, and B. Napoleon, "EUS contrast agents: what is available, how do they work, and are they effective?" *Gastrointestinal Endoscopy*, vol. 69, no. 2, pp. S71–S77, 2009.

[6] M. Kitano, M. Kudo, K. Maekawa et al., "Dynamic imaging of pancreatic diseases by contrast enhanced coded phase inversion harmonic ultrasonoqraphy," *Gut*, vol. 53, no. 6, pp. 854–859, 2004.

[7] S. Kersting, J. Roth, and A. Bunk, "Transabdominal contrast-enhanced ultrasonography of pancreatic cancer," *Pancreatology*, vol. 11, supplement 2, pp. 20–27, 2011.

[8] H. Sakamoto, M. Kitano, Y. Suetomi, K. Maekawa, Y. Takeyama, and M. Kudo, "Utility of contrast-enhanced endoscopic ultrasonography for diagnosis of small pancreatic carcinomas," *Ultrasound in Medicine and Biology*, vol. 34, no. 4, pp. 525–532, 2008.

[9] H. Sakamoto, M. Kitano, K. Kamata, M. El-Masry, and M. Kudo, "Diagnosis of pancreatic tumors by endoscopic ultrasonography," *World Journal of Radiology*, vol. 2, no. 4, pp. 122–134, 2010.

[10] C. F. Dietrich, A. Ignee, and H. Frey, "Contrast-enhanced endoscopic ultrasound with low mechanical index: a new technique," *Zeitschrift für Gastroenterologie*, vol. 43, no. 11, pp. 1219–1223, 2005.

[11] M. Kitano, H. Sakamoto, U. Matsui et al., "A novel perfusion imaging technique of the pancreas: contrast-enhanced harmonic EUS (with video)," *Gastrointestinal Endoscopy*, vol. 67, no. 1, pp. 141–150, 2008.

[12] S. Varadarajulu and M. A. Eloubeidi, "The role of endoscopic ultrasonography in the evaluation of pancreatico-biliary cancer," *Surgical Clinics of North America*, vol. 90, no. 2, pp. 251–263, 2010.

[13] Y. Michiko, Y. Yoshimitsu, S. Yasuyuki, and H. Hideyuki, "Gastrointestinal: contrast-enhanced harmonic EUS for pancreatic cancer," *Journal of Gastroenterology and Hepatology*, vol. 24, no. 10, p. 1698, 2009.

[14] E. Ohno, A. Itoh, H. Kawashima et al., "Malignant transformation of branch duct-type intraductal papillary mucinous neoplasms of the pancreas based on contrast-enhanced endoscopic ultrasonography morphological changes: focus on malignant transformation of intraductal papillary mucinous neoplasm itself," *Pancreas*, vol. 41, no. 6, pp. 855–862, 2012.

[15] M. Kitano, M. Kudo, H. Sakamoto, and T. Komaki, "Endoscopic ultrasonography and contrast-enhanced endoscopic ultrasonography," *Pancreatology*, vol. 11, supplemnt 2, pp. 28–33, 2011.

[16] A. Seicean, R. Badea, R. Stan-Iuga, T. Mocan, I. Gulei, and O. Pascu, "Quantitative contrast-enhanced harmonic endoscopic ultrasonography for the discrimination of solid pancreatic masses," *Ultraschall in der Medizin*, vol. 31, no. 6, pp. 571–576, 2010.

[17] P. Fusaroli, A. Spada, M. G. Mancino, and G. Caletti, "Contrast harmonic echo-endoscopic ultrasound improves accuracy in diagnosis of solid pancreatic masses," *Clinical Gastroenterology and Hepatology*, vol. 8, no. 7, pp. 629.e2–634.e2, 2010.

[18] J. Romagnuolo, B. Hoffman, S. Vela, R. Hawes, and S. Vignesh, "Accuracy of contrast-enhanced harmonic EUS with a second-generation perflutren lipid microsphere contrast agent (with video)," *Gastrointestinal Endoscopy*, vol. 73, no. 1, pp. 52–63, 2011.

[19] E. Ohno, Y. Hirooka, A. Itoh et al., "Intraductal papillary mucinous neoplasms of the pancreas: differentiation of malignant and benign tumors by endoscopic ultrasonography findings of mural nodules," *Annals of Surgery*. In press.

[20] N. Kobayashi, K. Sugimori, T. Shimamura et al., "Endoscopic ultrasonographic findings predict the risk of carcinoma in branch duct intraductal papillary mucinous neoplasms of the pancreas," *Pancreatology*, vol. 12, no. 2, pp. 141–145, 2012.

[21] B. Napoleon, M. V. Alvarez-Sanchez, R. Gincoul et al., "Contrast-enhanced harmonic endoscopic ultrasound in solid lesions of the pancreas: results of a pilot study," *Endoscopy*, vol. 42, no. 7, pp. 564–570, 2010.

[22] H. Imazu, Y. Uchiyama, K. Matsunaga et al., "Contrast-enhanced harmonic EUS with novel ultrasonographic contrast (Sonazoid) in the preoperative T-staging for pancreaticobiliary malignancies," *Scandinavian Journal of Gastroenterology*, vol. 45, no. 6, pp. 732–738, 2010.

[23] M. K. Hasan and R. H. Hawes, "EUS-guided FNA of solid pancreas tumors," *Gastrointestinal Endoscopy Clinics of North America*, vol. 22, no. 2, pp. 155–167, 2012.

[24] M. J. Hewitt, M. J. McPhail, L. Possamai, A. Dhar, P. Vlavianos, and K. J. Monahan, "EUS-guided FNA for diagnosis of solid pancreatic neoplasms: a meta-analysis," *Gastrointestinal Endoscopy*, vol. 75, no. 2, pp. 319–331, 2012.

[25] M. Kitano, H. Sakamoto, and M. Kudo, "Endoscopic ultrasound: contrast enhancement," *Gastrointestinal Endoscopy Clinics of North America*, vol. 22, no. 2, pp. 349–358, 2012.

[26] M. Kitano, H. Sakamoto, and T. Komaki, "FNA guided by contrast-enhanced harmonic EUS in pancreatic tumors," *Gastrointestinal Endoscopy*, vol. 69, pp. 328–329, 2009.

Research Article

Accuracy and Quality Assessment of EUS-FNA: A Single-Center Large Cohort of Biopsies

Benjamin Ephraim Bluen,[1] Jesse Lachter,[2,3] Iyad Khamaysi,[1,3] Yassin Kamal,[1,3] Leonid Malkin,[1] Ruth Keren,[1] Ron Epelbaum,[4] and Yoram Kluger[1]

[1] *Technion-Israel Institute of Technology, The Bruce and Ruth Rappaport Faculty of Medicine, Israel*
[2] *Technion-Israel Institute of Technology and EUS Service, The Bruce and Ruth Rappaport Faculty of Medicine, Rambam Healthcare Campus, Haifa, Israel*
[3] *Departments of Gastroenterology and Community Medicine, Rambam Health Care Campus, Haifa, Israel*
[4] *Oncology Ambulatory Care, Rambam Healthcare Campus, Haifa, Israel*

Correspondence should be addressed to Benjamin Ephraim Bluen, bbluen@gmail.com

Introduction. Thorough quality control (QC) study with systemic monitoring and evaluation is crucial to optimizing the effectiveness of EUS-FNA. *Methods.* Retrospective analysis was composed of investigating consecutive patient files that underwent EUS-FNA. QC specifically focused on diagnostic accuracy, impacts on preexisting diagnoses, and case management. *Results.* 268 patient files were evaluated. EUS-FNA cytology helped establish accurate diagnoses in 92.54% (248/268) of patients. Sensitivity, specificity, PPV, NPV, and accuracy were 83%, 100%, 100%, 91.6%, and 94%, respectively. The most common biopsy site was the pancreas (68%). The most accurate location for EUS-FNA was the esophagus, 13/13 (100%), followed by the pancreas (89.6%). EUS-FNA was least informative for abdominal lymph nodes (70.5%). After FNA and followup, eight false negatives for tumors were found (3%), while 7.5% of samples still lacked a definitive diagnosis. *Discussion.* QC suggests that the diagnostic accuracy of EUS-FNA might be improved further by (1) taking more FNA passes from suspected lesions, (2) optimizing needle selection (3) having an experienced echo-endoscopist available during the learning curve, and (4) having a cytologist present during the procedure. QC also identified remediable reporting errors. In conclusion, QC study is valuable in identifying weaknesses and thereby augmenting the effectiveness of EUS-FNA.

1. Introduction

Endoscopic ultrasound has proven to be a highly sensitive tool for diagnosing lesions in and adjacent to the gastrointestinal tract [1]. Aspirated samples can be sent for histological, cytological, and chemistry analyses, all of which may establish a lesion/tumor as being benign or malignant, without the need for more invasive interventions. Recent surveys have indicated that EUS-FNA has been well received by the medical community at large [2]. While it has been seen that EUS-FNA can effectively establish diagnoses, it is still a relatively new procedure with overall effects on patient management that remain to be fully investigated.

FNA, originally used by Martin and Ellis [3] to diagnose suspected neoplasms, was performed under the guidance of palpation. Newer technology has allowed real-time FNA to be performed under EUS guidance using various 19–25 gauge needles [4], which has markedly increased its accuracy [5] in detecting and staging lesions while evaluating the surrounding lymph and vascular networks [6]. Bentz et al. [7] summarized that real-time EUS-FNA makes possible the accurate definitive diagnosis of pancreatic, mediastinal, and retroperitoneal masses as malignancies by acquiring tissue at primary sites and via relevant lymph node and hepatic analyses. Establishing proper staging by EUS-FNA has led to a clinically significant decrease in immediate futile

surgical operations being performed, opting instead for a more appropriate palliative or neoadjuvant chemoradiation therapy for advanced cancers [8]. Also, EUS staging of tumors at the T1 level leads to endoscopic curative resections, again obviating unnecessary operations.

EUS-FNA has proven very useful diagnostically, obviating unwarranted procedures, and reduction of cost, all of which lead to improvements in overall patient care [9]. In studies byAlhayaf et al. [10] and Lachter et al. [11], EUS has been shown to be a valuable tool for diagnosing choledocholithiasis, demonstrating greater than 90% sensitivity and negative predictive values for stones in the biliary ducts. This obviates the alternative procedure, endoscopic retrograde cholangiopancreatography (ERCP), except for therapeutic usage as it is associated with far more complications than EUS. In another case, a patient presented with what was originally diagnosed as pancreatic cancer by CA 19–9 over 1000 ng/mL and negative hepatobiliary CT scan. However, EUS revealed a gallbladder adenocarcinoma [12], leading to successful surgical removal of the tumor.

The focus of this research was to continue the progress of the aforementioned studies of EUS-FNA affecting patient management in a study not limited to specific GI tract lesions. This large single-center quality control study investigated how EUS-FNA impacted patient care at one hospital and how its implementation might be improved to further increase its diagnostic accuracy. Such results might help to persuade the medical community at large to utilize EUS-FNA to efficiently obtain accurate diagnoses that can lead to speedier patient recovery, fewer unnecessary operations, reduced patient and hospital medical expenses, and, most important of all, lead to better patient care.

2. Materials and Methods

A retrospective clinical analysis was performed, followed by statistical analyses.

2.1. Research Population. Subjects for this research consisted of two hundred sixty-eight consecutive patients from computerized case files from 2008–2010 at Rambam Healthcare Campus in Haifa, Israel. These subjects were chosen from the hospital's gastrointestinal and cytology departments, all of whom had undergone EUS-FNA by Rambam gastroenterologists and have had cytological analysis performed. This population is representative of the population of Haifa, its immediate surroundings, and various communities of northern Israel.

2.2. Variables. Patient files were analyzed for management and diagnosis before and after EUS-FNA. Any change in diagnosis and/or treatment was noted, such as more aggressive or more conservative, more or fewer tests being performed, with chemotherapy and surgery among the various possibilities. Moreover, methods to improve the diagnostic accuracy of EUS-FNA were considered as to limit potential errors such as inadequate FNA samples or morbidities

associated with EUS-FNA. Demographics including age and gender were noted.

2.3. Research Methods. Data was collected from patient files and results were charted according to the target region of EUS-FNA aspiration and also according to overall results. Data was arranged into pre-EUS-FNA and postaspiration groups as described in Hirdes et al. [13] and Anand et al. [4]. Post-EUS-FNA results were analyzed to see if the FNA had any positive or negative impact on patient care in regard to its sensitivity, specificity, and its ability to withdraw sufficient material from lesions to be effective diagnostically. Statistical analysis was accomplished in collaboration with the hospital ward quality control (QC) department. Descriptive statistics including mean and standard deviation were performed for multiple variables in the study such as demographics. Sensitivity and specificity values were determined based upon the lesion status prior to and after EUS-FNA analyses by the use of SPSS version 18 program. P values less than 0.05 were indicated as statistically significant.

3. Results

A total of 268 patients' files comprised the study sample. The mean patient age was 66.6 years old. The majority (68%) of FNA samples were taken from the pancreas, with other frequent targets being the stomach, mediastinum, and abdominal lymph nodes (Figure 1). EUS-FNA diagnostic accuracy was found to be highest (100%) in the stomach and esophagus, while achieving 92.0%, 90.5%, and 74.1% accuracies in diagnosing pancreatic, mediastinal, and abdominal lymph lesions, respectively (Table 1).

226 of the total 268 patients (84.3%) lacked a definitive diagnosis prior to performing EUS-FNA. Examples commonly encountered were obstructive jaundice or a widened Wirsung duct that was found on computerized tomography (CT). After EUS-FNA, 134 of the cases were determined to be benign (59.3%), 67 cases of malignancy were found (29.6%), and 7.5% of cases still lacked a definitive diagnosis following the procedure (Figure 2).

EUS-FNA cytology proved useful in establishing the diagnosis in 248 out of 268 patients (92.54%). Sensitivity and specificity were established by evaluating diagnoses for changes prior to and after EUS-FNA. Prior to FNA, 27 of the 268 patients (10.1%) were determined to have benign lesions, 12 (4.5%) patients had malignant conditions, and 3 patients (1.1%) had lesions of chronic inflammation designed as "other." Positive values were indicated as malignant, and negative values were labeled as benign.

EUS-FNA diagnosed 10 out of 10 malignant cases for 100% positive predictive value (PPV). The PPV value indicates that 100% of cases having known malignancy tested positive for malignancy after EUS-FNA, indicating the importance of a positive result that EUS-FNA is diagnostic. This also indicates 100% specificity in ensuring no false positives, meaning that a lesion found to be malignant by EUS-FNA had a 100% of being malignant. EUS-FNA did not detect two other cases of malignancy, instead giving false
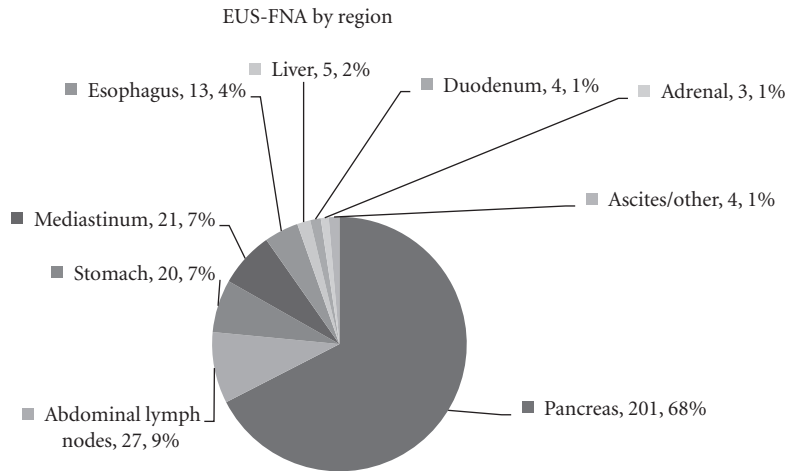
EUS-FNA by region

FIGURE 1: The chart represents the frequency EUS-FNA biopsy at analyzed regions. The pancreas was the most frequently biopsied organ.

TABLE 1: EUS-FNA by region and diagnostic accuracy.

Region	Frequency	FNA nondiagnostic or false negative	FNA diagnostic (%)
Pancreas	201	16	92.04
Abdominal lymph nodes	27	7	74.07
Stomach	20	0	100.00
Mediastinum	21	2	90.48
Esophagus	13	0	100.00
Liver	5	0	100.00
Duodenum	4	0	100.00
Adrenal	3	0	100.00
Ascites/other	4	1	75.00
Total	268	20	92.54

Various regions sampled by EUS-FNA cytology, showing frequency of FNA, number of false negatives or nondiagnostic samples, and overall diagnostic accuracy are displayed.

Total includes several cases of overlap in patients where multiple regions were sampled by FNA. For example, a patient had FNA biopsies taken from his pancreas and abdominal lymph nodes.
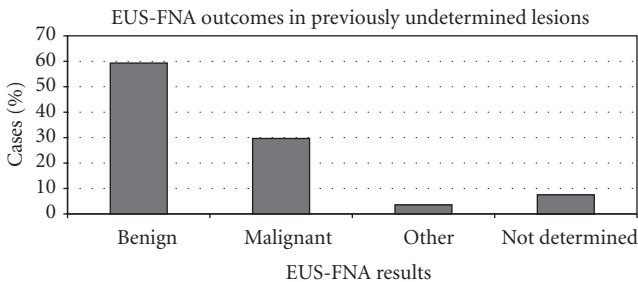

FIGURE 2: Charted is a breakdown of the diagnoses after EUS-FNA, cases of which prior diagnoses initially were undetermined. This population represented the majority of patients (84.3%, 226/268).

negatives results that resulted in 83.3% (10/12) sensitivity. False negatives represent lesions that EUS-FNA cytology determined as benign, but were soon after diagnosed as malignant. Therefore, the 83.3% sensitivity indicates that a negative result by EUS-FNA has an 83.3% chance of being benign, but does not always rule out a malignant condition

(see Table 3). Similarly, the NPV is an indicator for negative results. Out of 27 presumed to be benign cases prior to FNA, 22 cases were indeed benign by FNA, whereas 2 malignant cases were found: one case of chronic inflammation and two not determined. As the NPV of EUS-FNA is 91.6% (22/24), there is over a 90% chance that a negative result from EUS-FNA will indeed be a benign lesion. The overall accuracy of EUS-FNA was found to be 94.1%, which implies that 94% of the results are correct diagnostically, no matter if the result is benign or malignant (Table 3). This compares to a recent 2011 review of previous studies of diagnosing pancreatic solid masses by EUS-FNA since 1992 that established a sensitivity, specificity, PPV, NPV, and accuracy of 78–95%, 75–100%, 98–100%, 46–80%, and 78–95% [14].

The greatest percentage of false negatives or non-diagnostic FNAs was found in analysis of abdominal lymph nodes. 27 cases were identified in which EUS-FNA from abdominal lymph nodes was performed, two-thirds of which involved additional sites of EUS-FNA. Of these 27 patients, seven cases of nondiagnostic or false negative were found (25.9%), The majority of such nondiagnostic or

TABLE 2: FNA results for abdominal lymph nodes.

Region	Cases	FNA nondiagnostic or false negative	Percent of FNA diagnostically useful
Nodes alone	9	3	66.67
With pancreas	8	3	62.50
With stomach	2	0	100.00
With liver	2	0	100.00
With adrenal	1	0	100.00
With mediastinum	3	0	100.00
With mediastinum and pancreas	1	1	0.00
With other (ascites)	1	0	100.00
Total	27	7	70.47

Displayed in this chart are the various regions from which EUS-guided FNA was performed on abdominal lymph nodes either alone or in combination with other organs. Alongside each value is the number of cases that the FNA proved unhelpful (nondiagnostic or false negative) in establishing the patient's diagnosis.

false negative cases (6/7) of abdominal lymph nodes either involved FNA the nodes alone or with accompanying FNA from the pancreas (Table 2).

A total of 20 cases (7.5% of total) nondiagnostic and false negative FNA cases were identified. Eight of the twenty cases were false negatives; zero false positives were found. The column labeled "FNA nondiagnostic or false negative" includes the cases in which EUS-FNA and/or subsequent cytology could not effectively diagnose a suspected lesion or resulted in a false negative (Table 1). A false negative indicates that cytological analysis of EUS-FNA aspirate showed a benign result, yet further histological analysis during surgical removal of the lesion found a malignancy. Causes included the number of FNA passes, the character of the lesion, the type and gauge number of the needle, and the experience of the performing endoscopist (one senior operator performed or attended greater than 90% of the EUS-FNA procedures). See Discussion in regard to the row titled "cysts with CEA >192 ng/mL" (Table 3). During data analysis, it was found that patient files often did not completely detail the stage of lesions prior to FNA and also did not provide data about chemotherapeutic treatment when diagnosed with a malignant condition by EUS-FNA.

4. Discussion

EUS-guided FNA can have a profound influence on patient management. Its diagnostic ability is one of its greatest assets. Patients with benign conditions do not require intensive treatment and usually routine patient followup is needed, depending on the nature of the pathology. In contrast, the patients diagnosed with malignancies are referred for surgical resection when possible, chemo/radiation therapy, and/or appropriate palliative care. For both benign and malignant diseases, quality assessments of care may point to ways to improve the service provided to our patients. In providing accurate diagnoses, EUS-FNA helps to establish proper patient care while avoiding futile, costly, and potentially risky procedures and operations.

In regard to location, EUS-FNA was most accurate in the esophagus, stomach, and adrenal and peri-GI tract areas

(marked as "other" in the results section), demonstrating 100% accuracy. In the pancreas, which was the region of most frequent EUS-guided FNA usage (see Figure 1), 92.04% accuracy was achieved in correctly diagnosing pancreatic lesions. The present series reflects the local practice which involves EUS only through the upper gastrointestinal tract. Transrectal ultrasound and biopsies are performed by the proctologic surgeons using separate equipment and thus were not included in the present study.

Despite being a highly sensitive and selective method, EUS-FNA cytology was not equally accurate for several analyzed regions. One such area was in the assessment of abdominal lymph nodes, where the accuracy was 74.07%. Accuracy in assessing mediastinal lesions was 90.48% (see Table 2). This is in comparison to prior studies by Nakahara et al. that used 22 gauge needles to obtain adequate specimens from undiagnosed abdominal lymphadenopathies in 93% of cases ($n = 53$) that led to a sensitivity of 94%, 100% specificity, 100% positive predictive value (PPV), 90% negative predictive value (NPV), and an overall 96% accuracy [15]. For mediastinal lesions, comparative studies ($n = 37$) demonstrated 79.3% sensitivity, 100% specificity, and 85% accuracy overall in detecting malignant mediastinal lymphandenopathies [16].

Several factors can be responsible for the diminished accuracy of these selected areas. First, the number of passes made into the lesion of interest comes into question. In two out of the 20 cases (10.0%) of FNA being nondiagnostic or false negative, it was documented that three passes were made from the lesion by FNA. Five cases (25.0%) involved two passes and three cases (15.0%) were documented where only one pass was attempted to aspirate contents from suspicious lesions. This can be due to several reasons. Minimal fluid was reported to be withdrawn from eight of the 20 cases (40.0%), which likely made it difficult for cytologists to delineate or exclude a specific pathology if present (see Table 3). Moreover, minimal fluid withdrawal was a key reason found for the false negative cases seen (see bottom of Table 3). The local tendency to attempt FNA on cysts smaller than 2 cm when easily accessible for potential biopsy may lead to a high rate of inadequate fluid for evaluation. Fluid is tested by

TABLE 3: nondiagnostic EUS-FNA cases.

Reason	Frequency	Percent of total
Number of FNA passes		
3 passes	2	10.00
2 passes	5	25.00
1 pass	3	15.00
Not listed	10	50.00
Total	20	100.00
Other reasons		
Unidentifiable cause	10	50.00
Minimal fluid withdrawn	8	40.00
Difficult to pass needle*	3	15.00
Suspected autoimmune or chronic inflammation	2	10.00
False negatives	8	40.00
Total	20	100.00
Sensitivity	83.3%	
Specificity	100.00%	
Positive predictive value	100.00%	
Negative predictive value	91.6%	
Accuracy	94.1%	

Listed is a summary of suspected causes of nondiagnostic and false negative FNA cases, along with sensitivity, specificity, PPV, NPV, and overall accuracy of EUS-FNA.
*The category labeled "difficult to pass needle" is a subgroup of the cases that fall under the group "minimal fluid withdrawn."

performing a 1:2 or 1:3 dilution of the aspirated material so as to maximize the ability to allow analyses of the fluid in chemistry (CEA and amylase) and cytological tests.

Lesions with very viscous mucous contents often are unsuitable for obtaining adequate fluid for chemistry (CEA and amylase) evaluation. Data from samples taken from EUS-FNA biopsies of pancreatic cysts have shown that a CEA level above 192 ng/mL is indicative of mucinous neoplasms in 79% of cases [17]. In three of the original nondiagnostic 23 cases (13.0%), the measured CEA levels were 210, 1905, and 6740 ng/mL, respectively, which supported the diagnosis of a mucinous neoplasm or IPMN. Originally 245 out of 268 cases were diagnostic by EUS-FNA cytology (see Table 1); factoring in this diagnostic criteria adds three more cases to arrive at 248 out of 268 (92.54%) total diagnostic cases.

Issues that infrequently complicate EUS-FNA procedures are the vicinity of the lesion for biopsy and the condition of the patient. It was documented in three nondiagnostic FNA cases (15.0%) that fewer passes were taken of suspected lesions because the operator found it difficult to insert the needle into the lesion for biopsy. In one of these cases, multiple vessels surrounded the suspected mass, resulting in a narrow window to insert the needle for FNA. This may be remedied by using newer small 25 gauge or more flexible needles that can more easily penetrate hard lesions ensuring the ease of puncture and a greater quantity of aspirate extracted [18]. In two other cases, despite the standard eight hours fast patient preprocedure preparation, the patient's stomachs were still partly full of food contents. In such cases, EUS-FNA may best be postponed and the patients instructed to fast for a longer time. However, this may also be indicative

of a gastric outlet obstruction that may be in part due to tumors. Another case involved a duodenal obstruction that limited the passage of the endoscope, making it difficult for the endoscopist to pinpoint the lesion site for FNA biopsy. In addition, one EUS-FNA procedure caused a patient to bleed after one pass into the lesion, so no further attempts of performing FNA were made. Lastly, two of the cases (10.0%) that proved nondiagnostic by EUS-FNA were suspected by the operating endoscopist to be of autoimmune origin or of chronic inflammation. None of these cases manifested in being diagnostic cytologically, resulting in the need for further blood tests and biopsies.

Occasionally, the documentation on patient case files was insufficient to determine a specific cause of nondiagnostic FNAs. There are two junior echoendoscopists currently working in Rambam Healthcare Campus, to whom may be attributed several of the nondiagnostic FNAs. One senior operator performed or attended greater than 90% of the EUS-FNA procedures. However, it cannot be confirmed if the nondiagnostic FNAs were due to operator inexperience because the patient files investigated did not list the name of the doctor who performed the respective EUS-FNA. Reports may be written by either the attending or the in-training echoendoscopist. Furthermore, recent literature showed as good results among newly trained echoendoscopists as compared to experienced self-trained ones. The number and type of needles used were rarely documented, factors which may impact the amount of material for cytology and chemical analyses. Moreover, local compensation for EUS is nationally standardized and strongly discourages usage of more than one needle. One additional method to ensure diagnostic

accuracy of EUS-FNA samples is to have a cytologist present during the procedure to ensure the adequacy of the aspirated samples and has been shown in several centers to increase the accuracy of cytological diagnosis by 10–15% [19]. This has also been associated with shortening procedure time, thus theoretically reducing the risk of complications. Although this would impose somewhat increased cost and logistical burdens, a cytologist present during EUS-FNA along with further and more detailed documentation of FNAs could provide valuable insight into how important any of these aspects is when evaluating possible causes of fruitless FNA procedures.

In analyzing the 268 patient files from 2008–2010, there was one reported case of FNA-related complication in which a minor hemorrhage occurred near the site of aspiration. This required the patient to be hospitalized for several additional hours before being released. No other cases of EUS-FNA morbidity or mortality caused by EUS-FNA were found; therefore, the morbidity rate is 1/268, or 0.37% with a mortality of 0.0%. This is in comparison to published benchmark data, which showed that the morbidity rate from EUS-guided FNA was 0.98% overall, including postprocedural pancreatitis, pain, and mortality [20]. This retrospective analysis indicates that EUS-guided FNA is a useful diagnostic procedure that minimizes potential morbidity that patients may experience.

As previously noted, accurate diagnoses were made possible by EUS-FNA in 92.54% of evaluated cases, which minimized the overall health and financial costs brought about by the amount of extra tests, chemotherapy, and fruitless operations that patients may undergo as a result of misdiagnosis. A previous report found that EUS-FNA markedly decreased the frequency of futile surgery for pancreatic cancers while additionally aiding in the tailoring of optimal individualized patient treatment according to the stage of the patient's cancer [21]. This may also be due to the ability of EUS to visualize the surrounding lymph nodes around a lesion to determine the likely effectiveness of surgery. This overall correlates to a significant savings of time and money for patients, doctors, and hospitals alike.

5. Limitations

Limitations of this study included its retrospective nature at a single medical center. Although many of the computerized data files investigated contained fairly complete data, analysis was limited in a few files that consisted of incompletely documented reports. The study was also performed at a single healthcare center with its equipment and personnel. Therefore, it should be noted that the diagnostic accuracy of EUS-FNA may vary by several factors, including the experience of the center's echoendoscopists, cytologists, and lab personnel, and also by the sensitivity of its equipment. Rambam Healthcare Campus is also a training facility for many young doctors, and as such, there exist wide gaps in experience of the performing echoendoscopists, although a senior endoscopist supervises or consults on most procedures.

6. Conclusions

EUS-FNA was found to have 94.1% accuracy. Quality control analysis and literature suggest that this may be further improved by more thorough reporting of procedural information (perhaps with forcedfields in the electronic medical report), optimizing needle selection, and by having a senior echo-endoscopist and a cytologist present during each procedure.

Ethical Approval

Because patient files are their own personal property, this work underwent the formal approval of the institutional review board (IRB). In conducting this study, patients were not approached, nor were any adverse effects or harm brought upon them.

References

[1] P. Vilmann and A. Saftoiu, "Endoscopic ultrasound-guided fine needle aspiration biopsy: equipment and technique," *Journal of Gastroenterology and Hepatology*, vol. 21, no. 11, pp. 1646–1655, 2006.

[2] J. Lachter, R. Feldman, I. Krief, and R. Reshef, "Satisfaction of the referring physician: a quality control study focusing on EUS," *Journal of Clinical Gastroenterology*, vol. 41, no. 10, pp. 889–893, 2007.

[3] H. E. Martin and E. B. Ellis, "Biopsy by needle puncture and aspiration," *Annals of Surgery*, vol. 92, no. 2, pp. 169–181, 1930.

[4] D. Anand, J. E. Barroeta, P. K. Gupta, M. Kochman, and Z. W. Baloch, "Endoscopic ultrasound guided fine needle aspiration of non-pancreatic lesions: an institutional experience," *Journal of Clinical Pathology*, vol. 60, no. 11, pp. 1254–1262, 2007.

[5] A. S. Can, "Cost-effectiveness comparison between palpation- and ultrasound-guided thyroid fine-needle aspiration biopsies," *BMC Endocrine Disorders*, vol. 9, article 14, 2009.

[6] L. V. Hernandez and M. S. Butani, "Emerging applications of endoscopic ultrasound in gastrointestinal cancers," *Gastrointestinal Cancer Research*, vol. 2, no. 4, pp. 198–202, 2008.

[7] J. S. Bentz, M. L. Kochman, D. O. Faigel, G. G. Ginsberg, D. B. Smith, and P. K. Gupta, "Endoscopic ultrasound-guided real-time fine-needle aspiration: clinicopathologic features of 60 patients," *Diagnostic Cytopathology*, vol. 18, no. 2, pp. 98–109, 1998.

[8] A. Gines, S. D. Cassivi, J. A. Martenson et al., "Impact of endoscopic ultrasonography and physician specialty on the management of patients with esophagus cancer," *Diseases of the Esophagus*, vol. 21, no. 3, pp. 241–250, 2008.

[9] J. M. Dumanceau, M. Polkowski, A. Larghi et al., "Indications, results, and clinical impact of Endoscopic Ultrasound (EUS)-guided sampling in gastroenterology, European Society of Gastrointestinal Endoscopy (ESGE) clinical guideline," *Endoscopy*, vol. 43, pp. 1–16, 2011.

[10] N. Alhayaf, E. Lalor, V. Bain, J. McKaigney, and G. S. Sandha, "The clinical impact and cost implications of endoscopic ultrasound on the use of endoscopic retrograde cholangiopancreatography in a Canadian university hospital," *Canadian Journal of Gastroenterology*, vol. 22, no. 2, pp. 138–142, 2008.

[11] J. Lachter, A. Rubin, M. Shiller et al., "Linear EUS for bile duct stones," *Gastrointestinal Endoscopy*, vol. 51, no. 1, pp. 51–54, 2000.

[12] J. Lachter and S. Zelikovsky, "EUS changes diagnosis from pancreatic to gallbladder carcinoma," *International Journal of Gastrointestinal Cancer*, vol. 32, no. 2-3, pp. 161–164, 2002.

[13] M. M. C. Hirdes, M. P. Schwartz, K. M. A. J. Tytgat et al., "Performance of EUS-FNA for mediastinal lymphadenopathy: impact on patient management and costs in low-volume EUS centers," *Surgical Endoscopy and Other Interventional Techniques*, vol. 24, no. 9, pp. 2260–2267, 2010.

[14] S. Yoshinaga, H. Suzuki, I. Oda, and Y. Saito, "Role of endoscopic ultrasound-guided fine needle aspiration (EUS-FNA) for diagnosis of solid pancreatic masses," *Digestive Endoscopy*, vol. 23, no. 1, pp. 29–33, 2011.

[15] O. Nakahara, K. Yamao, V. Bhatia et al., "Usefulness of endoscopic ultrasound-guided fine needle aspiration (EUS-FNA) for undiagnosed intra-abdominal lymphadenopathy," *Journal of Gastroenterology*, vol. 44, no. 6, pp. 562–567, 2009.

[16] L. Bataille, M. Lonneux, B. Weynand, D. Schoonbroodt, P. Collard, and P. H. Deprez, "EUS-FNA and FDG-PET are complementary procedures in the diagnosis of enlarged mediastinal lymph nodes," *Acta Gastro-Enterologica Belgica*, vol. 71, no. 2, pp. 219–229, 2008.

[17] W. R. Brugge, K. Lewandrowski, E. Lee-Lewandrowski et al., "Diagnosis of pancreatic cystic neoplasms: a report of the cooperative pancreatic cyst study," *Gastroenterology*, vol. 126, no. 5, pp. 1330–1336, 2004.

[18] H. Imazu, Y. Uchiyama, H. Kakutani et al., "A prospective comparison of EUS-guided FNA using 25-gauge and 22-gauge needles," *Gastroenterology Research and Practice*, vol. 2009, Article ID 546390, 6 pages, 2009.

[19] R. A. Erickson, L. Sayage-Rabie, and R. S. Beissner, "Factors predicting the number of EUS-guided fine-needle passes for diagnosis of pancreatic malignancies," *Gastrointestinal Endoscopy*, vol. 51, no. 2, pp. 184–190, 2000.

[20] K. X. Wang, Q. W. Ben, Z. D. Jin et al., "Assessment of morbidity and mortality associated with EUS-guided FNA: a systematic review," *Gastrointestinal Endoscopy*, vol. 73, no. 2, pp. 283–290, 2011.

[21] J. Lachter, J. J. Cooperman, M. Shiller et al., "The impact of endoscopic ultrasonography on the management of suspected pancreatic cancer—a comprehensive longitudinal continuous evaluation," *Pancreas*, vol. 35, no. 2, pp. 130–134, 2007.

Research Article

Digital Chromoendoscopy for Diagnosis of Diminutive Colorectal Lesions

Carlos Eduardo Oliveira dos Santos,[1] Daniele Malaman,[1] César Vivian Lopes,[2] Júlio Carlos Pereira-Lima,[2] and Artur Adolfo Parada[3]

[1] *Department of Endoscopy and Gastroenterology, Dr Mario Araujo University Hospital, 96400-130 Bagé, RS, Brazil*
[2] *Department of Endoscopy and Gastroenterology, Santa Casa Hospital and Fundação Riograndense Universitária de Gastroenterologia (FUGAST), 90610-210 Porto Alegre, RS, Brazil*
[3] *Department of Endoscopy 9 de Julho Hospital, 01409-902 São Paulo, SP, Brazil*

Correspondence should be addressed to Carlos Eduardo Oliveira dos Santos, clinica@endosantos.com.br

Introduction. To compare the accuracy of digital and real-time chromoendoscopy for the differential diagnosis of diminutive (<5 mm) neoplastic and nonneoplastic colorectal lesions. *Materials and Methods.* This is a prospective randomized study comparing the Fujinon intelligent color enhancement (FICE) system (65 patients/95 lesions) and indigo carmine (69 patients/120 lesions) in the analysis of capillary meshwork and pit pattern, respectively. All lesions were less than 5 mm in diameter, and magnification was used in both groups. Histopathology was the gold standard examination. *Results.* Of 215 colorectal lesions, 153 (71.2%) were adenomas, and 62 were hyperplastic polyps (28.8%). Morphological analysis revealed 132 (61.4%) superficial lesions, with 7 (3.3%) depressed lesions, and 83 (38.6%) protruding lesions. Vascular meshwork analysis using FICE and magnification resulted in 91.7% sensitivity, 95.7% specificity, and 92.6% accuracy in differentiating neoplastic from nonneoplastic lesions. Pit pattern analysis with indigo carmine and magnification showed 96.5% sensitivity, 88.2% specificity, and 94.2% accuracy for the same purpose. *Conclusion.* Both magnifying virtual chromoendoscopy and indigo carmine chromoendoscopy showed high accuracy in the histopathological diagnosis of colorectal lesions less than 5 mm in diameter.

1. Introduction

Colorectal cancer is one of the most commonly diagnosed malignancies in Western countries and represents a major cause of morbidity and mortality associated with cancer [1]. The prevention of colorectal cancer requires the diagnosis and resection of precursor lesions, according to the adenoma-carcinoma sequence [2]. It is also important to consider the pathway of the *de novo* cancer (carcinoma without prior adenomatous tissue) because small (even diminutive) lesions, especially depressed ones, may be more malignant, even showing invasive behavior [3]. A diagnosis of early cancer is possible only if the minimal changes in structure and color (pale color or hyperemia) displayed on

the mucosal surface of the lesion can be recognized [4]. Endoscopic detection and treatment of these neoplasms is the most cost-effective strategy to reduce the incidence and mortality of colorectal cancer [5, 6]. Colonoscopy is the best diagnostic method, and the use of chromoendoscopy (CE) with indigo carmine and crystal violet may help characterize the morphology of lesions, whose correct interpretation is crucial in choosing the appropriate treatment. When associated with magnification, this method can provide high accuracy in differentiating neoplastic from non-neoplastic lesions after pit pattern analysis [7–12], in the assessment of invasion depth of carcinomas [13], and in the diagnosis of diminutive residual tumor after endoscopic resection [14], thus increasing the efficiency of the endoscopic procedure

[15]. Some studies indicate that CE may increase the detection rate of small flat adenomas in diagnostic colonoscopies [16, 17].

In recent years, new technologies have emerged and enabled the analysis of surface (pit-like pattern) and microvascular patterns, at the push of a button on the colonoscope and without the need for dyes, to achieve excellent results in the differential diagnosis between non-neoplastic and neoplastic colorectal lesions [18, 19] and to determine the depth of invasion of early cancer [20, 21]. This technology is known as digital chromoendoscopy (DCE) and, similarly to CE, allows a predictive *in vivo* histological diagnosis, reducing time and effort. New DCE techniques include the Fujinon intelligent color enhancement (FICE) system, narrow-band imaging (NBI), Olympus, and, more recently, i-Scan developed by Pentax. FICE and i-Scan systems are based on a computed spectral estimation technology that processes the reflected photons to reconstitute virtual images for a choice of different wavelengths of red, green, and blue signaling. The NBI system depends on optical filters within the light source, using a frame sequential lighting method.

Several series using this technology have shown similar results for CE and DCE, especially when associated with magnification [22–24], and some findings have demonstrated increased detection of small nonpolypoid neoplastic lesions using DCE when compared with conventional colonoscopy [25–27]. This study aimed to evaluate the ability of DCE (using the FICE system) to differentiate between neoplastic and non-neoplastic lesions less than 5 mm in diameter and to compare FICE accuracy with that of real-time CE (using indigo carmine) in the investigation of colorectal lesions.

2. Materials and Methods

Between December 2007 and June 2008, this prospective randomized study analyzed 215 colorectal lesions less than 5 mm in 134 patients (74 women; mean age, 60.6 years).

Patients were eligible for study participation if they were indicated for colon cancer screening or had diagnostic colonoscopy for abdominal pain. Exclusion criteria were coagulopathy, incomplete colonoscopy, poor bowel preparation, polyps with 5 mm or more, history or presence of inflammatory bowel disease, polyposis syndrome, and rectal bleeding in the last 6 months, patients with previous colonoscopy or surgical resection of colon or rectum.

Patients were randomly allocated by sealed envelope to colonoscopy with targeted magnification FICE (group I) or with indigo carmine chromoendoscopy (group II).

All lesions were analyzed with a high-resolution magnifying colonoscope (Fujinon 490ZW5, Fujinon Corp., Saitama, Japan), approximately 80–100X, equipped with the EPX 4400 processor. Only after examination under white light, the lesions were analyzed by DCE or real-time CE. Tap water was used to clean the surface when necessary to ensure optimal image quality.

In group I, 95 lesions in 65 patients were assessed with the FICE system at red, green, and blue wavelengths of R550(2), G500(3), and B470(2), respectively, used to evaluate the capillary pattern, which was defined as either negative (pale-colored surface and invisible vessels or only minute, thin, superficial capillaries) or positive (darkening of the mucosal pattern or a fine meshwork of brown/bluish vessels). Negative capillary meshwork is considered the typical pattern for non-neoplastic lesions and positive capillary meshwork for neoplastic lesions (Figure 1).

In group II, 120 lesions in 69 patients were examined under magnification after 0.8% indigo carmine with a dye spray catheter. The pit pattern analysis was based on the Kudo classification [28, 29], with type I or II pit pattern defining non-neoplastic and type III-V pit pattern defining neoplastic lesions (Figure 2).

All the procedures were performed by a single endoscopist (CEOS) who has routinely used magnifying colonoscopy for over 10 years. The transparent cap was not used.

Bowel preparation consisted of one-day clear liquid diet, with 10% mannitol solution, being considered appropriate in all patients. Procedures were performed with the patient under conscious sedation (intravenous midazolam and meperidine or fentanyl).

The morphology of lesions was determined according to the Paris classification [30]. Lesion size was estimated by comparison with the span of open (7 mm) biopsy forceps (FB-24U-1; Olympus Medical Systems Corp., Tokyo, Japan). The location was estimated by the anatomic landmarks.

All lesions were removed with biopsy forceps or by endoscopic mucosal resection, and specimens were fixed in 10% formalin and histologically examined using hematoxylin and eosin staining. Histologic diagnosis was performed by a pathologist blinded to colonoscopic results, and his definitions followed the guidelines of the World Health Organization classification of colorectal tumors [31]. In the case of multiple lesions in the same patient, each lesion was identified individually and placed in different flasks.

The study was performed in accordance with the principles of the Declaration of Helsinki, and written informed consent was obtained from all patients before endoscopy.

2.1. Statistical Analysis. For real-time CE with indigo carmine dye spraying and DCE using the FICE system, sensitivity, specificity, positive (PPV), and negative predictive values (NPV), with their 95% confidence intervals (CI), for the diagnosis of colorectal lesions were analyzed by comparing endoscopic diagnoses with histopathology findings (80% power; 5% significance level). Numerical variables were expressed as means and categorical variables as percentage. The Mann-Whitney U test was used for comparison of means. Fisher's exact test or the χ^2 test was used to compare prevalence of neoplasms according to the different imaging methods. A P value of less than 0.05 ($P < 0.05$) was considered to be statistically significant. Data were analyzed using the Stata 9.2 Statistical Package.
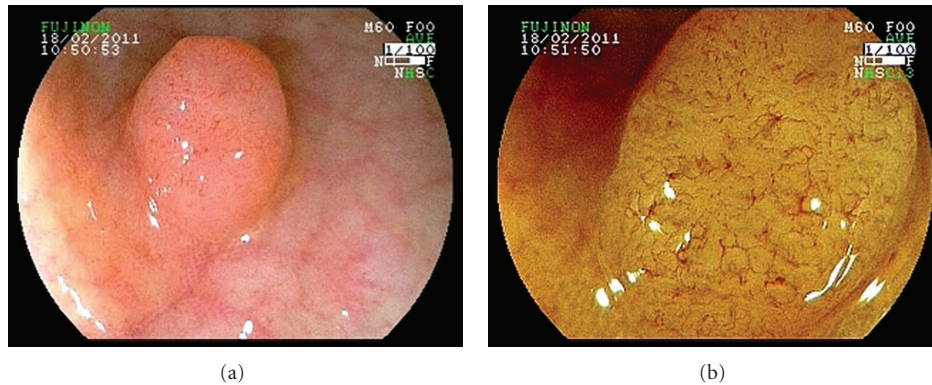
(a) (b)

FIGURE 1: (a) Standard endoscopic image of colorectal lesion type 0-Is. (b) FICE-magnifying observation image of the same lesion: a fine and regular meshwork of brown vessels (positive vascular pattern). Histopathology diagnosed a tubular adenoma.
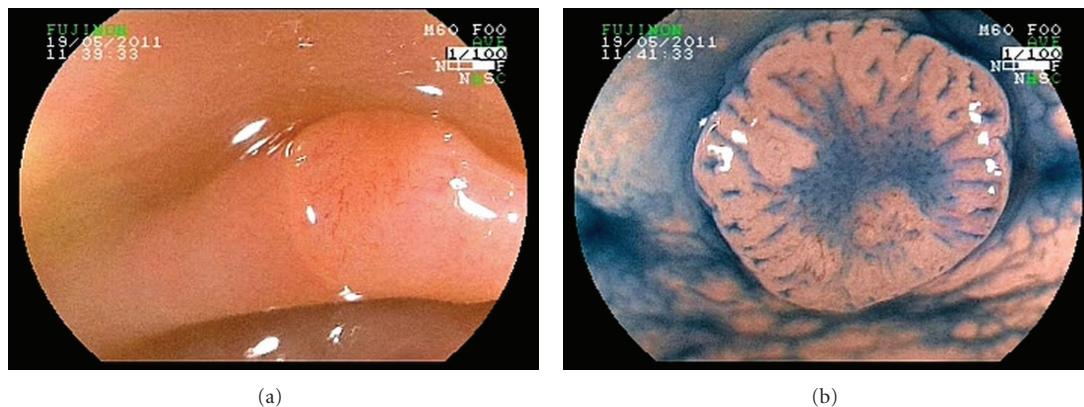

(a) (b)

FIGURE 2: (a) White light image of flat lesion. (b) Indigo carmine dye spraying magnifying showed a lesion type 0-IIa + IIc and the presence of type III L+ IIIs pit pattern. Histopathology identified a tubular adenoma.

3. Results

From 353 consecutive patients, 166 met primary study criteria. Thirty-two other cases were excluded after randomization due to failure to reach the cecum ($n = 2$), poor bowel preparation (at least semisolid stools at colonoscopy) ($n = 5$), or presence of lesions greater than 5 mm ($n = 25$). Finally, 134 patients with 215 colorectal lesions were analyzed (Figure 3).

Of 215 colorectal lesions, 153 (71.2%) were neoplastic lesions; of these, 125 (58.1%) were tubular adenomas. The mean size of all adenomas was 3.2 mm (DP = 1.1). All non-neoplastic lesions (62/28.8%) were hyperplastic polyps. The mean size of misdiagnosed lesions was 2.6 mm in diameter.

Regarding morphology, lesions were classified as follows: 132 (61.4%) superficial lesions, 116 (53.9%) type 0-IIa, 9 (4.2%) 0-IIa + dep, 4 (1.9%) 0-IIa + IIc, 2 (0.9%) 0-IIc + IIa, and 1 (0.5%) 0-IIc; and 83 (38.6%) protruding lesions, 78 (36.3%) 0-Is, 3 (1.4%) 0-Isp, and 2 (0.9%) 0-Ip.

Regarding lesion site, 39 (18.1%) lesions were located in the rectum, 48 (22.3%) in the sigmoid colon, 40 (18.6%) in the descending colon, 36 (16.7%) in the transverse colon, 38 (17.7%) in the ascending colon, and 14 (6.5%) in the cecum.
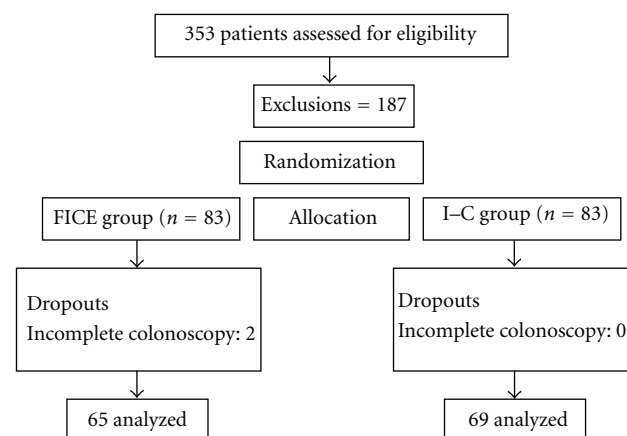

FIGURE 3: Study group.

The characteristics of patients and lesions analyzed are shown in Table 1. There were no significant differences between groups regarding sex, age, or lesion site, morphology, and histology.

TABLE 1: Characteristics of colorectal lesions analyzed by digital chromoendoscopy (FICE group) and real-time chromoendoscopy (indigo carmine group).

Variable	FICE (95) n (%)	Indigo carmine (120) n (%)
Sex		
Female	35 (53.8)	39 (56.5)
Male	30 (46.2)	30 (43.5)
Mean age (years)	60.2	60.9
Histopathology		
Neoplastic	67 (70.5)	86 (71.7)
Nonneoplastic	28 (29.5)	34 (28.3)
Histopathology		
Tubular adenoma	57 (60)	68 (56.7)
Tubulovillous adenoma	9 (9.5)	14 (11.6)
Serrated adenoma	1 (1.1)	4 (3.3)
Hyperplastic polyp	28 (29.5)	34 (28.3)
Macroscopic type		
Flat	55 (57.9)	77 (64.2)
Protruded	40 (42.1)	43 (35.8)
Macroscopic classification		
0-IIa	44 (46.3)	72 (60)
0-IIa + dep	7 (7.4)	2 (1.7)
0-IIa + IIc	2 (2.1)	2 (1.7)
0-IIc + IIa	1 (1.1)	1 (0.8)
0-IIc	1 (1.1)	0
0-Is	37 (38.9)	41 (34.1)
0-Isp	1 (1.1)	2 (1.7)
0-Ip	2 (2.1)	0
Location		
Rectum	19 (20)	20 (16.7)
Sigmoid colon	23 (24.2)	25 (20.8)
Descending colon	18 (18.9)	22 (18.3)
Transverse colon	15 (15.8)	21 (17.5)
Ascending colon	12 (12.6)	26 (21.7)
Cecum	8 (8.4)	6 (5%)

FICE: Fujinon intelligent color enhancement.

TABLE 2: Capillary meshwork (CM) by digital chromoendoscopy (FICE) and histopathologic findings.

	Neoplastic	Non-neoplastic
CM positive	66	1
CM negative	6	22

FICE: Fujinon intelligent color enhancement.

In group I (FICE), mean age was 60.2 years, 35 (53.8%) patients were female, and 30 (46.2%) were male. There were 67 (70.5%) neoplastic lesions—57 (60%) tubular adenomas, 9 (9.5%) tubulovillous adenomas, and 1 (1.1%) serrated adenoma—and 28 (29.5%) hyperplastic lesions. Of all 95 lesions, 55 (57.9%) were superficial, and 40 (42.1%) were protruding lesions. Nineteen (20%) lesions were located in the rectum, 41 (43.2%) in the left colon (sigmoid and descending), and 35 (36.8%) in the right colon (transverse, descending, and cecum). In the capillary pattern analysis, 67/95 lesions were classified as positive, 66 histologically confirmed as neoplastic lesions, and 28/95 were classified as negative, 22 confirmed as non-neoplastic lesions (Table 2). DCE with the FICE system showed 91.7% sensitivity, 95.7% specificity, 92.6% accuracy, 98.5% PPV, and 78.6% NPV in differentiating neoplastic from nonneoplastic lesions.

In group II (indigo carmine), mean age was 60.9 years, 39 (56.5%) patients were female, and 30 (43.5%) were male. Of 120 lesions, 86 (71.7%) were neoplastic lesions, of which 68 (56.7%) were tubular adenomas. Seventy-seven (64.2%) were superficial lesions. Twenty (16.7%) lesions were located in the rectum, 47 (39.2%) in the left colon, and 53 (44.2%) in the right colon. Real-time CE using indigo carmine dye spraying to evaluate pit pattern showed 96.5% sensitivity, 88.2% specificity, 94.2% accuracy, 95.4% PPV, and 90.9% NPV in differentiating neoplastic from non-neoplastic lesions.

Reproducibility and validity coefficients for the diagnosis of neoplastic lesions are described in Table 3.

The accuracy was 91% and 94% for capillary meshwork and pit pattern analysis in the diagnosed adenomas of the colon and rectum, respectively.

When comparing accuracy between superficial lesions and protruding lesions, the results are shown in Table 4.

TABLE 3: Comparison between digital chromoendoscopy (FICE) and real-time chromoendoscopy (indigo carmine) in differentiating neoplastic from non-neoplastic lesions.

	FICE (DCE)	Indigo carmine (CE)
Accuracy % (95% CI)	92.6 (87.3–98.0)	94.2 (90.0–98.4)
Sensitivity % (95% CI)	91.7 (82.7–96.9)	96.5 (90.1–99.3)
Specificity % (95% CI)	95.7 (78.1–99.9)	88.2 (72.5–96.7)
PPV % (95% CI)	98.5 (92–100)	95.4 (88.6–98.7)
NPV % (95% CI)	78.6 (59–91.7)	90.9 (75.7–98.1)
Kappa (95% CI)	0.81 (0.68–0.95)	0.86 (0.75–0.96)

95% CI: 95% confidence interval; FICE: Fujinon intelligent color enhancement; DCE: digital chromoendoscopy; CE: real-time chromoendoscopy; PPV: positive predictive value; NPV: negative predictive value.

TABLE 4: Accuracy between superficial lesion and protruding lesion using capillary pattern (FICE) and pit pattern analysis (Indigo carmine).

	FICE (DCE)	Indigo carmine (CE)
Superficial lesion	92.7%	96.1%
Protruding lesion	92.5%	90.7%

FICE: Fujinon intelligent color enhancement; DCE: digital chromoendoscopy; CE: real-time chromoendoscopy.

4. Discussion

The key to reducing the incidence of colorectal carcinoma is early detection of cancers of the colon and rectum, allowing the endoscopic treatment of these tumors. A representative part of small lesions is hyperplastic polyps, which have no

malignant potential and therefore do not require resection. The ability to differentiate neoplastic from non-neoplastic lesions contributes to avoid unnecessary resections and to reduce costs and test time, as well as procedure-related complications. Therefore, ideally, endoscopic resection should be indicated only in neoplastic lesions.

CE with indigo carmine and magnification is used to evaluate pit patterns and has shown good results in discriminating between neoplastic and non-neoplastic lesions, with accuracy ranging from 84 to 96.8%, sensitivity from 91.4–97.6%, and specificity from 67.2–93.9% [9–12]. However, real-time CE is a relatively laborious, time-consuming process, and its learning curve for interpreting pit patterns is considered slow. Thus, most endoscopists do not use CE because they consider it a laborious technique which can disrupt the flow of their routine examinations.

DCE has been recently developed, allowing more detailed examination of the mucosal surface and small superficial capillaries. FICE, i-Scan and NBI are noninvasive technologies that allow a faster, easier, and simpler analysis than CE. At the push of a button on the endoscope, it is possible to assess capillary and surface patterns of colorectal lesions. DCE has yielded overall satisfactory results, similar to those obtained with CE [22–24].

Experience with virtual or indigo carmine chromoendoscopy and colonoscopy without magnification presented a diagnostic accuracy between 68% and 93% [32–35]; however, most studies in the literature using magnification revealed better results.

A multicenter, prospective, randomized study reported that DCE (NBI) was able to detect more subjects with adenomas ($P = 0.014$), flat adenomas ($P = 0.003$), and right-sided adenomas ($P = 0.003$) compared with white-light colonoscopy. There was no difference in the total number of subjects with advanced adenomas (≥ 1.0 cm, villous, and high-grade dysplasia) ($P = 0.216$). NBI had longer withdrawal time (0.003), which may have contributed to these better results. Accuracy, sensitivity, and specificity for adenomas ≤ 5 mm were 79.4%, 85.9%, and 72.2%, respectively [25]. A meta-analysis by Jin et al. [26] also showed that endoscopy with the NBI system significantly increased the rate of flat adenoma detection compared with conventional colonoscopy, and withdrawal time was longer ($P = 0.0006$). Inoue et al. [27] compared conventional colonoscopy and pan-colonic NBI and showed that the latter significantly increased the number of adenomas detected ($P < 0.05$) and the number of diminutive (<5 mm) adenomas detected ($P < 0.05$).

The vessels of the microvascular structure of the normal colorectal epithelium are from 5 to $10 \mu m$ in diameter. Magnification may facilitate the recognition of minute surface capillaries, favoring the differential diagnosis between neoplastic and non-neoplastic lesions of the colon and rectum. However, visualization of the capillary pattern of lesions less than 5 mm in diameter is not easy, which may justify our mistaken judgments in the endoscopic evaluation of the capillary meshwork. The mean size of misdiagnosed lesions in our study was 2.6 mm.

Pohl et al. [36] compared the FICE system with low and high magnifications in the identification of adenomas and revealed a greater sensitivity, specificity, and accuracy using high magnification. The results were comparable to those using indigo carmine and higher than those using standard magnification. Kim et al. [37] also observed a significantly greater accuracy with high magnification and FICE for both small and diminutive lesions ($P < 0.05$). These findings are in accordance with a large number of articles showing higher diagnostic accuracy with high versus low magnifications [8–10, 24].

In our previous prospective randomized series on small lesions, using magnification and comparing DCE with CE, accuracy was similar for both methods: 92.8% (capillary pattern) and 90.1% (pit pattern) with the FICE system, and 94.9% with indigo carmine [38]. Likewise, the study by Su et al. [22] showed the same values for sensitivity, specificity, and accuracy (95.7%, 87.5%, and 92.7%, resp.) for both DCE and real-time CE. In our study of lesions less than 5 mm, DCE with high magnification showed 92.6% accuracy, 91.7% sensitivity, and 95.7% specificity, being as effective as real-time CE with indigo carmine in the analysis of the capillary meshwork (Table 3).

This study used a simplified classification based on two groups (positive or negative capillary meshwork), which has also been used by other authors with an accuracy above 90% [19, 34, 39]. As in our previous studies [12, 38], we performed DCE or real-time CE only after detection of lesions under high-definition white-light examination.

The Kudo classification was not designed to be used with DCE though some papers [12, 38, 40] have already shown that it could be employed for evaluation of the pit pattern, as well as the the capillary pattern with good results. East et al. [40] detected a very good agreement between both methods (kappa = 0.83), and, besides, the combination of both methods for evaluation of the pit and capillary patterns increased the sensitivity ($P = 0.06$) once compared to the single analysis of the pit pattern, although with a minimal difference ($P = 0.50$) when compared to the analysis of the capillary pattern. In our study, we did not evaluate the combination of both methods, but we do not believe that they could improve significantly the diagnostic accuracy of the DCE. Limitations of this study are as follow: no intraobserver evaluation, and the procedures were performed by a single endoscopist experienced in colonoscopy, especially DCE, whose experience may have influenced the results.

Yoshida et al. [34] studied the surface pattern of 151 polyps using the FICE system without magnification and reported an accuracy of 89.4% for lesions < 10 mm, and, when assessing lesions < 5 mm, accuracy was 82.7%. Teixeira et al. [41], using their classification of capillary pattern and FICE with magnification in 309 colorectal lesions, found a high accuracy of 98.3%, sensitivity of 99.2%, and specificity of 94.9%. Meta-analyses have shown high diagnostic accuracy using DCE in colorectal lesions in the assessment of both pit and capillary patterns, with no differences between them [42, 43], as demonstrated in our pilot study, in which we reported an accuracy of 94.9% and 93.6%,

respectively [12]. Studies using i-Scan have shown accuracy, sensitivity, and specificity ranging from 86.1 to 98.6%, 87.7 to 98% and 84.1 to 100% in differentiating neoplastic from non-neoplastic lesions [23, 44, 45]. In a prospective series comparing NBI versus i-Scan in the histological prediction of diminutive adenomas, no significant differences were evident between the two technologies (accuracy, 87.8% versus 90.7%; sensitivity, 88.8% versus 94.6%; specificity, 86.8% versus 86.4%), but both showed a difference in relation to high-definition white-light colonoscopy ($P = 0.046$ and $P = 0.017$, resp.) [46].

To date, some classifications have been proposed for the assessment of the capillary pattern [20, 39, 41], and even for surface patterns [34], but a reference classification, such as the Kudo classification [28, 29] for pit pattern analysis, has yet to be established.

In conclusion, technological advances are tools that help characterize and differentiate lesions of the colon and rectum, playing a role in the choice of appropriate treatment and avoiding unnecessary procedures. DCE and indigo carmine CE, both associated with magnification, showed high accuracy in the histopathological diagnosis of colorectal lesions less than 5 mm in diameter.

Conflict of Interests

The authors declare that they have no conflict of interests.

References

[1] C. Arditi, I. Peytremann-Bridevaux, B. Burnand et al., "Appropriateness of colonoscopy in Europe (EPAGE II): screening for colorectal cancer," *Endoscopy*, vol. 41, no. 3, pp. 200–208, 2009.

[2] B. Morson, "President's address. The polyp-cancer sequence in the large bowel," *Proceedings of the Royal Society of Medicine*, vol. 67, no. 6, pp. 451–457, 1974.

[3] T. Matsuda, Y. Saito, K. Hotta, Y. Sano, and T. Fujii, "Prevalence and clinicopathological features of nonpolypoid colorectal neoplasms: should we pay more attention to identifying flat and depressed lesions?" *Digestive Endoscopy*, vol. 22, no. 1, pp. S57–S62, 2010.

[4] Y. Sano, S. Tanaka, C. R. Teixeira, and N. Aoyama, "Endoscopic detection and diagnosis of 0-IIc neoplastic colorectal lesions," *Endoscopy*, vol. 37, no. 3, pp. 261–267, 2005.

[5] S. J. Winawer, A. G. Zauber, M. N. Ho et al., "Prevention of colorectal cancer by colonoscopic polypectomy (The National Polyp Study Workgroup)," *The New England Journal of Medicine*, vol. 329, pp. 1977–1981, 1993.

[6] F. Citarda, G. Tomaselli, R. Capocaccia, S. Barcherini, and M. Crespi, "Efficacy in standard clinical practice of colonoscopic polypectomy in reducing colorectal cancer incidence," *Gut*, vol. 48, no. 6, pp. 812–815, 2001.

[7] S. Kudo, C. A. Rubio, C. R. Teixeira, H. Kashida, and E. Kogure, "Pit pattern in colorectal neoplasia: endoscopic magnifying view," *Endoscopy*, vol. 33, no. 4, pp. 367–373, 2001.

[8] S. Tanaka, T. Kaltenbach, K. Chayama, and R. Soetikno, "High-magnification colonoscopy," *Gastrointestinal Endoscopy*, vol. 64, no. 4, pp. 604–613, 2006.

[9] K. Togashi, F. Konishi, T. Ishizuka, T. Sato, S. Senba, and K. Kanazawa, "Efficacy of magnifying endoscopy in the differential diagnosis of neoplastic and non-neoplastic polyps of the large bowel," *Diseases of the Colon and Rectum*, vol. 42, no. 12, pp. 1602–1608, 1999.

[10] M. Y. Su, Y. P. Ho, P. C. Chen et al., "Magnifying endoscopy with indigo carmine contrast for differential diagnosis of neoplastic and nonneoplastic colonic polyps," *Digestive Diseases and Sciences*, vol. 49, no. 7-8, pp. 1123–1127, 2004.

[11] E. C. A. Zanoni, R. Cutait, M. Averbach et al., "Magnifying colonoscopy: interobserver agreement in the assessment of colonic pit patterns and its correlation with histopathological findings," *International Journal of Colorectal Disease*, vol. 22, no. 11, pp. 1383–1388, 2007.

[12] C. E. O. Dos Santos, J. C. Pereira-Lima, C. V. Lopes, D. Malaman, A. A. Parada, and A. D. Salomão, "Comparative study between MBI (FICE) and magnification chromoendoscopy with indigo carmine in the differential diagnosis of neoplastic and non-neoplastic lesions of the colorectum," *Arquivos de Gastroenterologia*, vol. 46, no. 2, pp. 111–115, 2009.

[13] T. Matsuda, T. Fujii, Y. Saito et al., "Efficacy of the invasive/non-invasive pattern by magnifying chromoendoscopy to estimate the depth of invasion of early colorectal neoplasms," *American Journal of Gastroenterology*, vol. 103, no. 11, pp. 2700–2706, 2008.

[14] D. P. Hurlstone, S. S. Cross, S. Brown, D. S. Sanders, and A. J. Lobo, "A prospective evaluation of high-magnification chromoscopic colonoscopy in predicting completeness of EMR," *Gastrointestinal Endoscopy*, vol. 59, no. 6, pp. 642–650, 2004.

[15] C. E. dos Santos, D. Malaman, and J. C. Pereira-Lima, "Endoscopic mucosal resection in colorectal lesion: a safe and effective procedure even in lesions larger than 2 cm and in carcinomas," *Arquivos de Gastroenterologia*, vol. 48, pp. 242–247, 2011.

[16] R. Hüneburg, F. Lammert, C. Rabe et al., "Chromo-colonoscopy detects more adenomas than white light colonoscopy or narrow band imaging colonoscopy in hereditary nonpolyposis colorectal cancer screening," *Endoscopy*, vol. 41, no. 4, pp. 316–322, 2009.

[17] D. P. Hurlstone, S. S. Cross, R. Slater, D. S. Sanders, and S. Brown, "Detecting diminutive colorectal lesions at colonoscopy: a randomised controlled trial of pan-colonic versus targeted chromoscopy," *Gut*, vol. 53, no. 3, pp. 376–380, 2004.

[18] M. Hirata, S. Tanaka, S. Oka et al., "Magnifying endoscopy with narrow band imaging for diagnosis of colorectal tumors," *Gastrointestinal Endoscopy*, vol. 65, no. 7, pp. 988–995, 2007.

[19] J. J. W. Tischendorf, H. E. Wasmuth, A. Koch, H. Hecker, C. Trautwein, and R. Winograd, "Value of magnifying chromoendoscopy and narrow band imaging (NBI) in classifying colorectal polyps: a prospective controlled study," *Endoscopy*, vol. 39, no. 12, pp. 1092–1096, 2007.

[20] H. Kanao, S. Tanaka, S. Oka, M. Hirata, S. Yoshida, and K. Chayama, "Narrow-band imaging magnification predicts the histology and invasion depth of colorectal tumors," *Gastrointestinal Endoscopy*, vol. 69, no. 3, pp. 631–636, 2009.

[21] N. Yoshida, Y. Naito, M. Kugai et al., "Efficacy of magnifying endoscopy with flexible spectral imaging color enhancement in the diagnosis of colorectal tumors," *Journal of Gastroenterology*, vol. 46, no. 1, pp. 65–72, 2011.

[22] M. Y. Su, C. M. Hsu, Y. P. Ho, P. C. Chen, C. J. Lin, and C. T. Chiu, "Comparative study of conventional colonoscopy, chromoendoscopy, and narrow-band imaging systems in differential diagnosis of neoplastic and nonneoplastic colonic polyps," *American Journal of Gastroenterology*, vol. 101, no. 12, pp. 2711–2716, 2006.

[23] A. Hoffman, C. Kagel, M. Goetz et al., "Recognition and characterization of small colonic neoplasia with high-definition colonoscopy using i-Scan is as precise as chromoendoscopy," *Digestive and Liver Disease*, vol. 42, no. 1, pp. 45–50, 2010.

[24] H. M. Chiu, C. Y. Chang, C. C. Chen et al., "A prospective comparative study of narrow-band imaging, chromoendoscopy, and conventional colonoscopy in the diagnosis of colorectal neoplasia," *Gut*, vol. 56, no. 3, pp. 373–379, 2007.

[25] A. Rastogi, D. S. Early, N. Gupta et al., "Randomized, controlled trial of standard-definition white-light, love you. high-definition white-light, and narrow-band imaging colonoscopy for the detection of colon polyps and prediction of polyp histology," *Gastrointestinal Endoscopy*, vol. 74, pp. 593–602, 2011.

[26] X. F. Jin, T. H. Chai, and J. W. Shi, "Meta-analysis for evaluating the accuracy of endoscopy with narrow band imaging in detecting colorectal adenomas," *Journal of Gastroenterology and Hepatology*, vol. 27, pp. 882–887, 2012.

[27] T. Inoue, M. Murano, N. Murano et al., "Comparative study of conventional colonoscopy and pan-colonic narrow-band imaging system in the detection of neoplastic colonic polyps: a randomized, controlled trial," *Journal of Gastroenterology*, vol. 43, no. 1, pp. 45–50, 2008.

[28] S. Kudo, S. Hirota, T. Nakajima et al., "Colorectal tumours and pit pattern," *Journal of Clinical Pathology*, vol. 47, no. 10, pp. 880–885, 1994.

[29] S. E. Kudo, S. Tamura, T. Nakajima, H. O. Yamano, H. Kusaka, and H. Watanabe, "Diagnosis of colorectal tumorous lesions by magnifying endoscopy," *Gastrointestinal Endoscopy*, vol. 44, no. 1, pp. 8–14, 1996.

[30] "The Paris endoscopic classification of superficial neoplastic lesions," *Gastrointestinal Endoscopy*, vol. 58, pp. S3–S43, 2003.

[31] "Pathology and genetics of tumours of the digestive system," in *World Health Organization Classification of Tumours*, S. R. Hamilton and L. A. Aaltonen, Eds., pp. 104–119, IARC Press, Lyon, France, 2000.

[32] K. Konishi, K. Kaneko, T. Kurahashi et al., "A comparison of magnifying and nonmagnifying colonoscopy for diagnosis of colorectal polyps: a prospective study," *Gastrointestinal Endoscopy*, vol. 57, no. 1, pp. 48–53, 2003.

[33] J. Pohl, E. Lotterer, C. Balzer et al., "Computed virtual chromoendoscopy versus standard colonoscopy with targeted indigocarmine chromoscopy: a randomised multicentre trial," *Gut*, vol. 58, no. 1, pp. 73–78, 2009.

[34] N. Yoshida, Y. Naito, and Y. Inada, "The detection of surface patterns by flexible spectral imaging color enhancement without magnification for diagnosis of colorectal polyps," *International Journal of Colorectal Disease*, vol. 27, pp. 605–611, 2012.

[35] A. Rastogi, J. Keighley, V. Singh et al., "High accuracy of narrow band imaging without magnification for the real-time characterization of polyp histology and its comparison with high-definition white light colonoscopy: a prospective study," *American Journal of Gastroenterology*, vol. 104, no. 10, pp. 2422–2430, 2009.

[36] J. Pohl, M. Nguyen-Tat, O. Pech, A. May, T. Rabenstein, and C. Ell, "Computed virtual chromoendoscopy for classification of small colorectal lesions: a prospective comparative study," *American Journal of Gastroenterology*, vol. 103, no. 3, pp. 562–569, 2008.

[37] Y. S. Kim, D. Kim, S. J. Chung et al., "Differentiating small polyp histologies using real-time screening colonoscopy with Fuji Intelligent Color Enhancement," *Clinical Gastroenterology and Hepatology*, vol. 9, pp. 744–749, 2011.

[38] C. E. O. Dos Santos, J. C. P. Lima, C. V. Lopes et al., "Computerized virtual chromoendoscopy versus indigo carmine chromoendoscopy combined with magnification for diagnosis of small colorectal lesions: a randomized and prospective study," *European Journal of Gastroenterology and Hepatology*, vol. 22, no. 11, pp. 1364–1371, 2010.

[39] Y. Sano, T. Horimatsu, K. I. Fu, A. Katagiri, M. Muto, and H. Ishikawa, "Magnifying observation of microvascular architecture of colorectal lesions using a narrow-band imaging system," *Digestive Endoscopy*, vol. 18, no. 1, pp. S44–S51, 2006.

[40] J. E. East, N. Suzuki, P. Bassett et al., "Narrow band imaging with magnification for the characterization of small and diminutive colonic polyps: pit pattern and vascular pattern intensity," *Endoscopy*, vol. 40, no. 10, pp. 811–817, 2008.

[41] C. R. Teixeira, R. S. Torresini, C. Canali et al., "Endoscopic classification of the capillary-vessel pattern of colorectal lesions by spectral estimation technology and magnifying zoom imaging," *Gastrointestinal Endoscopy*, vol. 69, no. 3, pp. 750–756, 2009.

[42] J. E. East, E. K. Tan, J. J. Bergman, B. P. Saunders, and P. P. Tekkis, "Meta-analysis: narrow band imaging for lesion characterization in the colon, oesophagus, duodenal ampulla and lung," *Alimentary Pharmacology and Therapeutics*, vol. 28, no. 7, pp. 854–867, 2008.

[43] L. Wu, Y. Li, Z. Li et al., "The diagnostic accuracy of narrow-band imaging for the differentiation of neoplastic from non-neoplastic colorectal polyps: a meta-analysis," *Colorectal Disease*. In press.

[44] M. L. Han, Y. C. Lee, and C. C. Chen, "Computer-generated surface and tone enhancements to distinguish neoplastic from non-neoplastic colon polyps less than 1 cm in diameter," *International Journal of Colorectal Disease*, vol. 27, pp. 337–344, 2012.

[45] A. Hoffman, F. Sar, M. Goetz et al., "High definition colonoscopy combined with i-Scan is superior in the detection of colorectal neoplasias compared with standard video colonoscopy: a prospective randomized controlled trial," *Endoscopy*, vol. 42, no. 10, pp. 827–833, 2010.

[46] C. K. Lee, S. H. Lee, and Y. Hwangbo, "Narrow-band imaging versus I-Scan for the real-time histological prediction of diminutive colonic polyps: a prospective comparative study by using the simple unified endoscopic classification," *Gastrointestinal Endoscopy*, vol. 74, pp. 603–609, 2011.

Clinical Study

Successful Treatment of Early-Stage Jejunum Adenocarcinoma by Endoscopic Mucosal Resection Using Double-Balloon Endoscopy: A Case Report

Hirobumi Suzuki, Atsuo Yamada, Hirotsugu Watabe, Yuka Kobayashi, Yoshihiro Hirata, Yutaka Yamaji, Haruhiko Yoshida, and Kazuhiko Koike

Department of Gastroenterology, The University of Tokyo, 7-3-1 Hongo, Bunkyo-ku, Tokyo 113-8655, Japan

Correspondence should be addressed to Atsuo Yamada, yamada-a@umin.ac.jp

Small bowel adenocarcinoma (SBA) has generally been considered to have a poor prognosis because of nonspecific presentations and difficulties in detection of the disease. The advent of capsule endoscopy (CE) and double-balloon endoscopy (DBE) makes it possible to access to the small intestine for endoscopic interventions. We describe a successful case of early jejunum adenocarcinoma completely resected by endoscopic mucosal resection (EMR) using double-balloon endoscopy (DBE). Early diagnosis and EMR using new technologies such as CE and DBE may improve the recognition of this disease that, at present, has a poor prognosis.

1. Background

Small bowel adenocarcinoma (SBA) is a rare malignancy, but has generally been considered to have a poor prognosis, with a five-year survival rate of 48% (stage I-II), 28% (stage III), and 6% (stage IV) [1]. The majority of patients are diagnosed at an advanced stage due to nonspecific presentations and difficulties in detection of the disease. The advent of capsule endoscopy (CE) has allowed examination of the entire small intestine. In addition, double-balloon endoscopy (DBE) makes it possible to confirm the presence of small intestinal diseases and conduct an endoscopic intervention in the small intestine. We report here a successful case of early jejunum adenocarcinoma completely resected by endoscopic mucosal resection (EMR) using DBE.

2. Case Report

A 42-year-old man appeared with melena and underwent several examinations, including esophagogastroduodenoscopy (EGD), colonoscopy, and abdominal CT with a contrast agent. Abdominal CT scan revealed a wall thickness in the

small intestine (Figures 1(a) and 1(b)). The patient was referred to our hospital.

His hemoglobin level was 11.8 g/dl (normal range 11.3–15.5 g/dl). We conducted a capsule endoscopy and found part of a tumor in the small intestine, suggesting small bowel tumor (Figure 2(a)). In particular, the mucosal contrast of the tumor was enhanced by the effect of the spectral specification of flexible spectral imaging color enhancement (FICE) settings 1 and 2 (Figures 2(b) and 2(c)). In order to investigate the small bowel tumor, antegrade spiral enteroscopy (SE) was conducted [2]. SE showed a multinodular polyp (type Ip) 20 × 15 mm in diameter located about two meters distal to the ligament of Treitz (Figure 3). Biopsy specimen revealed an atypical epithelium. We considered that the lesion was located within the mucosa and decided to perform EMR. We used a DBE (EN-450T5/W, FUJIFILM Medical Co., Ltd., Japan) with an overtube (TS-13140, FUJIFILM Medical Co., Ltd., Japan) and a transparent cap (D-201-11304 Olympus Co., Ltd., Japan) attached to the endoscope tip, which is useful in the colon by pushing draped folds aside or helping luminal orientation at bends
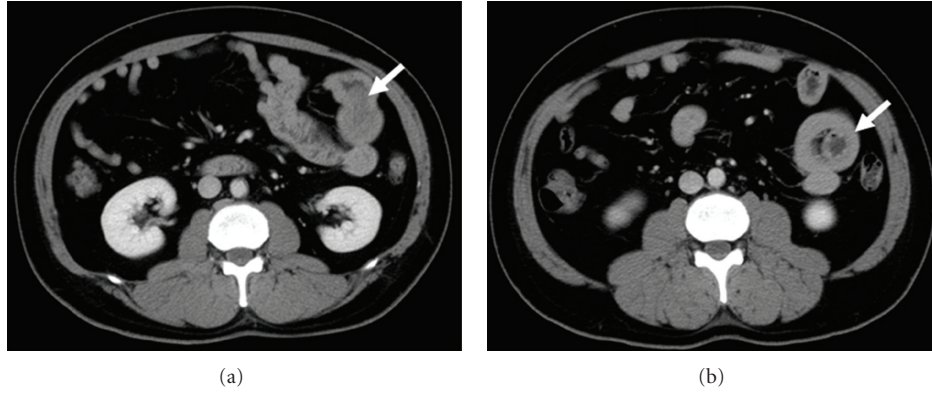
Figure 1: CT findings. (a) Abdominal CT showed the small bowel tumor (arrow). (b) Invagination of a part of the small bowel (arrow).
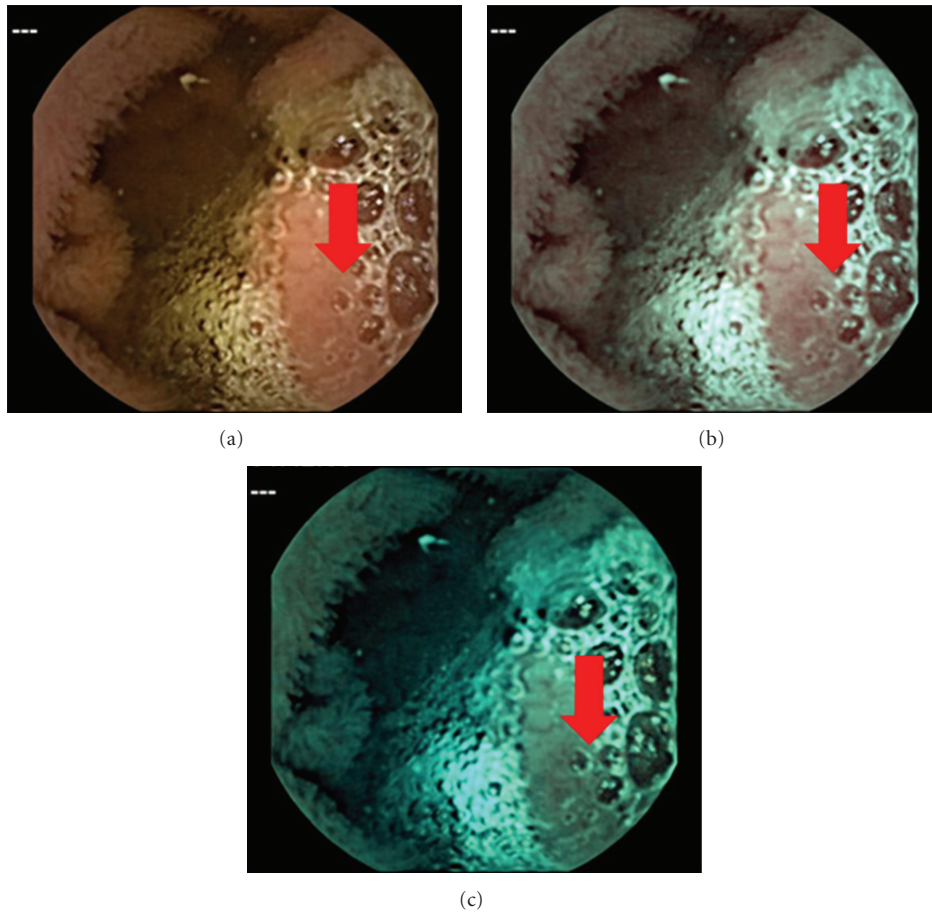

Figure 2: (a) Capsule endoscopy image: CE shows a mass located in the jejunum (arrow). (b) FICE image setting 1 (red 595 nm, green 540 nm, blue 535 nm). (c) FICE image setting 2 (red 420 nm, green 520 nm, blue 530 nm). The mucosal contrast of the tumor was enhanced by FICE settings 1 and 2.

by keeping appropriate distance between lens and mucosa [3]. In order to reduce intraluminal gas, a CO_2 insufflation pump was used during the procedure. It took 12 min to approach the jejunum polyp. Hyaluronic acid at 0.12% (MucoUp, Johnson & Johnson K.K., Japan) was injected into the submucosal layer to lift the surrounding mucosa using a 25-gauge needle (TOP Corp., Japan). A 15 mm electro-surgical diameter snare (Snare-Master, Olympus Medical Systems Corp., Japan) was placed around the lifted area. The lesion was strangulated and resected en bloc using blended electric current (Endocut 2 mode ICC200, ERBE, Germany). The electric current output was increased from
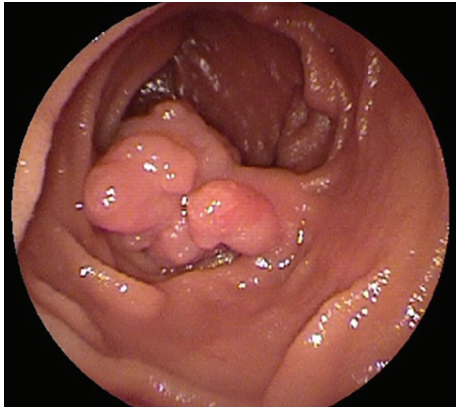
FIGURE 3: Double-balloon endoscopy showing a 0-Ip polyp in the jejunum. The surface of the polyp was multinodular and villous, and its stalk was slightly reddened.
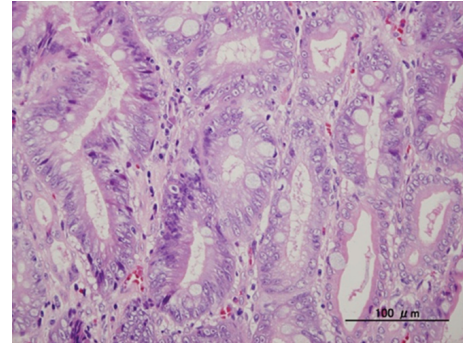

FIGURE 4: Histological analysis of the EMR specimen showed moderately-differentiated tubular adenocarcinoma with papillary adenocarcinoma. H&E stain. Magnification ×200 (bar = 100 μm).

60 to 100 W for final resection. Histological examination showed adenocarcinoma (Figure 4). The invasion depth of the carcinoma was limited to the mucosal layer. There was no lymphovascular invasion of carcinoma cells. The lateral and vertical margins of the specimen were negative. The patient was discharged seven days after EMR without any complications, such as perforation and bleeding. Follow-up endoscopy and abdominal CT scan four months after EMR showed no local or remote recurrences.

3. Discussion

In the last decade, CE and DBE have enabled visualization of the small bowel [4, 5]. In addition, DBE allows access to the small intestine for endoscopic intervention. In this case, the patient exhibited only nonspecific symptoms. Abdominal CT scan suggested wall thickening, and CE revealed a mucosal change. Spiral endoscopy confirmed the presence of an adenomatous lesion, and, finally, the tumor was completely resected by balloon endoscopy in which we had much more experiences than SE.

The American Gastroenterological Association (AGA) Institute states that patients with obscure gastrointestinal bleeding (OGIB) need comprehensive evaluation, including CE. In particular, CE is recommended as the third test in the evaluation of GI-bleeding patients after negative bidirectional endoscopy to obtain early diagnosis of small bowel tumors [6]. The frequency of small bowel tumors identified at CE was 2.4–9.6% in patients with a variety of indications, mainly OGIB [7].

Imagawa et al. reported that FICE improves the visibility of angioectasia, erosion/ulceration, and various tumors of the small intestine [8]. In particular, tumor visibility was improved with FICE settings 1 and 2. Indeed, these were useful for improving the image quality of the mucosal contrast of tumor.

In contrast, the usefulness of abdominal CT scans in patients with OGIB is unclear. We previously reported that abdominal CT scan is an effective modality to demonstrate duodenal varices in patients with OGIB [9]. This case

suggested that abdominal CT scan in patients with OGIB is useful to detect not only duodenal varices, but also early-stage small bowel carcinomas.

To our knowledge, there are few reports of EMR of benign tumors in small intestine such as polyps due to the Peutz-Jeghers syndrome with DBE [10, 11], and none include successful completion of endoscopic resection of pathologically diagnosed SBA. Early diagnosis and EMR using new technologies such as CE and DBE may thus improve the recognition of this disease that, at present, has a poor prognosis.

The present case implies that the combination of several imaging modalities, including CT scan, CE, and spiral or balloon endoscopies, is important to effectively manage a patient with OGIB.

References

[1] Talamonti, Goetz, Joehl, and Rao, "Primary cancers of the small bowel: analysis of prognostic factors and results of surgical management," *Archives of Surgery*, vol. 137, no. 5, pp. 564–571, 2002.

[2] P. A. Akerman, D. Agrawal, D. Cantero, and J. Pangtay, "Spiral enteroscopy with the new DSB overtube: a novel technique for deep peroral small-bowel intubation," *Endoscopy*, vol. 40, no. 12, pp. 974–978, 2008.

[3] S. Kondo, Y. Yamaji, H. Watabe et al., "A randomized controlled trial evaluating the usefulness of a transparent hood attached to the tip of the colonoscope," *American Journal of Gastroenterology*, vol. 102, no. 1, pp. 75–81, 2007.

[4] H. Yamamoto, Y. Sekine, Y. Sato et al., "Total enteroscopy with a nonsurgical steerable double-balloon method," *Gastrointestinal Endoscopy*, vol. 53, no. 2, pp. 216–220, 2001.

[5] G. Iddan, G. Meron, A. Glukhovsky, and P. Swain, "Wireless capsule endoscopy," *Nature*, vol. 405, no. 6785. article 417, 2000.

[6] E. Rondonotti, M. Pennazio, E. Toth et al., "Small-bowel neoplasms in patients undergoing video capsule endoscopy: a multicenter European study," *Endoscopy*, vol. 40, no. 6, pp. 488–495, 2008.

[7] S. D. Ladas, K. Triantafyllou, C. Spada et al., "European Society of Gastrointestinal Endoscopy (ESGE): recommendations (2009) on clinical use of video capsule endoscopy

to investigate small-bowel, esophageal and colonic diseases," *Endoscopy*, vol. 42, no. 3, pp. 220–227, 2010.

[8] H. Imagawa, S. Oka, S. Tanaka et al., "Improved visibility of lesions of the small intestine via capsule endoscopy with computed virtual chromoendoscopy," *Gastrointestinal Endoscopy*, vol. 73, no. 2, pp. 299–306, 2011.

[9] S. Yoshida, H. Watabe, M. Akahane et al., "Usefulness of multi-detector helical CT with multiplanar reconstruction for depicting the duodenal varices with multiple collateral shunt vessels," *Hepatology International*, vol. 4, no. 4, pp. 775–778, 2010.

[10] H. Gao, M. G. van Lier, J. W. Poley, E. J. Kuipers, M. E. van Leerdam, and P. B. Mensink, "Endoscopic therapy of small-bowel polyps by double-balloon enteroscopy in patients with Peutz-Jeghers syndrome," *Gastrointestinal Endoscopy*, vol. 71, no. 4, pp. 768–773, 2010.

[11] K. Mönkemüller, J. Weigt, G. Treiber et al., "Diagnostic and therapeutic impact of double-balloon enteroscopy," *Endoscopy*, vol. 38, no. 1, pp. 67–72, 2006.